

Magic states are rarely the most important resource to optimize

Marco Fellous-Asiani,^{1,*} Hui Khoon Ng,^{2,3,4,†} and Robert S. Whitney^{5,‡}

¹*Centre for Quantum Optical Technologies, Centre of New Technologies,
University of Warsaw, Banacha 2c, 02-097 Warsaw, Poland*

²*Yale-NUS College, Singapore*

³*Centre for Quantum Technologies, National University of Singapore, Singapore*

⁴*MajuLab, CNRS-UCA-SU-NUS-NTU International Joint Research Laboratory, Singapore*

⁵*Université Grenoble Alpes, CNRS, LPMMC, 38000 Grenoble, France.*

(Dated: November 4, 2024)

We propose a scaling approach to evaluating the qubit resources required by concatenated fault-tolerant quantum computing. The approach gives closed-form expressions, which remain simple for multiple levels of concatenation, making it an ideal tool to compare and minimize the resource costs of different concatenation schemes. We then use it to study the resources required for normal and magic operations. Here, magic operations require the preparation, verification and injection of complicated states called “magic states”, while normal operations do not. It is often expected that magic operations will dominate a computation’s physical resource requirements (qubits, gates, etc.), although this expectation has been cast in doubt for surface codes. Our results show that this expectation is also wrong for typical concatenated codes, with magic operations rarely being costly. We give concrete examples for the concatenated 7-qubit scheme with Steane error-correction gadgets or a flag-qubits approach. While optimizations that affect all operations are naturally more effective than ones that affect only magic operations, the surprising conclusion of our work is that the former can reduce costs by several orders of magnitude whereas the latter contributes only marginal reductions. This is particularly surprising given the numerous works on optimizations that affect only magic operations.

I. INTRODUCTION

Quantum computers can potentially exploit quantum phenomena like interference and entanglement to rapidly perform calculations intractable on existing classical computers. They are expected to be invaluable for tasks such as optimization [1, 2], simulation of quantum systems [3–5], attacking cryptographic protocols [6, 7], etc. Yet, there is an apparent contradiction at the heart of quantum computing: It exploits quantum phenomena extremely sensitive to noise and imprecision, but its calculations demand extremely low error rates. The proposed resolution of this contradiction is fault-tolerant quantum computing [8–11] (see also more recent references like [12–16]), which uses many lower-quality *physical qubits* to make high-quality *logical qubits* by relying on quantum error correction to remove errors. Error correction requires the use of many physical qubits for each logical qubit of information, as well as many ancillary qubits and additional operations, resulting in significant resource overheads in the hardware. It is thus natural to investigate ways to minimize the resources needed for fault-tolerant quantum computing.

For error correction to be effective, all quantum operations must be carried out in a fault-tolerant manner (see the precise definition in Sec. V), namely that all circuits must have certain error-propagation properties to

ensure errors are removed even with possibly noisy error-correction operations. A typical fault-tolerant quantum computing scheme has a computationally universal set of logical operations (gates, state preparations, and measurements) with two distinct types that we refer to as *normal* operations and *magic* operations. Magic operations are those whose fault-tolerant implementation requires having extra qubits present (in addition to the data qubits upon which the operation is carried out), and these extra qubits must be prepared, verified, and injected as special states called magic states. In contrast, normal operations are those whose fault-tolerant implementation does not require such magic states.

The prototypical example of this normal versus magic dichotomy is found in well-known fault-tolerant quantum computing schemes, including the currently popular surface-code schemes (see, for example, the review articles Refs. [16] and [13]), as well as the concatenated scheme of Ref. [12] based on the 7-qubit code (used as an example in this work). There, the normal operations include Clifford gates implemented transversally across physical qubits carrying the quantum information, with the transversality guaranteeing fault tolerance of the operations. The magic operations are non-Clifford gates, with the T -gate as the most common variety, needed to complete the universal set of logical gates.

Until recently, the complexity of magic-state preparation and distillation [17] led to the natural expectation that magic operations require a lot of resources [18–21], overwhelmingly more than normal operations [22–24]. This expectation is the basis for the strong focus of the community on minimizing the number of magic states

* fellous.asiani.marco@gmail.com

† huikhoon.ng@nus.edu.sg

‡ robert.whitney@grenoble.cnrs.fr

needed for a given algorithm [25], reducing the resources required to prepare the magic states [12, 18, 20, 22, 26–33], or replacing magic-state injection by something less resource-costly [19, 28, 34, 35]. This expectation was, however, questioned by Litinski in Ref. [36], where he compared the resources for magic and normal operations in surface-code schemes. He found that magic operations can be much less costly than expected, and gave examples of situations where they do not contribute significantly to the overall resource cost of the quantum computer. A very recent work along the same thread is Ref. [37]. This suggests that there may be little gain in further reducing the resources required for magic operations in surface-code scenarios.

For general fault-tolerant quantum computing schemes, however, it remains unclear whether one needs further optimization of the magic operations, or whether current approaches are already sufficiently resource efficient. In particular, schemes that rely on concatenation to scale-up magic operations can have a rapid growth in their resource requirements, since such schemes often require that each magic state is replaced by multiple magic states at each level of concatenation. This hints at the possibility that the excess resource requirements of magic operations over normal operations may quickly become significant. Thus, it is natural to consider concatenated fault-tolerant schemes, and quantify the resources required by magic operations and compare them to the resources required for normal operations.

To address this question, we develop a general scaling approach to evaluate the qubit costs required in concatenated fault-tolerant quantum computing schemes. Here we define *qubit costs* as the number of physical qubits needed for the computation. Our approach is analytical and shows how the qubit cost scales with the number of levels of concatenation. It gives closed-form expressions for these costs that remain simple for multiple concatenation levels. We find that the qubit costs depend on just a few parameters of the concatenated fault-tolerant scheme, making it straightforward to evaluate the physical qubit costs required by any such scheme. An earlier work [24] evaluated resources for a single concatenation level using Monte-Carlo simulations, but such a numerical approach is infeasible beyond a couple of concatenation levels [39]. In contrast, our analytical approach captures the full scaling of resources as concatenation level grows.

We use this general scaling approach to evaluate the resources required by different fault-tolerant schemes, looking at qubit resource costs of algorithms containing magic and normal operations. Specific scenarios we examined are plotted in Fig. 1. There, solid curves correspond to qubit costs for typical quantum algorithms, while dashed curves of the same color correspond to what would happen if magic operations were no more costly than normal ones. Optimizing magic operations would move the solid curves towards the dashed curves of the same color. This

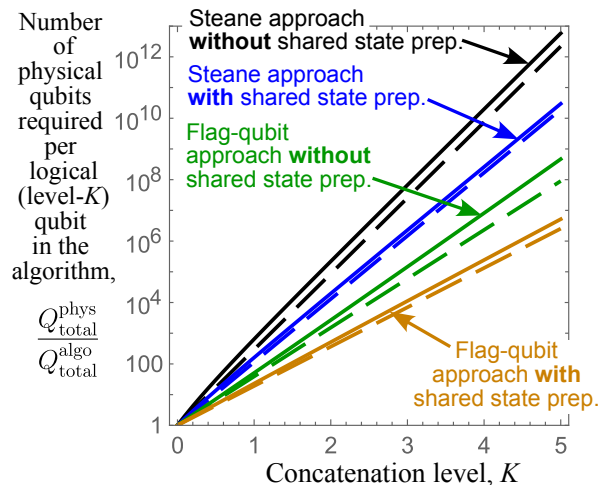


Figure 1. Plot of physical qubit costs for different error-correction schemes versus the number of levels of concatenation, K . The solid lines are when 5% of the gates in the logical algorithm are magic operations, which is typical of many algorithms (see appendix A). Where necessary we consider a large-scale algorithm requiring a few thousand logical qubits (for example, cracking RSA-2048 encryption [38]). The dashed lines are when all magic operations are replaced by normal operations at the level of the logical algorithm. On this scale the solid and dashed lines for the same error-correction scheme are very close. In contrast, the difference between the schemes is significant. Sharing state preparation reduces the qubit costs by a factor of about 100 at $K = 5$, switching from Steane to flag-qubits reduces the qubit costs by a factor of about 10^4 .

is a modest improvement compared to optimizations that affect all operations, such as switching to less costly error correction gadgets, and sharing state preparation for error correction and magic operations.

Given the huge challenge of building large quantum computers, no optimization is too small to be ignored. However, here we reach the surprising conclusion that optimizing magic states is rarely the most important optimization. It is more important to first optimize aspects of the fault-tolerant scheme that affect all gates (such as optimizing the error-correction gadget), and only consider optimizing specific gates (such as those requiring magic states) afterward.

More generally, this work’s scaling approach provides a tool to evaluate the qubit costs for any concatenated scheme. Its usefulness is enhanced by the fact it gives closed-form expressions that remain simple for multiple levels of concatenation. We give full details of its application to examples involving 7-qubit codes, to illustrate how it can be applied to any concatenated scheme. This includes our method of calculating the important but little-studied quantities, namely, the time and failure multiplicities that quantify the qubit costs associated with the time taken to prepare ancillary qubit states, and with preparing extra quantum states to replace those that fail verification (see Sec. VI) The failure multiplic-

ity is responsible for Fig. 1’s orders of magnitude difference between qubit costs with and without shared state-preparation. This makes it extremely clear that such little-studied quantities are crucial to get a realistic evaluation of the qubit resources for almost any fault-tolerant scheme.

The article is organized as follows. Sec. II presents a brief summary of the main methods and results. The rest of the manuscript then addresses those points in detail, starting with an introduction to the basic concepts in Sec. III. Sec. IV explains how our scaling approach works for a generic concatenated quantum computing scheme. We emphasize that this scaling approach can be understood without the full circuit details of the underlying scheme, as the scaling behavior is determined by only a few simple parameters. However, to get concrete values for the actual qubit costs for a given scheme, one must extract the values of those parameters from the details of the circuits that implement the operations of the scheme. For that, we explain the general properties of such circuits in Sec. V, and from them, we compute the associated qubit costs. In Sec. VI, we carefully derive the time and failure multiplicity factors that are crucial for computing the qubit costs. Sec. VII gives two examples for schemes based on the 7-qubit code. The first example uses the standard Steane error-correction gadget employed in the original scheme of Ref. [12], while the second replaces it with the more recent flag-qubits approach [32, 40, 41]. Motivated by our findings, we examine more generally in Sec. VIII the effect of reducing the size of the error correction gadget on the qubit costs. We conclude finally in Sec. IX.

II. SUMMARY OF MAIN METHOD AND RESULTS

In this work, we introduce a scaling approach to evaluating the “qubit cost” of performing concatenated fault-tolerant quantum computing protocols. Here “qubit cost” is the number of physical qubits necessary to perform the computation, which determines the size of the quantum computer required. We begin here with a summary of our methods and results, to give the reader the basic intuition, while leaving the many technical details to the remainder of the text.

We begin with an *abstract circuit* that carries out a specific computation (e.g., an algorithmic subroutine). An abstract circuit is one written in terms of idealized error-free qubits undergoing perfect gate operations. We choose a particular concatenated fault-tolerant quantum computing scheme to implement this circuit using real, potentially faulty, physical operations acting on real physical qubits; see Sec. III. At the lowest level of concatenation, each qubit in the abstract circuit is encoded into n physical qubits, as prescribed by the fault-tolerant scheme, forming a “logical qubit”. Each operation (gate, state preparation, and measurement) in the abstract cir-

cuit is implemented as an encoded — or logical — operation on the logical qubit, accompanied by error correction to remove errors. This base level — “level-1” — of encoding provides protection against a maximum number of errors assured by the fault-tolerant scheme. To correct more errors and achieve higher computational accuracy, we concatenate the circuit: Every physical qubit in the level-1 circuit is replaced by a logical qubit, and every physical operation is replaced by the corresponding logical operation accompanied by error correction. Each such replacement increases the concatenation by one level, and we go recursively from level-0 (i.e., no encoding at all), to level-1, to level-2, etc.

Each time we increase the concatenation level, we gain the ability to correct more errors, eventually reaching a level K adequate for the target computational accuracy. How large K is, for a target accuracy, depends on how the error-correction capability grows for the chosen fault-tolerant scheme. The increased accuracy, from increasing the concatenation level, comes at the cost of more physical qubits and operations. Again, how the qubit cost grows depends on the details of the scheme. Our main task in estimating the qubit cost of implementing an abstract circuit is to understand how the number of physical qubits grows each time we increase the concatenation level.

To facilitate that, we categorize all operations into normal and magic. Magic operations are those whose fault-tolerant implementations require the injection of additional ancillary qubit states called magic states, while normal operations are those that do not require the injection of a magic state. Which operations are normal or magic is determined by details of the fault-tolerant scheme in question; see Sec. IV. In many schemes, normal operations are those that are implemented transversally.

Since magic operations require more qubits than normal operations, we assume that the qubit cost of implementing the abstract circuit is determined by the level- K circuit layer with the largest number of (level- K) magic operations. When we look inside this layer, going down the concatenation levels towards the physical level, we see that level- k contains a sequence of many operations and many qubits. We refer to all these operations and qubits as \mathcal{L}_{\max} at level- k . There are some small subtleties in defining \mathcal{L}_{\max} at level- k (see Sec. IV A), but they are not necessary to understand our basic approach.

The qubit cost must count all qubits that participate in \mathcal{L}_{\max} . To do that, we assume that every level- k normal operation requires only normal operations at level $(k-1)$, while a level- k magic operation requires both normal and magic operations at level $(k-1)$. This describes many known concatenated fault-tolerant schemes, and is motivated by the desire to limit the use of resource-expensive magic operations in the design of fault-tolerant circuits. We then turn to qubits, and classify each of them as a “normal qubit” or a “magic qubit”; see Sec. IV B. For this classification, we say that a level- k qubit is magic if it experiences at least one level- k magic operation in \mathcal{L}_{\max} ;

the level- k qubit is normal otherwise. We then have the following mental picture when evaluating the qubit cost: At each concatenation level k , each normal level- k qubit is made up entirely of a certain number of level- $(k-1)$ normal qubits (with no magic qubits), with this number determined by the details of the fault-tolerant scheme. Here, all the level- $(k-1)$ qubits are normal qubits, because there are no magic operations within \mathcal{L}_{\max} on those level- $(k-1)$ qubits. In contrast, a magic level- k qubit, will be made of normal and magic level- $(k-1)$ qubits, with the number of each depending on the scheme's details.

With this, it becomes clear how the qubit cost calculation can be organized. We begin with the level- K qubits. Each level- K normal qubit requires $\lambda_{\text{normal},K}$ (say) level- $(k-1)$ normal qubits; each level- $(k-1)$ normal qubit requires $\lambda_{\text{normal},K-1}$ level- $(k-2)$ normal qubits; etc. For the magic qubits, we follow a separate thread: Each level- K magic qubit requires $\lambda_{\text{magic},K}$ level- $(k-1)$ magic qubits and b_K level- $(k-1)$ normal qubits, etc. We can have a more fine-grained counting, in the case where there are different kinds of magic qubits, corresponding to qubits that go through different kinds of magic gates with different number of ancillary qubits. We then divide $\lambda_{\text{magic},K}$ into branches for the different kinds of magic qubits. All these details can be concisely gathered into a matrix transformation \mathbf{M}_k for each level k that relates the number of normal and magic level- $(k-1)$ qubits needed for the level- k normal and magic qubits. An example of this is given in Eq. 2. In the situation where the concatenated fault-tolerant scheme has a recursive structure so that each level is self-similar (from using the same error-correction code over and over to increase the concatenation level), we have a single matrix \mathbf{M} for all k . Then, the qubit cost is particularly simple and one can analyze its growth, as K increases, through an eigen-analysis of \mathbf{M} .

The problem of evaluating the qubit cost for a given circuit and fault-tolerant scheme is thus reduced to finding the entries of these \mathbf{M} matrices. They depend on the intricate circuit details of the fault-tolerant scheme. Sec. V explains how to use such details to make such an evaluation for a generic concatenated fault-tolerant scheme. It shows that we need to account for two complications. The first is that many fault-tolerant schemes rely on probabilistic verification steps to assure fault-tolerant preparation of quantum states [42]. In the event of a verification failure, the state has to be re-prepared. To avoid holding up the computation, as any extra waiting time adds errors, we need to simultaneously prepare sufficiently many copies of the state, in the hope that we have at least the necessary number of copies passing the verification as needed by the computation. We refer to this increase in the qubit cost from the verification steps as the *failure multiplicity* (see Sec. VIB). Properly accounting for the failure multiplicities prevents an underestimate of the qubit cost.

We need to handle a second complication, namely, that

the same qubits can be re-used as they become available. Ancillary qubits participate in the computation for a certain number of time-steps, from their state preparation, interaction with the data qubits, to their measurement. Once they are measured, they are free to be reused as ancillary qubits for the next operation. This must be treated carefully to avoid over-simplified assumptions that lead to very poor resource estimates. For example, assuming ancillary qubits are always available for re-use gives a significant underestimate of qubit resource costs, while assuming ancillary qubits are never re-used gives a gross overestimate. Instead, we estimate the number of time steps an ancillary qubit is in use, and that tells us how often that qubit can be reused. We refer to this as the *time multiplicity* in our discussion (see Sec. VIA).

In Sec. VII we use our approach to carefully evaluate the qubit costs for concrete examples. We consider two variants of the 7-qubit concatenated fault-tolerant scheme. The first variant is the original protocol of Ref. [12] with the Steane EC gadgets, where simultaneous syndrome measurements can be done at the cost of verified encoded ancillary states, carried by the same number of physical qubits as for the logical qubits. Because EC gadgets are needed everywhere in the circuit, for both normal and magic operations, such a scheme incurs particularly high qubit costs. The second variant is the flag-qubit scheme of Ref. [32, 40, 41], aimed at reducing the ancillary qubit costs by not using verified encoded states. Instead, a small number of ancillary qubits are employed as flags to catch when a harmful fault might occur in the circuit.

Our results for the 7-qubit fault-tolerant scheme are summarized in Fig. 1, where we plot the qubit cost (measured per logical qubit) versus the maximum concatenation level K . Focusing on the black and green lines for the Steane and flag-qubit variants, respectively (without shared state-preparation; we come to this shared preparation in a moment), we see a markedly lower qubit cost for the flag-qubit scheme compared to the Steane version. To identify the proportion of the qubit costs attributable to the magic operations, we compare the solid and dashed lines: The solid lines give the qubit costs for the given abstract circuit, computed using \mathcal{L}_{\max} ; the dashed lines plot the costs for a fictitious circuit where all magic operations in \mathcal{L}_{\max} are replaced by normal operations. Surprisingly, the switch from magic to normal operations gave only a marginal reduction in qubit costs. Minimizing the costs of magic operations, e.g., reducing the qubit costs of magic-state preparations, would move the solid lines towards the corresponding dashed line, but we see that any resulting reduction in qubit costs would be modest.

In contrast, the large differences between the curves of different colors show that other optimizations achieve much more significant cost reductions. The lower ancillary qubit requirements of the EC gadgets in going from the Steane scheme to the flag-qubit approach gave orders-of-magnitude reductions in the qubit costs. Fur-

thermore, by taking into account the possibility of sharing state preparation across multiple magic operations that require the input of the same state at the same time, the failure multiplicities can be minimized, leading to the marked cost reductions that take us from the curves labeled “without shared prep.” to the ones “with shared prep.”.

Taken together, these optimizations can reduce the total qubit costs by multiple orders of magnitude (going from the black to orange solid curves in Fig. 1 is a reduction of nearly six orders of magnitude at $K = 5$) [43]. After these optimizations, one arrives at a circuit in which the extra cost of magic gates is sufficiently small that any further optimization of the magic operations could reduce the total resource cost only by a marginal amount.

Thus, we reach the conclusion, contrary to prior expectations, that reducing the costs of magic operations is far from the most important optimization. While the illustration of this in Fig. 1 relies on various assumptions (outlined later in this work), we believe this conclusion holds more generally for the following reason: The biggest reduction in qubit costs come from optimizations that affect *both* normal and magic operations, rather than optimizing the magic states that affect only the magic operations which rarely occur in a typical circuit anyway.

With this in mind, we identify two specific optimizations that affect both normal and magic operations, which then have the potential to significantly reduce the required qubit costs. The first optimization is to share the preparation and verification of quantum states, in particular the ancillary states needed in fault-tolerant schemes for the EC gadgets, and magic operations. By sharing this preparation and validation across multiple components that require the same states, we minimize the redundancy in the number of copies of these states needed to pass the probabilistic verification steps. The second optimization is to switch from an EC gadget that requires a relatively large number of ancillary qubits (like the Steane EC gadgets) to one that requires fewer qubits (like the flag-qubit ones).

To better understand this second aspect, we examine how the qubit costs vary with the size of the EC gadget. For this, we study a fictitious model for the EC gadget in the 7-qubit fault-tolerant scheme, where the ancillary qubit cost of error correction is captured by a continuous parameter δ , expressed as a fraction of the qubit cost of the Steane EC gadget; see Sec. VIII. Then, $\delta = 1$ corresponds to the Steane EC gadget cost in the case of shared state preparation, while $\delta = 0$ is the (unrealistic) case where the EC gadget requires no ancillary qubits at all. Then, the case of flag-qubit EC gadgets is analogous to $\delta \approx 0.06$ [44]. We find that, in going from $\delta = 1$ to $\delta = 0$, we can gain orders-of-magnitude improvement in the qubit costs, especially for larger K values. Furthermore, the relative costs of implementing the abstract circuit versus one with all magic operations replaced by normal operations remain fairly flat as δ decreases from

1, until we reach below $\delta \simeq 0.3$, i.e., a 70% decrease in the EC gadget qubit costs. This confirms the importance of optimizing the EC gadget costs.

Of course, building large and accurate quantum computers is a tremendous challenge and no optimization is too small to be ignored. However, it makes sense to first focus on optimizations that give large reductions in the required qubit costs, and only then turn to optimizations that allow further more modest reductions. We see here that reducing the costs of magic operations is one that gives only modest qubit-cost savings. Hence, it is rarely one of the first items to optimize in concatenated fault-tolerant quantum computing.

III. PRELIMINARIES

We begin by reviewing the key concepts in concatenated fault-tolerant schemes needed for our analysis, and then discuss how we can quantify the physical resource cost of a computation.

A. Concatenated fault-tolerant quantum computing

We first provide a quick review of the main features of concatenated fault-tolerant quantum computing schemes. We begin with the quantum error-correcting code \mathcal{C} that forms the basis of the error correction in any such scheme. We assume that \mathcal{C} uses n physical qubits — a “code block” — to carry a single “logical” qubit of information, and it can correct arbitrary errors on no more than t physical qubits within the same code block. Logical operations on these logical qubits are performed with some (non-uniquely) chosen physical operations that act on \mathcal{C} in the desired manner. Errors are diagnosed by measuring a set of check operators, and the measurement results are used to deduce the errors likely to have occurred. A correction operation — the “recovery” — is then applied to remove these errors.

Now, the above description of how the code removes errors from the physical qubits assumes perfect error-correction operations, i.e., ideal measurements and recovery. In reality, these error-correction operations are carried out by a physical circuit, with components that are themselves possibly faulty and can hence introduce — not just remove — errors into the encoded logical information. Fault tolerance theory addresses the question of how to remove errors, and do logical operations on the encoded information, despite using these possibly faulty components. Broadly speaking, fault-tolerant quantum computing focuses on designing computing circuits with the following properties: (1) physical circuits must not convert errors correctable by the code into uncorrectable ones; (2) the physical circuit that carries out error correction must still be able to remove errors to a certain extent (determined by the requirements of a given scheme), as

long as the error correction circuit is not too faulty. Any error-correcting code for use in a fault-tolerant quantum computer requires a detailed design of the physical circuits that carry out logical operations (i.e., state preparations, gates, and measurements) and error correction, satisfying the two broad properties above.

Fault-tolerant quantum computing schemes aim to achieve any desired level of computational accuracy, by scaling up the ability to remove errors. This is done by investing more physical resources — more qubits, more gates — to diagnose and correct more errors. Some fault-tolerance schemes correct more errors by scaling up a certain “area”, like surface codes and Bacon-Shor codes; there one scales up the ability to remove errors by increasing the area of the code (increasing n). Here, we focus instead on concatenated schemes, where we scale up by recursively encoding the information using multiple levels of the same code.

The basic idea of concatenation is to replace physical elements by logical ones, encoded with some code, and to do this recursively over multiple levels of encoding. For example, assuming that we always use the same code that employs n physical qubits, we begin with n physical qubits carrying a single logical qubit in the code space; we refer to this as “level-1” concatenation, the n physical qubits as a single level-1 code block, and the logical qubit a “level-1 qubit”. We will also refer to physical qubits as “level-0 qubits”, and logical qubits at level- k concatenation as “level- k qubits”. To concatenate the code, going from level-1 to level-2 concatenation, we replace each of the n physical qubits by a level-1 qubit (each carried by n physical qubits). This level-2 qubit is thus carried by n^2 physical qubits. More generally, to increase the code concatenation by one level, we replace each physical qubit by a level-1 qubit. Increasing the concatenation level increases the ability to correct errors for the following reason. The n -qubit code protects level-1 qubits by correcting errors on up to t physical qubits in each code block supporting a level-1 qubit. Now, errors that occur on more than t physical qubits in a code block lead to a level-1 logical error, but as long as it is one out of no more than t level-1 qubits for a level-2 code block in error, that level-1 logical error will be corrected by the error correction at level 2.

The fault-tolerant circuits associated with a level- k concatenated scheme are constructed in a similar manner, namely, for a given circuit that implements a particular operation, to increase the concatenation by one level, we replace every physical component — a preparation, a gate, or a measurement — by its level-1 version. Just as for qubits, we can then talk about a level- k operation, referring to the logical operation at the k th level of concatenation. Each level- $(k+1)$ operation is made up of level- k operations. Note that circuit concatenation differs from code concatenation in one critical respect, each operation needs to be implemented in a fault-tolerant manner, such that a certain amount of faults in the level-0 operations do not cause an error in the level-1 operation. The

level-1 version of a physical component is not just the corresponding level-1 logical operation acting on level-1 qubits, but also includes the error-correction (EC) circuit (called an EC gadget) for each code block involved in that operation. Furthermore, it requires that certain types of gate operations are implemented via magic-state injection [45]. We will make this more precise below when we discuss specific schemes and circuit designs.

The increase of concatenation level by recursively replacing physical qubits or components by level-1 versions, using the same code at each level, describes the typical concatenated schemes discussed in the community. Our scaling approach is straightforward in such cases, as we will show in Sec. IV. We believe our analytical approach to resource estimates is also a simple way to treat resources in more complicated concatenated schemes, where the prescription to construct level- k components from level- $(k-1)$ components is different at each level of concatenation.

B. Quantifying physical resource costs

There are many physical resources we wish to minimize when building a quantum computer, including the number of qubits, the number of operations, the energy consumption, the materials required, and the financial costs. The minimization of the resources is a challenging problem, and some of them are only starting to be tackled, see e.g. Refs. [46–49]. In this work, we focus on the number of qubits needed, and quantify the qubit cost of implementing both normal and magic operations.

1. Assumptions about the logical algorithm

We begin with a logical algorithm of interest, represented by an abstract circuit $\mathcal{C}_{\text{algo}}$ (recalling that an abstract circuit is one written in terms of idealized error-free qubits and gates-operations). We choose a particular concatenated fault-tolerant scheme to carry out the computation to some desired computational accuracy using real (faulty) operations. The target accuracy determines the maximum concatenation level K we need for the fault-tolerant implementation. This abstract circuit is assumed now to be written in terms of the (level- K) logical operations (state preparations, gates, and measurements) implementable in the fault-tolerant scheme that employs both normal and magic operations.

We now make assumptions about the operations at the logical level, $\mathcal{C}_{\text{algo}}$, often known as the “standard circuit model” of the computation for the abstract circuit. Firstly, we assume that the circuit $\mathcal{C}_{\text{algo}}$ requires that all (level- K) qubits are initialized in $|0\rangle$ and are measured in their Pauli Z basis. Secondly we assume that such level- K preparations and measurements are normal operations (rather than magic operations). Thirdly, we assume that the algorithm has a rectangular shape, namely, that all

level- K qubits are prepared at the same initial time-step, and measured at the same final time-step, with logical gate operations (but no measurements) in between.

Note that we only make these three assumptions at the logical level, i.e. at level- K , with none of them holding at level- k for $k < K$. For example, to perform level- K gates we often have to prepare lower level states which are not $|0\rangle$, for example magic gates at level K require the preparation of magic-states at level $K-1$, and this preparation requires magic operations at level $K-2$. Thus neither of the first two assumptions hold at lower levels. Similarly, at lower levels the third assumption does not hold because the circuit ceases to be rectangular, and contains many measurements throughout the algorithm (in both EC gadgets and in magic operations).

In principle, our scaling approach does not require these “standard circuit model” assumptions for the logical algorithm being implemented. However, they simplify its application. Thus, we assume them throughout, mentioning the places where they allow us to simplify the analysis.

2. Comparing costs of normal and magic operations

With the full circuit details for the chosen fault-tolerant quantum computing scheme, and going from level K down to the physical level (level 0), we can estimate — as we will do below — the total qubit cost, $Q_{\text{total}}^{\text{phys}}$, i.e., the total number of physical qubits needed to implement the circuit $\mathcal{C}_{\text{algo}}$ for the given target accuracy and chosen fault-tolerant scheme.

We then want to understand how much of the qubit cost $Q_{\text{total}}^{\text{phys}}$ is due to the magic operations in the circuit $\mathcal{C}_{\text{algo}}$. To do that, we consider a fictitious logical circuit $\mathcal{C}_{\text{normal}}$, which is the same as $\mathcal{C}_{\text{algo}}$, except that we replace every logical (level- K) magic operation in $\mathcal{C}_{\text{algo}}$ by a normal operation. We then evaluate the qubit cost $Q_{\text{total}}^{\text{phys}}$ for the circuit $\mathcal{C}_{\text{normal}}$, in the same manner as for $\mathcal{C}_{\text{algo}}$. The difference between the $Q_{\text{total}}^{\text{phys}}$ values for $\mathcal{C}_{\text{algo}}$ and $\mathcal{C}_{\text{normal}}$ can be attributed to the qubit cost of doing the magic operations in $\mathcal{C}_{\text{algo}}$.

Note that $\mathcal{C}_{\text{normal}}$ is, of course, not a uniquely defined circuit: There are usually many different normal gate operations, and we can choose which one we use to replace the magic operations in $\mathcal{C}_{\text{algo}}$ to get $\mathcal{C}_{\text{normal}}$. Nevertheless, in the examples we will study, magic operations are single-qubit gates and all single-qubit normal gates have the same qubit cost. Thus, any replacement of magic operations by single-qubit normal gates will yield the same $Q_{\text{total}}^{\text{phys}}$ for $\mathcal{C}_{\text{normal}}$. In appendix B 2, we explain how to treat more general cases. In addition, we will also assume that the chosen fault-tolerant scheme is such that a level- k normal operation is composed only of level- $(k-1)$ normal operations (see next section), irrespective of whether that operation is a gate operation, a state preparation or a measurement. Hence, since $\mathcal{C}_{\text{normal}}$ contains only

normal operations at level- K , then there are no magic operations at any level in $\mathcal{C}_{\text{normal}}$.

To quantify the cost of the magic operations, we define the ratio between $Q_{\text{total}}^{\text{phys}}$ for the two circuits:

$$R = \frac{Q_{\text{total}}^{\text{phys}} \text{ for } \mathcal{C}_{\text{algo}}}{Q_{\text{total}}^{\text{phys}} \text{ for } \mathcal{C}_{\text{normal}}}. \quad (1)$$

For $R \gg 1$, magic operations require significantly more physical qubits than normal operations, while $R = 1$ means that magic and normal operations require the same physical qubit costs.

Of crucial interest for the scalability of a fault-tolerant scheme is the behavior of R as K grows. An R that grows unchecked suggests a limit to scalability, and a need to reduce the cost of magic operations. R is also an important ingredient in estimating any resource (such as power or energy) in a full-stack quantum computing model. Specifically, such estimations are simpler when $R \sim 1$, because one can neglect resource-cost differences between magic and normal operations, as in Ref. [47].

In the rest of the paper, we evaluate $Q_{\text{total}}^{\text{phys}}$ and R , using a general scaling argument in Sec. IV. We then use this argument to estimate these quantities for concatenated schemes based on the 7-qubit code.

IV. A GENERAL SCALING APPROACH

Here, we derive a simple scaling approach to how the number of qubits scales with the level of concatenation of the fault-tolerant quantum computing scheme. As we will see, our approach shows that the qubit costs depend on only a few parameters of the scheme, and allows us to understand the scaling behavior of the resource costs without requiring the full, and often highly complicated, details of the circuit designs underlying a scheme. For example, it tells us that the values of the parameters for which the resources required by magic states will explode as we increase the concatenation level k , and the values for which those resources remain finite.

Our scaling approach relies on two assumptions, valid for well-known concatenated fault-tolerant schemes:

- **Assumption 1:** For any $k \geq 1$, a level- k normal operation is built out of only normal operations at level- $(k-1)$.
- **Assumption 2:** For any $k \geq 1$, a level- k magic operation is built out of a combination of normal and magic operations at level- $(k-1)$.

Here, $k = 1, 2, 3, \dots$ denotes the level of concatenation in the fault-tolerant scheme, and an operation refers to a fault-tolerant state preparation, gate, or measurement. The level- $k-1$ operations include all the preparation and usage of all the ancillary-states necessary at level- $k-1$ (for EC gadgets, magic-state injection, etc.).

These two assumptions hold for many fault-tolerant quantum computing schemes, where the repeatedly used subroutines like the EC gadgets are designed to use only normal operations. One also usually tries to implement as many logical gates as possible using only normal operations, completing the universal gate set with only a small number of magic operations (often only a single type of magic gate).

As explained in the introduction, magic operations are logical operations that require magic states for their fault-tolerant implementation; normal operations do not. Thus, this split into magic and normal only formally makes sense for $k \geq 1$; in contrast, all level-0 (i.e., physical) gates are assumed to be direct operations on the physical qubits and do not need magic states. Nevertheless, it is convenient for book-keeping in our scaling argument to still classify level-0 gates into normal and magic. Specifically, we say that a level-0 operation is magic if the logical version of that operation is magic; it is normal otherwise.

A. Definition of a layer

To find the physical qubit cost of a given algorithm, one notes that the circuit implementing that algorithm $\mathcal{C}_{\text{algo}}$ (described in Sec. III B 1) requires different resources at different moments in the calculation. Hence, we cut $\mathcal{C}_{\text{algo}}$ into what we call *layers*, each of which is a single time step of $\mathcal{C}_{\text{algo}}$. The physical qubit cost of an algorithm is then given by the layer that requires the most physical qubits, we call this the bottleneck layer, \mathcal{L}_{max} . To evaluate the physical qubit costs, we need to extend the definition of such layers to lower levels, all the way down to the level of physical qubits (level-0). We explain this in the next paragraph, however some readers may wish to skip that explanation, because the details are not necessary to grasp the logic of the scaling approach that follows.

To detail the definition of a given layer at level- k , we start with the above definition of that layer at the algorithm level (level- K), and iteratively define that layer at lower levels. For any $k \in [0, K]$, the layer at level- $(k - 1)$ is defined to include all the operations necessary to perform that layer, at level- k . Thus, it includes the full level- $(k - 1)$ circuit that prepares and measures all ancillary states that are used in all operations occurring in the layer at level- k . To avoid any risk of underestimating costs, we make two further inclusions in the layer. Firstly, when going from level- k to level- $(k - 1)$ we include the ancillary states used to prepare those level- k qubits, even if that preparation is at an earlier time in the level- k circuit. Secondly, as fault-tolerant schemes often require multiple time-steps to prepare and measure ancillary states, we include in the layer the full circuits for all ancillary states used in preceding or subsequent layers, if they are being prepared or measured at the same time as the layer of interest. These two inclusions allow us to be

sure that the level-0 layer has enough physical qubits for the computer to implement that layer at the level of the algorithm $\mathcal{C}_{\text{algo}}$. After that the qubit cost for the *whole algorithm* is given by the layer requiring the most physical qubits, which we call the bottleneck layer, \mathcal{L}_{max} . In all our examples, we assume that \mathcal{L}_{max} is a level- K layer containing the largest number of magic operations, since we are considering magic operations that cost more than normal operations. This is typically the case when the algorithm requires the same number of level- K qubits in each layer [50]. We next need to make an assumption for the ancillary states being prepared and measured during \mathcal{L}_{max} for previous or subsequent layers. For simplicity of our calculations, and to ensure our cost evaluations apply for any algorithm $\mathcal{C}_{\text{algo}}$, we assume that all layers preceding and following \mathcal{L}_{max} require the same ancillary states as \mathcal{L}_{max} [51]. In other words, we assume that every layer in the algorithm is as costly as the most-costly layer, \mathcal{L}_{max} .

B. Classifying operations and qubits

Now, we take the classification of operations into normal and magic, and use it to classify the qubits. We define a qubit at level- k to be normal if it experiences *only* normal operations throughout the whole of the level- k implementation of the bottleneck layer \mathcal{L}_{max} , as defined above. We define a qubit at level- k to be magic, if it experiences at least one level- k magic operation during the level- k implementation of \mathcal{L}_{max} [52]. When we want to categorize then count the level- k normal and magic qubits for a concrete fault-tolerant scheme, there are a numerous details to take into account (see Sec. V B and Appendix B), however such details are not necessary to understand our scaling approach.

To explain our scaling approach, we start with a simple case. For this, we imagine that any level- k normal qubit has the same level-0 requirements (i.e. same physical qubits count) as any other level- k normal qubit, irrespective of what combination of initial preparation, gate-operation and measurement it experiences. In the same manner, we imagine that any level- k magic qubit has the same level-0 requirements as any other level- k magic qubit. It can sometimes be tedious to uncover whether this simple case describes a given fault-tolerant scheme (see Appendix B), however Sec. VII shows that this simple case is sufficient for the well-known 7 qubit code with Steane EC gadgets (even if it is insufficient for flag EC gadgets). In this simple case, we can say that

- each level- k normal qubit is built out of λ_{normal} level- $(k - 1)$ normal qubits;
- each level- k magic qubit is built out of λ_{magic} level- $(k - 1)$ magic qubits and b level- $(k - 1)$ normal qubits.

The value of the three parameters, λ_{normal} , λ_{magic} and b depends on numerous details, which are explained in

much of the rest of this paper. However, once these parameters are known, the scaling for this simple case requires minimal mathematics, while also being representative of the scaling for more complicated cases. So it makes sense to understand how this simple case works, before exploring when it is applicable. Hence, we now explain our scaling approach for the simple case.

Let us define $Q_{\text{normal}}(k)$ and $Q_{\text{magic}}(k)$, respectively, as the number of level- k normal and magic qubits. Then the above discussion of the simple case allows us to write

$$\begin{pmatrix} Q_{\text{normal}}(k-1) \\ Q_{\text{magic}}(k-1) \end{pmatrix} = \mathbf{M} \begin{pmatrix} Q_{\text{normal}}(k) \\ Q_{\text{magic}}(k) \end{pmatrix},$$

with $\mathbf{M} = \begin{pmatrix} \lambda_{\text{normal}} & b \\ 0 & \lambda_{\text{magic}} \end{pmatrix}$. (2)

This equation can be used directly to determine the qubit resources for a single level of concatenation. However, the matrix \mathbf{M} is also the key ingredient for evaluating resources with multiple levels of concatenation, as we will see next.

However, before turning to multiple concatenation levels, we recall that \mathbf{M} is only a 2×2 matrix in the simple case considered above. More generally, there can be multiple types of normal and magic qubits, for which \mathbf{M} becomes an $n \times n$ matrix with $n > 2$. Appendices B1 and B2 discuss when this occurs, and how to treat it. They show that while the mathematics for an $n \times n$ matrix \mathbf{M} is more complicated, the basic structure of the scaling approach is unchanged. Thus we proceed here to describe the scaling approach with multiple levels of concatenation in terms of the simpler 2×2 matrix.

C. Scaling with multiple level of concatenation

To calculate the physical qubit cost of a particular algorithm, we take the number of levels of concatenation, K , that achieves the desired computational precision [53]. We then iterate Eq. (2) from $k = K$ down to $k = 0$ to obtain the number of level-0 normal and magic qubits required. This gives the total number of physical qubits needed for the algorithm, as follows. At the highest level $k = K$, we have a total of $Q_{\text{total}}^{\text{algo}}$ level- K qubits — equal to the number of logical qubits needed to carry out the algorithm. Of these, $Q_{\text{magic}}^{\text{algo}} = Q_{\text{magic}}(K)$ of them participate in a level- K magic operation in the layer \mathcal{L}_{max} , while $Q_{\text{normal}}^{\text{algo}} \equiv Q_{\text{total}}^{\text{algo}} - Q_{\text{magic}}^{\text{algo}} = Q_{\text{normal}}(K)$ participate only in normal operations in layer \mathcal{L}_{max} . Here the classification of qubits into normal and magic is based on whether gate operations are normal and magic, since we assumed all state preparation and measurements in $\mathcal{C}_{\text{algo}}$ are normal operations (see Sec. III B). As level 0 (i.e., $k = 0$) corresponds to physical qubits, we have $Q_{\text{normal}}^{\text{phys}} \equiv Q_{\text{normal}}(0)$ and $Q_{\text{magic}}^{\text{phys}} \equiv Q_{\text{magic}}(0)$. So the total number of physical qubits required is $Q_{\text{normal}}^{\text{phys}} + Q_{\text{magic}}^{\text{phys}}$.

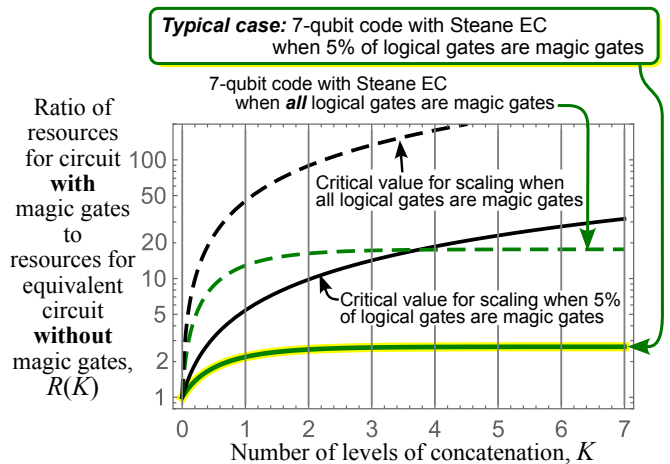


Figure 2. Ratio of resources $R(K)$ for a circuit of interest, $\mathcal{C}_{\text{algo}}$, divided by the resources for the equivalent circuit $\mathcal{C}_{\text{normal}}$ in which all level- K magic operations are replaced by normal ones; see Eq. (1). The solid lines are for a $\mathcal{C}_{\text{algo}}$ where 5% of the gates are magic operations (comparable to some real algorithms in Appendix A). The dashed lines are for a $\mathcal{C}_{\text{algo}}$ with only magic operations (an unrealistic worst-case scenario). The parameters for the green curves correspond to a typical example ($\lambda_{\text{normal}} = 294, \lambda_{\text{magic}} = 84, b = 3702$) for the 7-qubit code with Steane EC gadget; see Sec. VII B. The black curves also have $\lambda_{\text{magic}} = 84, b = 3702$, but λ_{normal} is reduced to its critical value $\lambda_{\text{normal}} = \lambda_{\text{magic}}$. We see that the 7-qubit code with Steane EC gadget is deep in the regime below criticality, which means that the proportion of resources for magic operations remains finite even as $K \rightarrow \infty$.

Then, iterating Eq. (2) from $k = K$ to $k = 0$ gives,

$$\begin{pmatrix} Q_{\text{normal}}^{\text{phys}} \\ Q_{\text{magic}}^{\text{phys}} \end{pmatrix} = \mathbf{M}^K \begin{pmatrix} Q_{\text{normal}}^{\text{algo}} \\ Q_{\text{magic}}^{\text{algo}} \end{pmatrix}. \quad (3)$$

To evaluate \mathbf{M}^K , we diagonalize \mathbf{M} in a straightforward manner. The zero in the lower-left corner of \mathbf{M} is a consequence of Assumption 1 above, and it means that the eigenvalues of \mathbf{M} are equal to its diagonal entries, λ_{normal} and λ_{magic} . We write \mathbf{M}^K in terms of its eigenvalues and eigenvectors, and find that the total number of physical qubits required is

$$\begin{aligned} Q_{\text{total}}^{\text{phys}} &\equiv Q_{\text{normal}}^{\text{phys}} + Q_{\text{magic}}^{\text{phys}} \\ &= \lambda_{\text{normal}}^K Q_{\text{normal}}^{\text{algo}} \\ &\quad + \left(\lambda_{\text{magic}}^K + b \frac{\lambda_{\text{normal}}^K - \lambda_{\text{magic}}^K}{\lambda_{\text{normal}} - \lambda_{\text{magic}}} \right) Q_{\text{magic}}^{\text{algo}}. \end{aligned} \quad (4)$$

This shows that the required physical qubit costs grow exponentially with K , as shown in Fig. 1 (accompanied by a double-exponential increase in accuracy; see Eq. 7 below).

To get a sense of excess cost due to the magic operations, we consider the quantity R from Eq. (1). In this case, the numerator of R is given by Eq. (4), while the

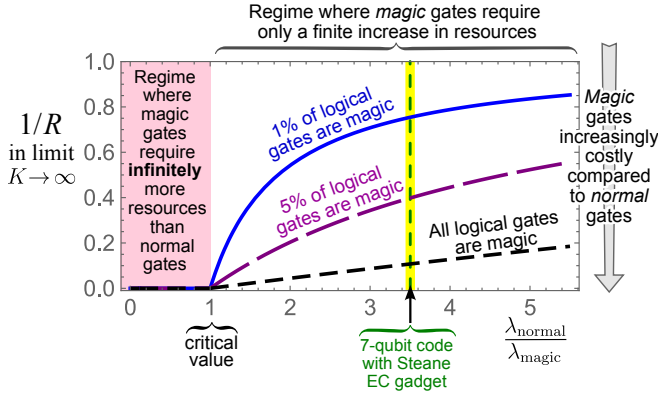


Figure 3. Analogy with a phase transition for the resource requirements in the limit of many levels of concatenation, $K \rightarrow \infty$. The role of the order parameter is played by $1/R$ on the vertical axis, with R defined in Eq. (1). Hence, “0.0” on the vertical axis means magic operations require infinitely more resources than normal operations, while “1.0” means they require the same resources. Each curve indicates the resources for a circuit with a given percentage of magic operations in the algorithmic circuit $\mathcal{C}_{\text{algo}}$. There are two regimes of behavior, with a transition between them at the critical value, $\lambda_{\text{magic}} = \lambda_{\text{normal}}$.

denominator is the same equation, but with magic operations replaced by normal operations at the logical level ($k = K$) so $Q_{\text{magic}}^{\text{algo}} = 0$ and $Q_{\text{normal}}^{\text{algo}} = Q_{\text{total}}^{\text{algo}}$. We thus have

$$R(K) = \frac{Q_{\text{normal}}^{\text{algo}}}{Q_{\text{total}}^{\text{algo}}} + \frac{b}{\lambda_{\text{normal}} - \lambda_{\text{magic}}} \frac{Q_{\text{magic}}^{\text{algo}}}{Q_{\text{total}}^{\text{algo}}} + \left(1 - \frac{b}{\lambda_{\text{normal}} - \lambda_{\text{magic}}}\right) \frac{Q_{\text{magic}}^{\text{algo}}}{Q_{\text{total}}^{\text{algo}}} \left(\frac{\lambda_{\text{magic}}}{\lambda_{\text{normal}}}\right)^K. \quad (5)$$

We note that Eqs. (4) and (5) fully describe the resource scaling for a given concatenated scheme with the above properties, and they are determined by only three circuit parameters, λ_{normal} , λ_{magic} and b as defined above.

Equation (5) tells us that R grows monotonically with K [54]; Fig. 2 shows this behavior. This monotonic behavior makes it natural to look at R in the limit of infinite K , as it will be smaller at any finite K . In this limit, the scaling behavior changes with the ratio $\lambda_{\text{magic}}/\lambda_{\text{normal}}$, and exhibits a transition at $\lambda_{\text{normal}} = \lambda_{\text{magic}}$, as seen by noting that

$$\lim_{K \rightarrow \infty} R = \begin{cases} C & \text{for } \lambda_{\text{normal}} > \lambda_{\text{magic}} \\ \infty & \text{for } \lambda_{\text{normal}} \leq \lambda_{\text{magic}} \end{cases}, \quad (6a)$$

$$\text{with } C \equiv \frac{Q_{\text{normal}}^{\text{algo}}}{Q_{\text{total}}^{\text{algo}}} + \frac{b}{\lambda_{\text{normal}} - \lambda_{\text{magic}}} \frac{Q_{\text{magic}}^{\text{algo}}}{Q_{\text{total}}^{\text{algo}}}. \quad (6b)$$

Hence, for $\lambda_{\text{normal}} > \lambda_{\text{magic}}$, the qubit cost required by magic operations grows with K but remains a finite proportion of the overall resources. In contrast, if

$\lambda_{\text{normal}} \leq \lambda_{\text{magic}}$, the excess resource required by magic operations grows without limit to become infinite when $K \rightarrow \infty$. Hence, to know if magic states will dominate the resource requirements for a given scheme at large K , one first checks if $\lambda_{\text{magic}} \geq \lambda_{\text{normal}}$.

We note that the behavior for $K \rightarrow \infty$ is reminiscent of a phase transition (one could think of $K \rightarrow \infty$ as the thermodynamic limit), with an order parameter $1/R(K \rightarrow \infty)$; see Fig. 3. When $\lambda_{\text{magic}}/\lambda_{\text{normal}}$ is below the critical value of 1, we have $1/R(k \rightarrow \infty) = 0$; when $\lambda_{\text{magic}}/\lambda_{\text{normal}}$ is above the critical value, $1/R(k \rightarrow \infty)$ is finite.

Above we did the scaling analysis in the simple case, where every normal qubit at each level k is made up from the same number λ_{normal} of level- $(k-1)$ normal qubits; similarly for the magic qubits. This can be generalized in two ways. First, λ_{normal} and λ_{magic} can have a k dependence, applicable for schemes that do not have a simple recursive rule for concatenation but a prescription for increasing the concatenation level that can differ from level to level. We can accommodate this generalization by a k -dependent \mathbf{M} matrix at each level, so that the \mathbf{M}^K on the right-hand side of Eq. (3) is replaced by the product $\mathbf{M}_1 \mathbf{M}_2 \dots \mathbf{M}_K$, with the matrix \mathbf{M}_k specifying the number of level- $(k-1)$ qubits needed for each level- k qubit.

A second generalization is possible when one has different types of normal and magic qubits that require different resources. In this situation, the simplistic case with just the two (constant) parameters λ_{normal} and λ_{magic} can be regarded as giving an upper bound on the qubit cost, if we define λ_{normal} , λ_{magic} and b to be the upper bound, over all types, on the number of level- $(k-1)$ qubits needed for the level- k normal and magic qubits [55]. However, if the resource costs of the different types differ significantly, such a simple upper bound may give a poor estimate of the actual resource cost. In this case, this is accommodated by using larger \mathbf{M} , matrices whose eigenvalues and eigenvectors must be found, leading to similar conclusions about the qubit costs as in the simple case above (see Appendix B). We will see a concrete example of this when we discuss the case of the 7-qubit concatenated scheme with flag-qubit error correction (see Sec. VII D). Thus, while both generalizations involve more parameters, the scaling behavior for the qubit cost can be derived following the same logic as in the simple case explained above.

We conclude this section with its main message, which is also one of the main messages of this work: The scaling of qubit costs as one increases the number of levels of concatenation K , depends only on a small number of parameters. In the simple case, treated fully above, these parameters are λ_{normal} , λ_{magic} , and b . These parameters fully determine the physical qubit costs required by a given concatenated fault-tolerant scheme, and allow one to write relatively simple closed-form algebraic expressions for those costs — expressions like that in Eq. (4). These, in turn, allows us to identify the relative cost of gate operations that require magic states (magic oper-

ations) to those that do not require magic states (normal operations). The only problem is that it is tedious work to extract concrete values of these parameters in a given fault-tolerant scheme. It requires studying the circuits that implement the error-correction scheme of the scheme, counting how many qubits are necessary when going from level k to level $(k - 1)$. The remainder of the paper elaborates on this for a common class of concatenated schemes, and discusses the specific examples of the 7-qubit concatenated scheme with either the Steane or flag-qubit error correction approach.

V. EVALUATING QUBIT RESOURCE COSTS FOR CONCATENATED FAULT-TOLERANT SCHEMES

The previous section described behaviors that arise for the qubit costs (quantified in terms of the number of physical qubits needed) for a given computation. However, to find the specific concatenated fault-tolerant scheme, we need to extract the parameters for the scaling approach (for example, the parameters λ_{normal} , λ_{magic} , and b). That requires understanding the detailed circuit designs for the concatenated scheme of interest.

Here, we focus on concatenated schemes that are recursively defined using the same code at every level, a general class that includes some of the most commonly discussed examples in the literature of concatenated fault-tolerant quantum computing. For such schemes, we need only specify the circuit details for how to go from level-0 to level-1 concatenation; further increase in the concatenation level is carried out by recursively replacing level-0 components by the level-1 versions.

Before we discuss the circuit designs, we first recall the notion of the quantum accuracy threshold associated with such recursive schemes. As explained earlier, in a fault-tolerant quantum computation, a given $\mathcal{C}_{\text{algo}}$, specifying a sequence of logical operations that carries out an algorithm, is built from potentially faulty physical (i.e., level-0) qubits and operations following the fault-tolerance prescription. As we increase the concatenation level k , the error probability per logical operation after k levels scales according to the formula [12],

$$p_k = \frac{1}{B^{1/t}} (B^{1/t} p_0)^{(t+1)^k}, \quad (7)$$

where t is the number of errors the underlying code corrects. Here, p_0 bounds the error probability of a physical operation, and B is a numerical constant that captures the increased complexity of the physical circuit due to the error correction (for each level of concatenation). B depends on the number of fault locations in an “exRec” for the scheme (see Ref. [12] for details) and determines the quantum accuracy threshold $p_{\text{thres}} \equiv B^{-1/t}$ below which p_k shrinks as k grows. Using this formula, we can determine the maximum concatenation level K needed to achieve a target computational accuracy, provided we

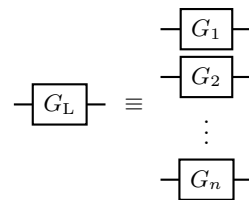


Figure 4. A transversal logical-qubit gate G_L , with $G_1, G_2, \dots \in \mathcal{G}_{\text{phys}}$ as physical single-qubit gates. Each horizontal line on the right-hand side represents a single physical qubit; the horizontal lines on the left-hand side represents a single logical qubit.

are below the threshold. Our goal here is to estimate, for a given value of K , an upper bound — hopefully, a close-to-tight one — on the number of physical qubits $Q_{\text{total}}^{\text{phys}}(K)$ needed to implement $\mathcal{C}_{\text{algo}}$ to a desired target accuracy.

Below, we begin with a review of the circuit designs for recursive concatenated schemes. We then explain how to extract the parameters of interest for characterizing the resource scaling, and specialize in the case of the 7-qubit concatenated scheme for concrete numbers. Of course, circuit designs are specific to a particular fault-tolerant scheme with its choice of underlying code. Nevertheless, there are common features, at least in the known examples so far, that allow us to come up with concrete formulas for our resource estimates below.

A. Circuit designs

We begin with the physical operations that can be performed. We assume we can do a set of physical gates $\mathcal{G}_{\text{phys}}$, prepare a physical qubit in some (usually small) set of “default” physical states $\mathcal{S}_{\text{phys}}$, as well as do measurements on the physical qubits for some (again, usually small) set of observables $\mathcal{M}_{\text{phys}}$. Each of these physical operations (gates, preparations, and measurements) are each assumed to take time τ_{phys} . In practice, of course, the different operations may take different times. For example, in many implementations, a two-qubit gate takes a longer time than single-qubit ones; measurement times can be significantly longer than gate times; preparation of different states may also take a different number of timesteps. Here, we ignore these device-dependent variabilities, and opt for the simplicity of a single time parameter τ_{phys} for all physical operations.

Next, we discuss logical gates. Below, we indicate logical operations and states with a subscript “L”. Logical gates can be separated into the normal and magic classes as discussed earlier. Again, the normal gates are those that can be done fault-tolerantly in a direct manner by applying a fixed number of gates on the data qubits; the magic operations are those whose fault-tolerant implementations require ancillary qubits prepared in a special magic state. We assume each normal gate takes a fixed

time $\tau_G \equiv g\tau_{\text{phys}}$ to complete, with g is a positive integer, assumed for simplicity to be the same for all normal gates. The prototypical example of normal gates are logical gates that can be done transversally, i.e., the logical gate is achieved by applying a physical gate to each physical qubit in the code block; see Fig. 4. In this transversal case, $g = 1$.

We assume the magic operations we need are single-logical-qubit gates, as is often the case for lower implementation demands. The normal and magic operations that we can implement fault-tolerantly together form the set of logical gates \mathcal{G}_L , which we assume to be computationally universal. Before we go on to describe how these magic operations are implemented, we need a few additional ingredients, namely, fault-tolerant measurements and preparations, as well as a circuit for the error-correction operations.

We assume that a set of logical measurements (e.g., measurement of the \bar{Z} operator) \mathcal{M}_L can be implemented as normal operations (requiring no magic states): A logical measurement in \mathcal{M}_L requires no ancillary qubits, and can be done in a fixed time $\tau_M \equiv m\tau_{\text{phys}}$, with m a positive integer. Again, a prototypical example for an element of \mathcal{M}_L is a logical measurement performed by doing transversal physical measurements, i.e., measurements from $\mathcal{M}_{\text{phys}}$ on each individual physical data qubit.

Next, we assume that a set of states \mathcal{S}_L can be fault-tolerantly prepared, but in a manner that requires the use of ancillary physical qubits to verify that the state is correctly (i.e., fault-tolerantly) prepared. Here we differentiate between physical qubits that carry the logical information — referred to as “data qubits” — and extra physical qubits — referred to as “ancillary qubits” — needed to help carry out the operations. In the verification step, the ancillary qubits interact with the data qubits carrying the (yet-to-be-verified) prepared state, and those ancillary qubits are measured to check for possible errors; see Fig. 5. The state is considered fault-tolerantly prepared only if the “pass” measurement outcome is obtained. If a “fail” outcome occurs, that copy is discarded. Of course, such a repeat-until-success strategy that may require indefinite waiting times is often difficult to incorporate; long waiting times entail more noise in the qubits waiting to interact with the ancillary state. Instead, a more practical approach is to have a parallel procedure where multiple copies of the needed state are prepared at once, so that there is a high chance that at least one copy will pass the verification. This requires extra qubits, an increase we will quantify by a “failure multiplicity” factor (see Sec. VI).

\mathcal{S}_L can contain standard logical states like $|0\rangle_L$ or $|+\rangle_L$, but also multi-physical-qubit states needed in the fault tolerance scheme. These multi-qubit states need not be logical states, and the subscript L in \mathcal{S}_L simply indicates that it contains states needed in the fault-tolerance scheme. Each round (pass or fail) of preparation of $|\psi\rangle \in \mathcal{S}_L$ requires v_ψ ancillary qubits, takes total time

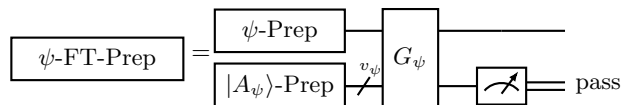


Figure 5. The method to prepare an arbitrary state $\psi \in \mathcal{S}_L$ in a fault-tolerant manner (indicated as ψ -FT-Prep). One first prepares the qubits carrying the (yet-to-be-verified) ψ state (indicated as ψ -Prep). To ensure fault-tolerance this state must then be verified via the verification step, G_ψ . This verification step requires an input made of v_ψ ancillary (physical) qubits prepared in the state $|A_\psi\rangle$ (indicated as $|A_\psi\rangle$ -Prep). These ancillary qubits are then measured after G_ψ . If the measurement result gives a “pass”, the state is fault-tolerantly prepared, and can be used as a ψ -FT-Prep state in the calculation. In contrast, if a “fail” result is obtained, the state is useless. Thus one should be running multiple such preparation circuits in parallel to ensure a very high chance that at least one of them passes verification and so generates the ψ -FT-Prep state to be used in the calculation. Note that this preparation circuit includes the circuits that give ψ -Prep and $|A_\psi\rangle$ -Prep, which states themselves require ancillary qubits. In many cases, the states being prepared are logical states (like $|0\rangle_L$ or $|+\rangle_L$); in such cases we call them $|\psi\rangle_L$ rather than ψ -FT-Prep. Thus $|\psi\rangle_L$ in Figs. 6 and 7 was prepared in the manner shown here.

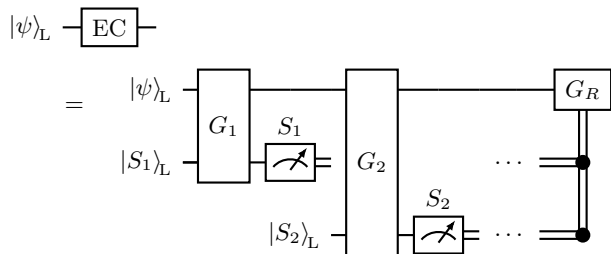


Figure 6. The circuit for a generic EC gadget acting on a state $|\psi\rangle_L$. The gadget involves I_S syndrome operators S_i sequentially, using fault-tolerantly prepared ancillary states $|S_i\rangle_L \in \mathcal{S}_L$. Each G_i gate is a sequence of d_i normal gates, and the measurement of S_i is assumed to be in the set of easily-implemented measurements, \mathcal{M}_L . The measurement outcomes are used to deduce what errors occurred and hence what recovery to apply. The recovery operation, denoted simply as G_R above, is a sequence of d_R normal gates on the physical qubits in the code block, controlled on the I_S measurement outcomes.

τ_ψ and has probability p_ψ of getting the “pass” outcome.

We also need the circuit design for the fault-tolerant implementation of the EC gadget, i.e., the circuit that implements the syndrome measurement and recovery to remove errors. Here, we assume a generic structure for the EC gadget; see Fig. 6. v_i ancillary qubits, fault-tolerantly prepared in a multi-qubit state $|S_i\rangle \in \mathcal{S}_L$, are used to measure syndrome operator S_i , for $i = 1, \dots, I_S$. We will refer to the $|S_i\rangle$ s as the “syndrome states”. The I_S syndrome operators are measured sequentially as shown in the figure, with each G_i comprising a sequence of d_i normal gates, and thus taking time $d_i\tau_G = d_i g\tau_{\text{phys}}$

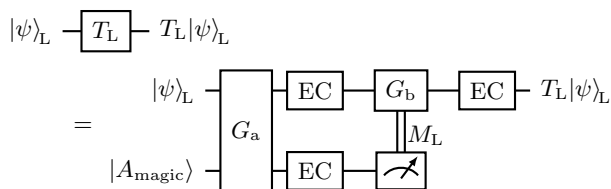


Figure 7. Magic-state implementation of a magic operation T_L on the input logical state $|\psi\rangle_L$ via the use of a magic state $|A_{\text{magic}}\rangle \in \mathcal{S}_L$. G_a and G_b are normal gates, and $M_L \in \mathcal{M}_L$. The G_b gate is applied controlled on the measurement result of M_L . Each horizontal line here is a logical qubit, and the boxes marked “EC” are the EC gadgets of Fig. 6.

to complete. The recovery operation G_R is then performed, using normal gates only, depending on the measurement outcomes. Note that the syndrome operators S_i need not be the check operators for the code; instead, in some EC-gadget designs, a single measured syndrome operator can yield the results of multiple check operators at once. Note also that, since the syndrome states come from \mathcal{S}_L , their fault-tolerant preparation is non-deterministic, and one requires again multiple preparation attempts at the same time, to be assured of available syndrome states when they are needed for the EC gadget.

Now, we can return to the magic operations. We assume, as is the case in known schemes, a magic operation is implemented using a magic-state approach; see Fig. 7. In this approach, a magic operation T_L — a single-logical-qubit gate — is implemented using only normal gates and measurements from \mathcal{M}_L (interspersed with error correction to maintain fault tolerance), but the process consumes a resource state $|A_{\text{magic}}\rangle \in \mathcal{S}_L$ carried by ancillary qubits, a so-called “magic state” appropriate for that magic operation. In general, $|A_{\text{magic}}\rangle$ can be carried by some n_A physical qubits and need not be a logical state for the underlying code; for simplicity, however, we will assume that $|A_{\text{magic}}\rangle$ is a logical state, carried by n qubits, on which we can perform logical gates as well as error correction using same EC gadget as for the data qubits. In Fig. 10, we show the situation where G_a and G_b are each a single normal gate; this is what we will assume in our resource estimates below. More generally, G_a and G_b can be composed from a sequence of normal gates interspersed with the EC gadgets (after every normal gate).

We need an additional feature to ensure fault tolerance of the resulting circuit. As mentioned earlier, we increase the circuit concatenation by one level by replacing every physical component — a preparation, a gate, or a measurement — by its level-1 version. This level-1 version is a fault-tolerantly implementable logical counterpart of the corresponding gate (with this logical counterpart of magic operations being implemented using magic-state injection). The level-1 version is not just the corresponding level-1 version of the logical operation; it includes also the error-correction circuit for each code block involved in that operation. We use the terminology of Ref. [12]

and refer to this level-1 version (including the error correction) as a “1-Rec”. This applies for gates, preparation and measurement. Every gate in $\mathcal{G}_{\text{phys}}$ is replaced by a “1-gate-Rec”, comprising the circuit that performs the corresponding level-1 logical gate, followed by the EC gadget. Every state preparation in $\mathcal{S}_{\text{phys}}$ is replaced by a “1-prep-Rec”, comprising the fault-tolerant preparation of those states, followed by the EC gadget. Finally, every measurement in $\mathcal{M}_{\text{phys}}$ is replaced by a “1-meas-Rec”, which is simply the measurement of level-1 logical operator.

Ref. [12] showed that we can then repeat the above fault-tolerant construction to go from level-1 to level-2, thereby concatenating up to an level- K of fault-tolerant error correction. Such a “recursive simulation” gives a fault-tolerant construction at every level. To make our notation clear, we will reserve the subscript L for level-1 elements (so the earlier figures for the circuit designs are understood to be for level-1 concatenation); we will specify the concatenation level when talking about higher concatenation levels.

Finally, we need one more critical assumption about the circuit designs for fault-tolerant gate implementation: Logical normal operations are assumed to be implementable using only physical normal operations. In contrast, logical magic operations can in general also make use of physical magic operations, for example, in the preparation of the magic states. This, together with the recursive manner of concatenation, assures that Assumptions 1 and 2 of Sec. IV are valid.

B. Qubit costs for basic components

We start by evaluating the qubit costs for the basic components of the fault-tolerance scheme introduced in the previous section. The normal gates and measurements in \mathcal{M}_L require no additional ancillary qubits, and hence require no additional qubit costs. However, extra ancillary qubits are required for state preparation of elements in \mathcal{S}_L , the EC gadget and the magic operations. Let us treat these one by one, for the first level of concatenation ($k = 1$); we extend this to multiple levels of concatenation in subsequent subsections.

When evaluating the qubit costs for a given component in a concrete fault-tolerant scheme, the first step is to take that component’s circuit diagram and simply count the number of qubits (qubits carrying data plus qubits involved in ancillary states). For simplicity, we first explain this for the simple case which gave the 2×2 scaling in Sec. IV (the case in which there is only one type of normal qubit, and one type of magic qubit); we describe the generalization to other cases at the end of this section. The second step is then to account for two factors that are rarely shown in circuit diagrams, but have a crucial effect on the qubit costs. These two factors are the following.

- **Time multiplicity:** Ancillary states take multi-

ple time-steps to prepare, but must be ready when needed. Thus, at a given time-step in the calculation, one may be preparing the ancillary states for multiple subsequent time-steps. In short, if a certain type of ancillary state takes a time τ_{anc} to be prepared, but is required by the calculation at time-intervals of τ_L , then we assume that we have $r = \lceil \tau_{\text{anc}}/\tau_L \rceil$ ancillary states at the same time [56], with one such state used in the current time-step and the others being prepared for the subsequent $(r - 1)$ time-steps. We call r the ancillary state's *time multiplicity*. It takes a different value for each type of ancillary state, and its calculation is explained in Sec. VIA.

- **Failure multiplicity:** The preparation of quantum states usually requires a verification procedure to guarantee that the state has been prepared in a fault-tolerant manner before it is used. Usually, the verification of each of these μ copies requires ancillary qubits that are prepared in a specific way, interact with the qubits encoding the state, and are then measured to tell us if the state is verified or not. The states that fail verification should not be injected into the calculation, and are thrown away. Thus, whenever the circuit diagram indicates a verification of such a state, we must prepare μ copies of that state in parallel (along with the ancillary states used to verify them) to account for the fact that there is a chance that each one will fail verification. We call μ the state preparation *failure multiplicity*. It is different for each type of quantum state, because each one has a different probability of failing verification. The larger the failure probability, the larger μ must be to ensure a high enough probability for a successful verification of the state. We quantify what we mean by “high enough probability” in Sec. VIB, where we also calculate μ for different states.

Such time and failure multiplicities appear in the qubit costs required by quantum states used in state preparation, EC gadgets, and magic states. Our strategy in determining their values is to ensure that data qubits *never* need to wait mid-calculation for a verified ancillary state to become available, to avoid accumulation of errors when the data qubits are waiting. In principle, one could reduce the time multiplicity by making the data qubits wait longer between uses of ancillary states (increasing τ_L to reduce r). Similarly, one could eliminate the failure multiplicity by preparing only one quantum state for each usage, then if it fails verification, one starts preparing a new quantum state, making the calculation wait for a verified state to become available. However, such waiting times come at the cost of many more errors, and hence a worse fault-tolerance threshold (for instance in the case of ancillary states required by the EC-gadgets, or magic states). Thus, we do not consider any reductions of multiplicities that come from making data qubits

wait.

The first component to consider in any fault-tolerant scheme is the state preparation shown in Fig. 5. The fault-tolerant preparation of a state $|\psi\rangle \in \mathcal{S}_L$ carried by n physical qubits requires a verification with an additional v_ψ ancillary qubits. The number of physical qubits needed for the fault-tolerant preparation of the state $|\psi\rangle \in \mathcal{S}_L$ is thus given by

$$\lambda_\psi \equiv \mu_\psi(n + v_\psi). \quad (8)$$

where the failure multiplicity that appears here μ_ψ corresponds to preparing multiple states in parallel to account for the fact we need to verify the state $|\psi\rangle$ before use, and each one has a chance of failing verification. In contrast, there is no time multiplicity (in other words $r_\psi = 1$), because one prepares each state only once.

The next component to consider is the EC gadget shown in Fig. 6. We see that ancillary qubits are required to carry the syndrome states $|S_i\rangle \in \mathcal{S}_L$, for $i = 1, 2, \dots, I_S$. The total number of physical qubits needed to prepare and carry the syndrome states for an EC gadget is thus given by

$$\lambda_{\text{EC}} = \sum_{i=1}^{I_S} r_i \mu_i(n_i + v_i). \quad (9)$$

Here, μ_i , n_i , and v_i are, respectively, the failure multiplicity, number of physical qubits carrying the state $|S_i\rangle$, and the associated number of verification ancillary qubits for the state preparation. This counting assumes that it is impossible to re-use any ancillary qubits within the same EC gadget, e.g., none of the qubits employed in preparing $|S_1\rangle$ can be reused for preparing $|S_i\rangle$, for some $i > 1$. Such a re-use would allow one to reduce the qubit costs in the EC gadgets, but it is not possible in the examples that we consider in this work.

With this, we can already obtain an expression for λ_{normal} , the number of physical qubits needed for a level-1 normal qubit. A normal qubit, by definition, never goes through a magic operation, and it requires ancillary physical qubits only for two things: its initial fault-tolerant state preparation, and in the subsequent EC gadgets. We thus have

$$\begin{aligned} \lambda_{\text{normal}} &= \lambda_\psi + \lambda_{\text{EC}} \\ &= \mu_\psi(n + v_\psi) + \sum_{i=1}^{I_S} r_i \mu_i(n_i + v_i), \end{aligned} \quad (10)$$

with the time multiplicity r_i accounting for the qubit costs needed to run consecutive EC gadgets on the same level-1 qubit. Note that Eq. (10) is an overestimate, since, while $\mu_\psi(n + v_\psi)$ qubits are used in the preparation of the initial state, only n of them carry the state through to subsequent timesteps, leaving $\mu_\psi(n + v_\psi) - n$ ancillary qubits for re-use in later EC gadgets. However, when there are multiple levels of concatenation, the possibility for such re-use may be limited and anyway complicated to keep track of. We thus prefer the simplicity of an overestimate.

Finally, we consider a single magic gate applied on a single qubit. At level-1 concatenation, the qubit is replaced by a logical qubit carried by n physical qubits, and the physical magic gate is promoted to a 1-gate-Rec, with a logical magic gate (implemented using magic-state injection) followed by the EC gadget. We have already discussed the qubit costs for the EC gadget, so let us focus on the logical magic gate.

The magic gate requires a magic state $|A_{\text{magic}}\rangle$ for fault-tolerant implementation. Here $|A_{\text{magic}}\rangle$ is a logical state carried by n physical qubits and inside \mathcal{S}_L . Its preparation requires $v_{A;\text{prep}}$ ancillary qubits, followed by an EC gadget consisting of λ_{EC} ancillary qubits. The magic state must be verified, with a chance of failing verification, so one must add a failure multiplicity factor μ_A . The total qubit cost for $|A_{\text{magic}}\rangle$ is thus

$$\lambda_A \equiv \mu_A(n + v_A). \quad (11)$$

where $v_A = v_{A;\text{prep}} + \lambda_{EC}$. Note that including the ancillary qubits required by the EC gadget, λ_{EC} , inside v_A means that we will also throw away these qubits whenever the magic state fails verification. While it may seem an excessive over-counting of resources, in practice, an EC gadget is often used inside the actual fault-tolerant magic-state preparation circuit. This is at least the case in the schemes we study (see Figs. 11 a), and 17). It is thus natural to directly include the qubit cost for the EC gadget applied on the magic state in v_A itself. In addition, there is the qubit cost for the state carrying the data $|\psi\rangle_L$ associated with the EC gadget that must be applied after the gate operation between it and $|A_{\text{magic}}\rangle$. The qubit cost for $|\psi\rangle_L$ is thus the same as for a normal gate and given by λ_{normal} . Hence, the total qubit cost for the magic gate is

$$\lambda_{\text{magic,total}} = \lambda_{\text{normal}} + r_A \lambda_A. \quad (12)$$

The term λ_{normal} counts the physical qubits needed to prepare, carry, and protect the logical data qubit. The remaining term counts the qubits needed for the magic state, with an added time multiplicity r_A to account for the possibility of multiple magic gates applied on the same logical qubit close in time.

Now we are ready to divide the total qubit cost in Eq. (12) into two categories: normal and magic. There are only normal gates in the EC gadget, and there are only normal gates applied between the magic-state qubits and the data qubits. Hence, the only qubits in Eq. (12) that could be magic qubits are the $r_A \lambda_A$ qubits involved in the magic-state preparation. Looking at the magic-state preparation circuit allows us to identify the number of magic qubits in it, λ_{magic} , with the remaining $b = \lambda_{\text{magic,total}} - \lambda_{\text{magic}}$ qubits being normal. These are the remaining two numbers, λ_{magic} and b , needed for the scaling approach in Sec. IV.

For a concrete example of finding λ_{magic} and b , consider the 7-qubit scheme that we analyze in sec. VII. There only the n qubits carrying the magic state undergo magic

gates, all other qubits undergo only normal gates. Thus, the number of magic qubits in a magic gate is

$$\lambda_{\text{magic}} = r_A \mu_A n, \quad (13)$$

and the number of normal qubits in a magic gate is

$$\begin{aligned} b &\equiv \lambda_{\text{magic,total}} - \lambda_{\text{magic}} \\ &= \lambda_{\text{normal}} + r_A \mu_A v_A. \end{aligned} \quad (14)$$

Other schemes may give different numbers, but the principle used to identify λ_{magic} and b remains the same.

It is worth recalling that below Eq. (5), we used the fact $b > \lambda_{\text{normal}}$ to show that $R(K)$ grows monotonically with K , specifically in the regime $\lambda_{\text{normal}} > \lambda_{\text{magic}}$. Now we have all the ingredients to see why $b \geq \lambda_{\text{normal}}$. A magic gate requires us to perform normal gates on the qubits that carry the logical state, in addition to the preparation of the magic state $|A_{\text{magic}}\rangle$. Hence, b (the number of normal qubits in this magic gate) must equal the number of normal qubits in a normal gate, λ_{normal} , plus the number of normal qubits in the preparation of the magic state $|A_{\text{magic}}\rangle$. This means that $b \geq \lambda_{\text{normal}}$. Further, we assumed here that the preparation of the magic state involves an EC gadget (which requires λ_{EC} normal qubits), which means that $b \geq \lambda_{\text{normal}} + \lambda_{EC}$. Generically, b will be even larger than this because of the factors of time and failure multiplicities that appear in the preparation of the magic state. Thus it is no surprise that our examples have b larger than λ_{normal} . This has an interesting consequence for the results of the scaling approach in sec. IV; it means that generically $b/(\lambda_{\text{normal}} - \lambda_{\text{magic}})$ in Eq. (6) is notably larger than one, as we will see in our examples.

Note that to keep the logic clear here, we assumed that there is only one type of normal qubit and one type of magic qubit. More generally, there can be multiple types of both that follow different scaling rules, for example if different gates have different qubit costs, or if some ancillary states prepared to carry out a given gate have higher qubit costs than others. Then one might have j_{normal} types of level- k normal qubits, and j_{magic} types of level- k magic qubits. The scaling analysis for such a situation is described in Appendix B; it is more complicated than the simple case presented in sec. IV, but the logic is the same, so the simple case remains representative of more general cases. As a concrete example, we will see that there is one type of magic gate, but two types of magic qubits in the flag-qubit example of Sec. VII D. With multiple types of magic qubits, the b and λ_{magic} parameters have multiple components. In such a case, one can calculate each component of λ_{magic} and b by following the same recipe as above. First, one identifies the total number of qubits necessary for a given type of magic qubit, with terms coming from preparation, error correction, and verification of its magic state. Some of these terms are likely to be different for different types of magic qubits, each with a different $\lambda_{\text{magic,total}}$. Second, one separates this total into the different types of qubits, identifies the number

of each type of normal qubits (these are the components of b), and the number of each type of magic qubits (these are the components of λ_{magic}). We will discuss this more carefully in the flag-qubit example; see Sec. VII D.

C. Resources for “normal” circuits with multiple levels of concatenation

Having understood the resource costs of the basic components, we now turn to logical circuits formed from these components, beginning with “normal” circuits, namely, those that employ only normal operations. Once again, we assume all normal qubits are the same — the simple case in Sec. IV — while noting that the extension to more general cases are straightforward but tedious (using the method in App. B). In this case, as the circuit has no magic operations, we have $Q_{\text{magic}}^{\text{algo}} = 0$ and $Q_{\text{total}}^{\text{algo}} = Q_{\text{normal}}^{\text{algo}}$. We start with $K = 1$. We encode each logical qubit as a level-1 logical qubit carried by n physical qubits. Each logical qubit is prepared at the start of the computation in state $|\psi_0\rangle \in \mathcal{S}_L$ with a 1-prep-Rec, namely, the fault-tolerant preparation of $|\psi_0\rangle$ followed by the EC gadget. Each logical gate is promoted to a 1-gate-Rec, comprising a normal gate implementable in time τ_G with no need for any ancillary qubits, followed by the EC gadget.

The qubit costs are then estimated using Eq. (10), we have

$$Q_{\text{total}}^{\text{phys}} \equiv Q_{\text{total}}^{\text{phys}}(K = 1) = \lambda_{\text{normal}} Q_{\text{total}}^{\text{algo}} \quad (15)$$

for this $K = 1$ situation.

Now, for $K > 1$, we simply treat the *physical* circuit for the above $K = 1$ case as if it is the new logical circuit, set $Q_{\text{total}}^{\text{algo}}$ in the formula above to now be $Q_{\text{total}}^{\text{phys}}(K = 1)$, and then reapply the above logic. We need only check that the physical circuit after each additional level of concatenation remains a normal circuit. This is the case since logical normal operations are implemented in a fault-tolerant manner using only physical normal operations, as per our earlier assumption; the EC gadget also only employs normal operations. Every logical qubit then again requires λ_{normal} physical qubits, and we pick up one additional factor of λ_{normal} for every additional level of concatenation. Thus, for K levels of concatenation, we have

$$Q_{\text{total}}^{\text{phys}}(K) = \lambda_{\text{normal}}^K Q_{\text{total}}^{\text{algo}}, \quad (16)$$

where $Q_{\text{total}}^{\text{algo}}$ here still refers to the number of logical qubits in the original level- K logical circuit. An implicit assumption made here is that the failure and time multiplicity factors are the same for all levels $k \leq K$ of concatenation (so that λ_{normal} is a k -independent constant). This will be the case in all the concrete examples we will treat.

D. Resources for general computational circuits with multiple levels of concatenation

In the previous section, a logical circuit that contains only normal operations gives circuits that contain only normal operations at all levels of concatenation. In that case, ancillary qubits are needed only for the EC gadget, but not the gate operations themselves. For general algorithmic circuits, we will need, in addition, ancillary qubits for the magic-state preparation for any magic operations. Our resource analysis thus needs to account for those extra ancillary qubits.

Here, our goal is to give a more rigorous explanation of the formulas in Sec. IV, in terms of the details of the recursive schemes introduced above. We consider a general algorithmic circuit $\mathcal{C}_{\text{algo}}$ of the type described in Sec. III B 1, that employs $Q_{\text{total}}^{\text{algo}}$ qubits. We consider the bottleneck layer \mathcal{L}_{max} in $\mathcal{C}_{\text{algo}}$, which is the step of the logical algorithm that requires the most physical qubits. Under the assumptions explained in detail in Sec. III B 1 and Sec. IV A, this is the time-step of the logical (level- K) circuit that has the most magic gates. As in Sec. IV C, we denote by $Q_{\text{magic}}^{\text{algo}}$ the number of level- K qubits on which those magic gates are applied in layer \mathcal{L}_{max} , and set $Q_{\text{normal}}^{\text{algo}} \equiv Q_{\text{total}}^{\text{algo}} - Q_{\text{magic}}^{\text{algo}}$. For simplicity, we assume that all the magic gates have the same qubit cost given by Eqs. (13) and (14). This corresponds to the simple case in Sec. IV, while again noting that the extension to the general case is straightforward but tedious (see App. B).

We now begin with a physical circuit (this can be the unencoded algorithmic circuit, or the physical circuit at some intermediate level of concatenation) comprising a certain number of normal and magic operations, applied on a number of physical qubits. We note that a physical qubit that is acted upon only by normal operations, when promoted to a logical qubit upon concatenation, will be carried by physical qubits that undergo only normal operations (as per our earlier assumption). However, a physical qubit that undergoes a physical magic operation, at the next level of concatenation, will require $\lambda_{\text{magic, total}}$ physical qubits from Eq. (12) above, but this can be split into λ_{magic} qubits that will undergo at least one physical magic operation (see Eq. (13)), and the remaining $b \equiv \lambda_{\text{magic, total}} - \lambda_{\text{magic}}$ qubits that are acted upon by normal operations only (see Eq. (14)). Then a single step in the recursion is given by the matrix equation in Eq. (2). Thus the recursion for K levels of concatenation can be concisely written as in Eq. (3).

As explained in Sec. IV, we see that the number of physical qubits grow exponentially with K , at a speed dictated by the two eigenvalues of \mathbf{M} , namely, λ_{normal} and λ_{magic} . In our examples below, we will explore the relative sizes of the two eigenvalues, which will then determine the dominant scaling behavior, quantified by how R grows with K [see Eq. (5)].

E. This scaling approach gives an overestimate on qubit costs

Our application of the scaling approach is actually computing an overestimate of the qubit's requirements. This is because there are a few places where we make simplifying assumptions that overestimate the qubit costs of a calculation. Some of these assumptions could be improved upon within our scaling approach (at the cost of making the calculations more complicated), thereby reducing the estimate that it predicts.

As a first example of our overestimating of the qubit cost of magic-gates, we assume that a single magic gate at level- K in the layer \mathcal{L}_{\max} has the same qubit cost as doing a magic-gate at every step at level- K during \mathcal{L}_{\max} . While this may sometimes be an overestimate of the cost of magic-gates, it is not a bad estimate in our examples, for which this overestimate (solid lines Fig. 1) is within an order of magnitude of an under-estimate (dashed lines in Fig. 1) in which we assume magic qubits cost no more than normal qubits.

A second example is that we overestimate the costs when we assume that each normal qubit always requires λ_{normal} qubits, assigning the same time-multiplicity to all of them. (as outlined above, and calculated in detail below in Sec. VI A). Yet, a few of the ancillary qubits are measured earlier than others, making them available for re-use earlier. If the circuit can be designed to re-assign and re-use them as soon as they become available (which would probably require a complicated numerical optimization of the full circuit), then we would require less qubits than our scaling approach indicates. However, such optimizations are likely to be numerically heavy and highly algorithm dependent. So our feeling is that such algorithm-specific numerical optimization should only be considered after we have applied the scaling approach presented here to identify more generic optimizations, such as those identified in this article and shown in Fig. 1.

VI. MULTIPLICITY FACTORS

For a given fault-tolerant quantum computing scheme, most of the quantities that determine λ_{normal} , λ_{magic} , and b (e.g., n_A , n , v_i , etc.) come directly from the scheme's circuit designs; we show how to write them down for the 7-qubit-code scheme in Sec. VII. The time and failure multiplicity factors, r_{iS} and μ_{iS} , however, go beyond circuit designs and warrant a separate explanation of how we can determine them. We note that the considerations discussed in this section are often neglected in standard fault-tolerance analysis. As we will see below, however, they can play a significant role in properly accounting for the qubit costs of a computation, and hence warrant a careful treatment.

A. Time multiplicity

In our formulas for λ_{normal} and $\lambda_{\text{magic, total}}$, we assume that once ancillary qubits are measured, they become immediately available to be reused to prepare whatever new ancillary state is needed at that moment. We noted earlier, however, that the preparation time for these ancillary states (such as syndrome states necessary for EC gadgets or magic states necessary for magic gates) is often longer than the time between two consecutive uses of those ancillary states in the same code block. The time-multiplicity for a given type of ancillary state accounts for the additional ancillary qubits needed to prepare multiple copies of that state at the same time, to have enough of them ready for all upcoming usages. To establish the upcoming usage of ancillary states, let us recall that we want the physical qubit resources for the bottleneck layer of the algorithm, \mathcal{L}_{\max} (the moment when the algorithm requires the most physical qubits) defined in Sec. IV A. As we want to allow for any algorithm, we assume that all subsequent layers use the same number of ancillary states as the bottleneck layer, \mathcal{L}_{\max} (see Sec. IV A for details). This assumption makes the required number of ancillary states unvarying in time, greatly simplifying the calculation of the time-multiplicity.

Here, we explain in detail how to get an expression for time multiplicity r for syndrome states used in EC gadgets. The expression for the time multiplicity for other states — such as the time multiplicity for a magic state, r_A — follows the same logic.

Let us consider the preparation of syndrome states that are used in EC gadgets. We begin as usual with $k = 1$. We first count how often the EC gadget is employed for each code block. This is simply the time τ_L for the 1-gate-Rec, assumed to be for a normal gate. τ_L is given by a sum of the time τ_G for the normal gate itself and the time of the EC gadget $\sum_{i=1}^{I_S} d_i \tau_G + d_R \tau_G$, where d_i is the number of gates in the sequence that performs G_i in the EC gadget, and d_R is the number of gates in the sequence implementing G_R (see Fig. 6). The measurements of S_i s are assumed to be done in the same timestep as the subsequent gates on the data qubits within the EC gadget and hence take no extra computational time. This thus gives

$$\tau_L = \left(1 + \sum_{i=1}^{I_S} d_i + d_R \right) \tau_G \quad (17)$$

as the time between two consecutive applications of the EC gadget. τ_L tells us how often fault-tolerantly prepared syndrome states are needed.

We want to compare τ_L with the total time τ_{anc} the ancillary qubits needed in the EC gadget are in use, from the initial state preparation to their final measurement. After that time, the qubits can be reused. For simplicity, we compute τ_{anc} by considering the longest time among all ancillary qubits used in the EC gadgets (note that not all ancillary qubits carry information for the same

amount of time). From Fig. 6, we find

$$\tau_{\text{anc}} = \max_{i=1,2,\dots,I_S} (\tau_i + d_i \tau_G + \tau_M). \quad (18)$$

Here, $\tau_i \equiv \tau_{S_i}$ is the time taken for the fault-tolerant preparation of the ancillary state $|S_i\rangle$; the second term $d_i \tau_G$, as before, gives the time taken for the G_i gate in the EC gadget; τ_M is the time for the measurement of S_i in the EC gadget.

Comparing τ_{anc} and τ_L , we find that often $\tau_{\text{anc}} > \tau_L$. Then for the computation to continue uninterrupted (under the above assumption that the required number of ancillary states is unvarying in time), we need at least

$$r \equiv \lceil \tau_{\text{anc}} / \tau_L \rceil \quad (19)$$

sets of ancillary qubits at any one time [56]. Put differently, at any given moment in the computation, we need to be preparing the syndrome states for $r - 1$ future EC gadgets, as well as using syndrome states in the current EC gadget.

A similar argument gives r_A , which is the time multiplicity for the ancillary qubits carrying the magic states, and depends on the depth of circuit that prepares the magic-state. We explain how to obtain r_A in Sec. VII, using the specific example of the 7-qubit-code scheme.

Now, the above discussion was for one level of concatenation. In principle, r can depend on k . For simplicity, we remove this dependence by redefining $r \equiv \max_{k \geq 1} \lceil \tau_{\text{anc}}(k) / \tau_L(k) \rceil$, a maximum that can be found for a given fault-tolerance scheme complete with the full circuit designs [57]. We also assume we do not mix ancillary qubits, in other words we assume certain ancillary qubits are reserved for EC gadgets throughout the calculation, while others are reserved for magic-states. One can imagine lowering the qubit costs by using qubits wherever and whenever they are needed, but such a complicated orchestration can be devised only for a given scheme and a given computational algorithm, and is beyond the scope of the current paper.

B. Failure multiplicity

Let us now discuss how to compute the failure-multiplicity factors μ_{iS} and μ_A . Recall that the failure multiplicity accommodates the finite probability of failure of the verification test during the preparation of a state in \mathcal{S}_L (i.e., the initial computational state, the syndrome states, or the magic states). To avoid holding up the computation, we must prepare more copies than actually required, so that we have a good chance that at least one copy passes the verification to be used in the computation at the time of need. For this, we imagine preparing μ copies of the state every time the circuit requires a single verified copy, i.e., a copy that passes the verification. Of course, it might happen that all μ copies fail verification, and so are considered useless, and we are forced to inject one of these useless states into the circuit,

possibly causing an error. However, we face a contradiction: On the one hand, we want a μ large enough that this failure case happens only very rarely; on the other hand, it is prohibitively costly to take an extremely large μ . We hence want to find the smallest μ that is “good enough”.

To resolve this contradiction, and identify when μ is “good enough”, we note that the injection of a useless state (because all μ states failed verification) gives a potential preparation fault in the circuit, occurring with a probability given by the likelihood of all μ states failing verification. This is an additional fault location in the circuit, not counted in the standard case when μ is taken as infinite so that we never inject a useless state. This increases the total number of fault locations that determines the threshold p_{thres} [as explained below Eq. (7)], hence reducing the value of p_{thres} . This interplay between the code’s threshold, and the number of states prepared for verification, μ , has often been ignored. Some works explicitly make the assumption that there is always a prepared state that successfully passed verification when needed [12, 28]. Other studies do acknowledge the extra resources verification failure implies under simplifying assumptions, but ignore how these events modify the fault-tolerance threshold. They typically compute an average number of qubits required per verified state, relying on the law of large numbers [28, 58]. In contrast, we show below that even very large quantum circuits are not in the regime governed by the law of large numbers, and its use under-estimates qubit costs.

Now, we want the smallest μ for which the probability that all μ copies fail verification is small enough to not *significantly* reduce the fault-tolerance threshold. While we analyze the general case below, when we want precise numbers for μ , we decide that μ should take the smallest value large enough that the threshold is only reduced by 1%.

We start with the probability that a copy fails verification, and use the fact that this is upper-bounded by Np , where p is the probability of a fault per gate, and N is an upper bound on the number of locations inside the preparation and verification circuit where a single fault can lead to failed verification. Typical values of N are shown in Table I (for the examples discussed Sec. VII). If we prepare μ copies every time the circuit requires a single *verified* copy of a state, the probability we lack a verified state is the probability that all μ copies fail verification. This is upper bounded by [59]

$$p_{\text{Lack}} = (Np)^\mu. \quad (20)$$

The exRec — see below Eq. (7) — will require M such verified states [60]. Then the probability of that exRec lacking verified states is upper bounded by $M p_{\text{Lack}}$.

If all μ do fail, then one is forced to use a possibly badly prepared state in the circuit, potentially introducing an error in the quantum computation. Otherwise, with probability $> 1 - p_{\text{Lack}}$, one has a verified state to use in the circuit, and one can throw away the other

Fault-tolerant scheme	State being prepared	Circuit diagram	N ^o of fault locations per verification, N	Verification failure probability $\leq Np_{\text{thres}}$	N ^o of verifications per exRec, M	Failure multiplicity <i>without</i> shared prep.	Failure multiplicity <i>with</i> shared prep.
Steane approach	$ 0\rangle$ or $ +\rangle$	Fig. 5	50	$\leq 0.10\%$	8	$\mu_{0/+} = 3$	$\mu_{0/+} = 1.16$
	$ A_{\pi/4}\rangle$	Fig. 11	521	$\leq 1.0\%$	8	$\mu_{\Lambda} = 4$	$\mu_{\Lambda} = 1.30$
	$ \text{Rep}\rangle$	Fig. 11c	17	$\leq 0.034\%$	8	$\mu_{\text{Rep}} = 2$	$\mu_{\text{Rep}} = 1.13$
Flag-qubit approach	$ 0\rangle$ or $ +\rangle$	Fig. 15	36	$\leq 0.072\%$	1	$\mu_{0/+}^{\text{flag}} = 3$	$\mu_{0/+}^{\text{flag}} = 1.19$
	$ H\rangle$	Fig. 17	$\approx \sqrt{\frac{2}{p_{\text{thres}}}} = 316$	$\leq 0.63\%$	1	$\mu_H^{\text{flag}} = 4$	$\mu_H^{\text{flag}} = 1.31$

Table I. A list of the parameters needed to evaluate failure probability and failure multiplicity for the 7-qubit code examples considered in Sec. VII. In all cases we assume the physical error probability per gate to be $p_0 < p_{\text{thres}} = 2 \times 10^{-5}$. We identify M as the number of such verified states needed in whichever exRec requires the most such verified states. For Steane EC gadgets, the exRec with the maximum number is that of the CNOT, with $M = 8$. For flag-qubits, the only verification is a single one needed in the preparation of $|H\rangle$ or $|0/+ \rangle$, so $M = 1$. The probability that any exRec lacks a verified state is then upper bounded by Mp_{Lack} ; see below Eq. (20). For the 7-qubit code with the Steane approach, $|0\rangle$ or $|+\rangle$ are required for all gates (normal and magic), while $|A_{\pi/4}\rangle$ and $|\text{Rep}\rangle$ are only required for magic gates. The failure probabilities (upper bounded by Np_{thres}) are relatively small (1% or less). Yet they are much too big for a successful fault-tolerant quantum computation. This is why we need to prepare multiple copies of a state to ensure that the probability p_{Lack} of all μ copies failing is many orders of magnitude smaller. For the 7-qubit code with the flag-qubit approach, $|0\rangle$ or $|+\rangle$ are required for all gates (normal and magic), while $|H\rangle$ is only needed for magic gates. The failure multiplicity without shared state-preparation (labeled “without state prep.”) is the smallest integer satisfying Eq. (27) for $\kappa = 1\%$. The last column uses the approach in Sec. VIC that shares state preparation for a group of 100 gates. In this case, the failure multiplicity drops to fairly close to one.

$(\mu - 1)$ copies. Throwing away the other $(\mu - 1)$ copies is wasteful, since many may have passed verification, but it keeps the algebra simple; we will be less wasteful in Sec. VIC.

Verification failure is a source of errors usually ignored in standard treatments of fault-tolerant quantum computing, which assume, for simplicity, that the circuit *never* lacks verified states, implicitly assuming that $\mu \rightarrow \infty$. To incorporate verification failure in the description, it is useful to recall how the Eq. (7) is derived. We do this here for the situation where the code underlying the fault-tolerant quantum computing scheme corrects $t = 1$ error; it is straightforward to generalize the analysis below to $t > 1$. We begin with p_k , which is the upper bound on the probability of error for a logical gate after k levels of concatenation. For $\mu \rightarrow \infty$ (and $t = 1$), we have

$$p_{k+1} = Bp_k^2, \quad (21)$$

The right-hand side of Eq. (21) is the probability that there is an error that the circuit cannot correct. Such an uncorrectable error comes from at least a pair of faults in the exRec of interest (namely, the largest one, which hence determines the threshold), and B is primarily the number of such pairs that are malignant (i.e., causes an uncorrectable error in the end), corrected to account also for uncorrectable errors from more than two faults in the circuit. The error probability per logical gate operation after k levels of concatenation is then

$$p_k = \frac{1}{B}(Bp_0)^{2^k}, \quad (22)$$

which corresponds to Eq. (7) for the case considered here with $t = 1$. This gives the usual fault-tolerance threshold that requires that $p < p_{\text{thres}} \equiv 1/B$, for p_k to decrease with increasing k .

The above analysis was for $\mu \rightarrow \infty$. For finite μ , Eqs. (21) and (22) must be modified to account for errors that come from the lack of verified states to inject at the relevant moment. This is another source of uncorrected errors that must be added to the right-hand side of Eq. (21), so that we have

$$p_{k+1} = Bp_k^2 + Mp_{\text{Lack}}. \quad (23)$$

We want the value of μ for which the additional contribution from the Mp_{Lack} term is *no worse* than a small reduction of the threshold from $1/B$ to $1/[(1 + \kappa)B]$ for small κ (below we choose $\kappa = 0.01$). In other words, we want

$$Bp_k^2 + Mp_{\text{Lack}} \leq (1 + \kappa)Bp_k^2. \quad (24)$$

This would guarantee that $p_{k+1} \leq (1 + \kappa)Bp_k^2$, meaning that the error per logical gate operation after k levels of concatenation would obey

$$p_k \leq \frac{(B(1 + \kappa)p_0)^{2^k}}{B(1 + \kappa)}. \quad (25)$$

In this case, the logical error rate after k levels would be about the same as if one never lacked verified states but the inverse of the threshold, B is larger by a factor of κ . If we take $\kappa = 1\%$, then this can be interpreted in an approximate way as follows: A quantum computer with

μ satisfying Eq. (26) is about as reliable as a quantum computer with infinite μ (so it never lacks verified states) but with a physical error probability about 1% higher. So, if one can reduce the physical error probability by about 1%, one has compensated for μ not being infinite.

To find the value of μ that ensures Eq. (24) holds for a chosen κ , we substitute in Eq. (20) and rearrange it to get the inequality

$$\mu \geq \frac{2 \ln[1/p_k] + \ln[1/\kappa] - \ln[B] + \ln[M]}{\ln[1/p_k] - \ln[N]}. \quad (26)$$

In the regime of interest ($p_k < p_0 < p_{\text{thres}} \equiv 1/B$), the right-hand side of Eq. (26) decays monotonically as we reduce errors, so will never exceed the value given by replacing p_k by p_{thres} . Hence, to be sure Eq. (26) is satisfied for any p_k of interest, it is sufficient to satisfy it when p_k is replaced by p_{thres} . Then, Eq. (26) becomes

$$\mu \geq \frac{\ln[MB/\kappa]}{\ln[B/N]}. \quad (27)$$

Of course, μ must be an integer, and we will take it to be the smallest integer satisfying this inequality.

As the right-hand side of Eq. (27) only depends logarithmically on B , κ , M , and N , it only depends weakly on the exact choice of these parameters. To get a feeling for the typical values of μ given by Eq. (27), we can look at the column of Table I labeled “Failure multiplicity without shared prep.”. It gives μ for the N and M typical of states in the two fault-tolerant schemes considered in Sec. VII, assuming we want $\kappa = 1\%$. The important thing we learn from this is that these failure multiplicities are typically fairly small integers (typically two, three or four). So one can expect that each time one requires a single verified state, one must prepare between two and four copies of that state for verification. In principle, μ can depend on k , but we neglect that here. To be rigorous, we can say that we take the largest μ over all k values, and use that value for all k , thereby overestimating this failure multiplicity μ .

C. Lowering the failure multiplicity by sharing state preparation

In the previous section, we assume that each time we need a verified copy of a state at a given place in the circuit, we prepare μ copies of that state, but in the end, we discard all but one copy for use in the actual circuit. This is extremely wasteful, because the majority of those discarded states also successfully passed verification. We will show here that it is vastly less wasteful if we created a shared reservoir of each type of state that needs to be prepared, do verification on each of them, and then distribute those that successfully passed verification to where they are needed (while throwing away those that fail verification). If the probability that each state is verified is of order $(1 - Np_{\text{thres}})$, then the “law of

large numbers” means that you might immediately guess that when preparing a very large number of copies, one only needs to prepare a bit more than $1/(1 - Np_{\text{thres}})$ unverified copies for every verified state needed, implying a failure multiplicity $\sim 1/(1 - Np_{\text{thres}})$, which is clearly much smaller than without sharing. Unfortunately, this sort of “large-number” arguments are too simplistic for finite numbers (e.g., it cannot tell us what happens if we need only 100 verified states, thus we treat the problem differently here. However, as we explain below, we do reach the conclusion that sharing the preparation of verified states in this manner greatly reduces the failure multiplicity.

To see how much it can reduce the failure multiplicity in practical situations, one can compare the last two columns of Table I, and note that sharing state preparation can reduce failure multiplicities from 4 to less than 1.3 [61]. As we will see, the reduction is based on a simple argument that overestimates the failure multiplicity for shared resources, so one can hope it could be even smaller. However, it cannot be smaller than one, so this already gives us a good idea of its order of magnitude.

To be more precise, we note that in a typical computation, multiple verified copies of the *same* state will be needed at different parts of the circuit at the same time. For example, every single level- k qubit experiences an EC gadget at the same moment, so a vast number of verified ancillary states will be used at the same time for the EC gadgets. To a lesser extent, in a large quantum computer, a large number of qubits will be undergoing a magic gate at the same time, so many qubits will require verified magic states at the same time. It is thus natural to consider sharing resources between all those gates that require the same type of verified states in the same time-step.

We imagine that copies of a state are produced and verified centrally in a state-preparation factory, often called an *ancilla factory*. This factory prepares and verifies as many copies as necessary (throwing away those that fail verification) to ensure that it produces enough *verified* states to distribute to all parts of the circuit in need of such a state at that timestep. This, of course, assumes the possibility of long-range gates or transport for distributing the states across the circuit, but long-range gates are usually already a requirement for implementing concatenated schemes, and this also fits well with architectures that have different zones for different computational functions (e.g., in the recent neutral-atom experiments [62]).

Let us try to estimate the resource savings arising from such a shared state-preparation factory. Suppose we need V verified copies of a state in a given timestep. For that, we prepare $V + S$ copies, each of which has a probability Np of failing the verification. We define $p_{\text{Lack}}^{\text{Share}}$ as the probability that we are short of copies that pass the verification, and are hence forced to use at least one failed copy, possibly introducing an error into our computation. We want to understand how large S has to be, to assure

a small enough $p_{\text{Lack}}^{\text{Share}}$. If the EC gadgets of two logical gates (gates i and j) use states coming from the same shared ancilla factory, if the logical gate i lacks a verified state, it is more likely that the logical gate j will also lack a verified state: the events are correlated, making the gate failure correlated. These correlations complicate the analysis.

Here, we prefer to simplify the analysis by making simple overestimates. These overestimates will be enough to show that sharing resources reduces the failure multiplicity to fairly close to one for reasonable values of V , for practical values of the maximum concatenation level K (we assume that K does not exceed 5 in practical situations). Our simplification is to decide that it is enough to find the value of S that ensures that $p_{\text{Lack}}^{\text{Share}}$ is so extremely small that there is a probability close to one that the whole calculation occurs without any gate-operation (at any level of k) in that calculation lacking a verified state. A lack of verified states only occurs if $S + 1$ of the $V + S$ copies fail verification. Hence, $p_{\text{Lack}}^{\text{Share}}$ is the probability that more than S of the $V + S$ copies of the state fail verification. We take the probability that each copy fails verification as Np . Then we can see, using the binomial distribution, that

$$p_{\text{Lack}}^{\text{Share}}(S, p) = \sum_{l=S+1}^{V+S} \binom{V+S}{l} (Np)^l (1-Np)^{V+S-l}. \quad (28)$$

This is in fact a slight overestimate of $p_{\text{Lack}}^{\text{Share}}(S, p)$, because Np is a slight overestimate of the probability that a copy fails verification (just as in Sec. VIB above). We now make another overestimate: We replace p by p_{thres} in Eq. (28), and work with $p_{\text{Lack}}^{\text{Share}}(S, p_{\text{thres}})$ from now on. Since $p \leq p_{\text{thres}}$, we know that $p_{\text{Lack}}^{\text{Share}}(S, p_{\text{thres}})$ is a significant overestimate of the probability of lacking a verified state. This means that when we next impose an upper bound on $p_{\text{Lack}}^{\text{Share}}(S, p_{\text{thres}})$, we are safe in the knowledge that the true probability to lack a verified copy of the state is smaller.

We now require that $p_{\text{Lack}}^{\text{Share}}$ is so small that there is only a small chance κ of lacking a verified state of a given type in the whole calculation, when $p = p_{\text{thres}} \equiv 1/B$. The probability to lack a verified state (of any type) in the whole computation is upper bounded by $\alpha \kappa$, where α is the number of different types of verified states needed in the computation (e.g., $\alpha = 4$ for the example discussed in Sec. VII B, with the four types of verified states being $|0\rangle$, $|+\rangle$, $|A_{\pi/4}\rangle$, and $|\text{Rep}\rangle$). To ensure that $p_{\text{Lack}}^{\text{Share}}$ is small enough for a state of type ν , we need to choose the number of spares for that type of states, S_ν , to be large enough to ensure that the probability to lack type ν states $p_{\text{Lack};\nu}^{\text{Share}}(S_\nu, p_{\text{thres}})$ obeys

$$p_{\text{Lack};\nu}^{\text{Share}}(S_\nu, p_{\text{thres}}) \leq \frac{\kappa}{N_{\text{states}}^{(\nu)}}, \quad (29)$$

where $N_{\text{states}}^{(\nu)}$ is the number of type ν states required in the whole calculation.

Now, we note that the following inequality holds:

$$N_{\text{states}}^{(\nu)} < KM N_{\text{gates}}^{\text{level-1}}, \quad (30)$$

where $N_{\text{gates}}^{\text{level-1}}$ is the total number of gates in the entire algorithm at level 1. This inequality is based on two observations. The first observation is that the number of verified states needed at level-1 concatenation is larger than at any other levels. This is because the number of verified states needed scales like the number of gates, and so grows exponentially as one goes down the concatenation levels towards the physical level; yet the physical level (level 0) itself requires no verified states. So the total number of verified states required must be much fewer than K times the number required at level 1. The second observation is that the number of verified states required at level 1 must be fewer than $M N_{\text{gates}}^{\text{level-1}}$. Inequality (30) overestimates $N_{\text{states}}^{(\nu)}$, but it allows for a simple sufficient bound: We assume we choose the smallest S_ν that ensures that

$$p_{\text{Lack};\nu}^{\text{Share}}(S_\nu, p_{\text{thres}}) \leq \frac{\kappa}{KM N_{\text{gates}}^{\text{level-1}}}, \quad (31)$$

since any S_ν that satisfies this will easily satisfy Eq. (29). We then use this S_ν to get the failure multiplicity for states of type ν as

$$\mu_\nu = \frac{V + S_\nu}{V}, \quad (32)$$

where we recall that V is the number of verified states we want to produce at a given timestep.

For a given fault-tolerant quantum computing scheme, it is fairly easy to get reasonable estimates of V , M , K and $N_{\text{gates}}^{\text{level-1}}$. We do not need rigorous values; we simply need to show that there is a clear advantage in sharing resources and how it can significantly reduce the value of μ to something fairly close to 1. We give a worked example for the case of the 7-qubit code scheme with Steane EC gadgets in Sec. VII C. It is more involved to estimate the number of level-1 gates, $N_{\text{gates}}^{\text{level-1}}$, in a circuit with K levels of concatenation, however the concatenated structure means that it should be well approximated by the number of physical gates (level-0 gates) in a circuit with $(K - 1)$ levels of concatenation, and this number scales, at worst, like $Q_{\text{total}}^{\text{phys}}(K - 1) \times D^{K-1} \times 2D_L$. Here $Q_{\text{total}}^{\text{phys}}(K - 1)$ is the number of physical qubits for $(K - 1)$ concatenations, and $D^{K-1} \times 2D_L$ is the physical circuit depth for $(K - 1)$ concatenations, where D_L is the algorithm's depth and D is how the physical circuit depth increases with each concatenation level. The factor of 2 in front of D_L acknowledges the fact that a magic gate in $\mathcal{C}_{\text{algo}}$ takes two logical-step to be implemented, as shown in Fig. 7 (we implement two normal gates G_a and G_b to perform state injection) [63]. These quantities ($Q_{\text{total}}^{\text{phys}}$, D and D_L) are all accessible for a given calculation with a given fault-tolerant scheme, as we will show in sec. VII, allowing us to find μ_ν in such cases.

Note that, formally, as K increases, the right-hand side of Eq. (31) vanishes. Hence, satisfying the inequality requires increasingly large S_ν , as K increases. However, we consider $K = 5$ (or fewer) for conceivable middle-term computers [64], and we will see in the examples that S_ν remains small enough for $K = 5$ that μ_ν is fairly close to one.

We conclude this section on sharing resources by recalling that it contains big overestimates of both the likelihood of lacking verified states, and the consequential danger for the results of a calculation. Despite these overestimates, we find that when sharing resources for reasonable parameters in the specific examples that we consider, the failure multiplicity drops to fairly close to one (see examples in the last column of Table I). As these multiplicity factors cannot be below one, our overestimates nevertheless provide fairly tight bounds on the true failure multiplicity values for shared resources.

VII. EXAMPLE: THE 7-QUBIT CODE SCHEME

As a concrete example, we look at the well-studied concatenated fault-tolerance scheme built upon the 7-qubit code; see Ref. [12] for the full description of the scheme. The underlying 7-qubit code is a Calderbank-Shor-Steane (CSS) stabilizer $[[n, k, d]] = [[7, 1, 3]]$ (n physical qubits encoding k logical qubits, with distance $d \equiv 2t + 1$, and hence corrects t errors) code. The two-dimensional code space — the logical qubit — is the $+1$ joint eigenspace of the stabilizer group generated by the set of X -type operators $\mathcal{X}_{\text{gen}} \equiv \{IIIXXXX, IXXIXXI, XIXIXIX\}$ and the Z -type version $\mathcal{Z}_{\text{gen}} \equiv \mathcal{X}_{\text{gen}}(X \rightarrow Z)$. The logical X and Z operators can be taken to be $XXXXXXX$ and $ZZZZZZZ$, respectively. The code corrects arbitrary errors on a single one of the seven physical qubits carrying the logical qubit: Pauli X errors are diagnosed by the X -type operators and Z errors by the Z -type operators; Y errors are considered as simultaneous X and Z errors; any single-qubit error can be written as a linear combination of X , Y , and Z errors and are hence correctable by the code. The error diagnosis involves the nondestructive (through the use of ancillary qubits) measurement of the \mathcal{X}_{gen} and \mathcal{Z}_{gen} operators. The measurement results (the syndromes) uniquely identify the qubit with the error and the type of error (X , Y , or Z). The recovery for this code can be performed “virtually”, via what is known as a Pauli-frame rotation, so that no actual quantum gates need to be carried out. This means that $d_R = 0$ (see Fig. 6) for this code.

A. Circuit designs

To analyze the qubit costs for this scheme, we need the detailed circuit designs for the 7-qubit code scheme. Here, we simply reproduce the designs devised

in Ref. [12], leaving the reader to refer to the original paper for the reasoning behind those designs.

We begin with the physical operations that can be performed. We make the common assumption that we can do six physical gates: the single-qubit Hadamard gate, $H \equiv \frac{1}{\sqrt{2}}(|+\rangle\langle 0| + |-\rangle\langle 1|)$; the phase gate, $S \equiv \exp(-i\frac{\pi}{4}Z)$; its Hermitian conjugate S^\dagger ; the two-qubit controlled- X gate, $\text{CNOT} \equiv |0\rangle\langle 0| \otimes \mathbb{1} + |1\rangle\langle 1| \otimes X$; the T -gate, $T \equiv \exp(-i\frac{\pi}{8}Z)$, and its Hermitian conjugate T^\dagger . These form the set $\mathcal{G}_{\text{phys}}$. H , S , and CNOT together generate the Clifford group of operations; adding the T -gate (and T^\dagger) gives full universality over qubit operations. In addition, we assume we can prepare a physical qubit in the states $|0\rangle$ and $|+\rangle$ — these form the set $\mathcal{S}_{\text{phys}}$ — and that we can do a physical Z measurement or a physical X measurement, giving $\mathcal{M}_{\text{phys}}$. Each of these physical operations is assumed to take time τ_{phys} to complete.

Many logical operations for the 7-qubit code can be done transversally, automatically ensuring their fault tolerance. The code admits transversal constructions of the logical H and S , i.e., the logical gate is achieved by applying physical gates to individual physical qubits. The logical CNOT is also transversal, composed from physical CNOT gates acting on corresponding pairs of physical qubits in the two code blocks. H , S , and CNOT are hence all normal gates, and since they generate the whole Clifford group, any Clifford operation is a normal operation. The measurement of the logical Z operator is transversal as well: It can be achieved by measuring the physical Z operator on each of (a subset of) the physical qubits (e.g., qubits 1, 2, and 3) and then classically computing the parity of the measurement outcomes. The same is true of the logical X measurement.

The fault-tolerant procedure for preparing the logical $|0\rangle$ state is given in Fig. 8. The circuit that verifies this state (necessary for a fault-tolerant procedure) is shown in Fig. 8(a); it takes as input two copies of the unverified state $|0\rangle_L$ -Prep prepared by the circuit in Fig. 8(b). One can fault-tolerantly prepare a logical $|+\rangle$ with the same procedure, except that we need an $X \leftrightarrow Z$ transformation; this simply swaps the roles of the target and control for every CNOT gate, every Z measurement becomes an X measurement, and the preparation of each physical $|+\rangle$ becomes a preparation of a physical $|0\rangle$ (and vice-versa) [12]. Each attempt at preparing the logical $|0\rangle$ or $|+\rangle$ state thus takes exactly the same number of qubits, gates, measurements, and timesteps.

We also need the circuit design for the fault-tolerant implementation of the error-correction gadget. Here, we consider two different circuit designs: the Steane EC gadget in Fig. 9 from Ref. [12], and the flag-qubit EC circuit in Fig. 16 [41]. The Steane EC gadget requires the syndrome states $|0\rangle_L$ and $|+\rangle_L$, used to detect X and Z errors, respectively, in the data-carrying block. The CNOT gates followed by the X and Z measurements together measure the stabilizer generators of the 7-qubit code, which allow for diagnosis of the errors in the data. As mentioned earlier, the recovery operation is done only

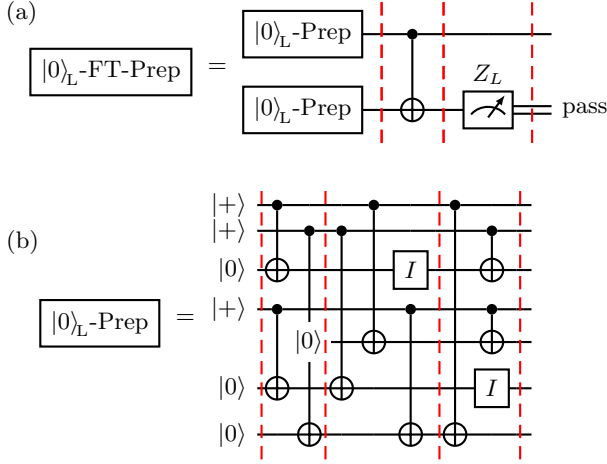


Figure 8. Fault-tolerant preparation of the logical (level-1) $|0\rangle$ state [12]; the logical $|+\rangle$ state is prepared using the same circuits, except for an $X \leftrightarrow Z$ transformation (see main text). (a) A verification step, involving two (unverified) copies of $|0\rangle_L$ (indicated in the figure as $|0\rangle_L$ -Prep), is carried out to assure fault tolerance. A logical $|0\rangle$ (indicated as $|0\rangle_L$ -FT-Prep) is successfully prepared if the measurement result gives a “pass”; if a “fail” result is obtained, the entire preparation procedure is repeated. (b) The circuit to prepare $|0\rangle_L$ -Prep, with $|0\rangle$ and $|+\rangle$ as physical states.

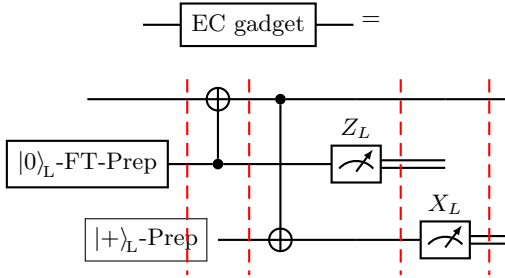


Figure 9. The Steane error-correction (EC) gadget for the 7-qubit code. Two logical ancillary states are fault-tolerantly prepared in $|0\rangle_L$ and $|+\rangle_L$ (see Fig. 8 for the preparation procedure). They interact with the data block (top line) via logical CNOTs (which are transversal) and are measured in the Z_L and X_L bases (again, transversally), respectively. The measurement outcomes are the syndrome results used for error correction.

virtually. Comparing Fig. 9 and the earlier general Fig. 6, we see that $I_S = 2$, with $S_1 = X_L$, $S_2 = Z_L$, $d_1 = d_2 = 1$, and $d_R = 0$.

The logical universal gate-set for the 7-qubit code is completed by a logical T -gate. We will find it useful to also be able to implement the logical T^\dagger -gate. Both can be done via the magic-state approach, in fact, with the same magic state $|A_{\text{magic}}\rangle$. The T and T^\dagger gates are hence the magic gates in this scheme. We first recall the magic-state implementation of a *physical* T gate [12], employs only Clifford operations (S , CNOT, and a Pauli- Z measurement) but consuming the magic state

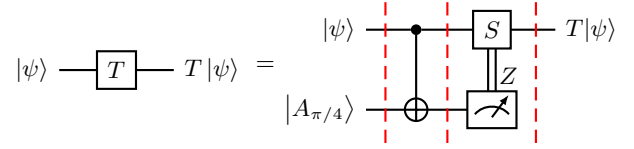


Figure 10. Implementation of a T -gate on the single-qubit input $|\psi\rangle$ via the use of the magic state $|A_{\pi/4}\rangle$.

Fault-tolerant scheme	State being prepared	Time multiplicity
Steane approach	syndrome	$r_s = 3$
	$ A_{\pi/4}\rangle$	$r_A = 3$
	$ \text{Rep}\rangle$	$r_{\text{Rep}} = 2$
Flag-qubit approach	syndrome	$r_s^{\text{flag}} = 2$
	$ H\rangle$	$r_H^{\text{flag}} = 2$

Table II. The time multiplicity for the various states discussed in the examples in this work. In Sec. VII B [around Eq. (34)], the details on how r_A can be determined is provided as an example.

$|A_{\pi/4}\rangle \equiv T|+\rangle$, where $|+\rangle \equiv \frac{1}{\sqrt{2}}(|0\rangle + |1\rangle)$; see Fig. 10. To promote this to an implementation of a logical T -gate, we replace every physical qubit in Fig. 10 by a logical qubit, every physical operation is replaced by its 1-Rec version, and the physical magic state is replaced by a fault-tolerantly prepared logical state, $|A_{\pi/4}\rangle_L$ -FT-Prep. The procedure for preparing $|A_{\pi/4}\rangle_L$ -FT-Prep is given in Fig. 11, which involves verification steps that employ verified “cat” states. Using the fact $T^\dagger = S^\dagger T$, the T^\dagger gate can be implemented with the same circuit as Fig. 10 with an extra S^\dagger applied on the top qubit at the end of the circuit. This S^\dagger can in practice be incorporated in the classically controlled operation so that if the magic state collapses to $|0\rangle$, S^\dagger is implemented and if it collapses to $|1\rangle$, no gate is applied. Importantly, S^\dagger can then be implemented transversally in the 7-qubit code and is hence a normal gate.

B. Evaluating qubit costs with the Steane EC gadget

With the circuit designs in place, we can now apply our earlier formulas for qubit costs to this 7-qubit example. We begin with the case where the EC gadget is done using the Steane EC circuit. To proceed, we take the circuits in Figs. 8-11 for the 7-qubit code with Steane EC gadgets, and combine them all into the simplified sketches in Fig. 12, where all circuit details irrelevant to the evaluation of qubit costs have been removed. Next to each part of the circuit, we indicate the number of qubits needed, allowing us to simply read off the qubit costs for the normal and magic qubits.

We now need Eqs.(8)–(10), (13), and (14), which we

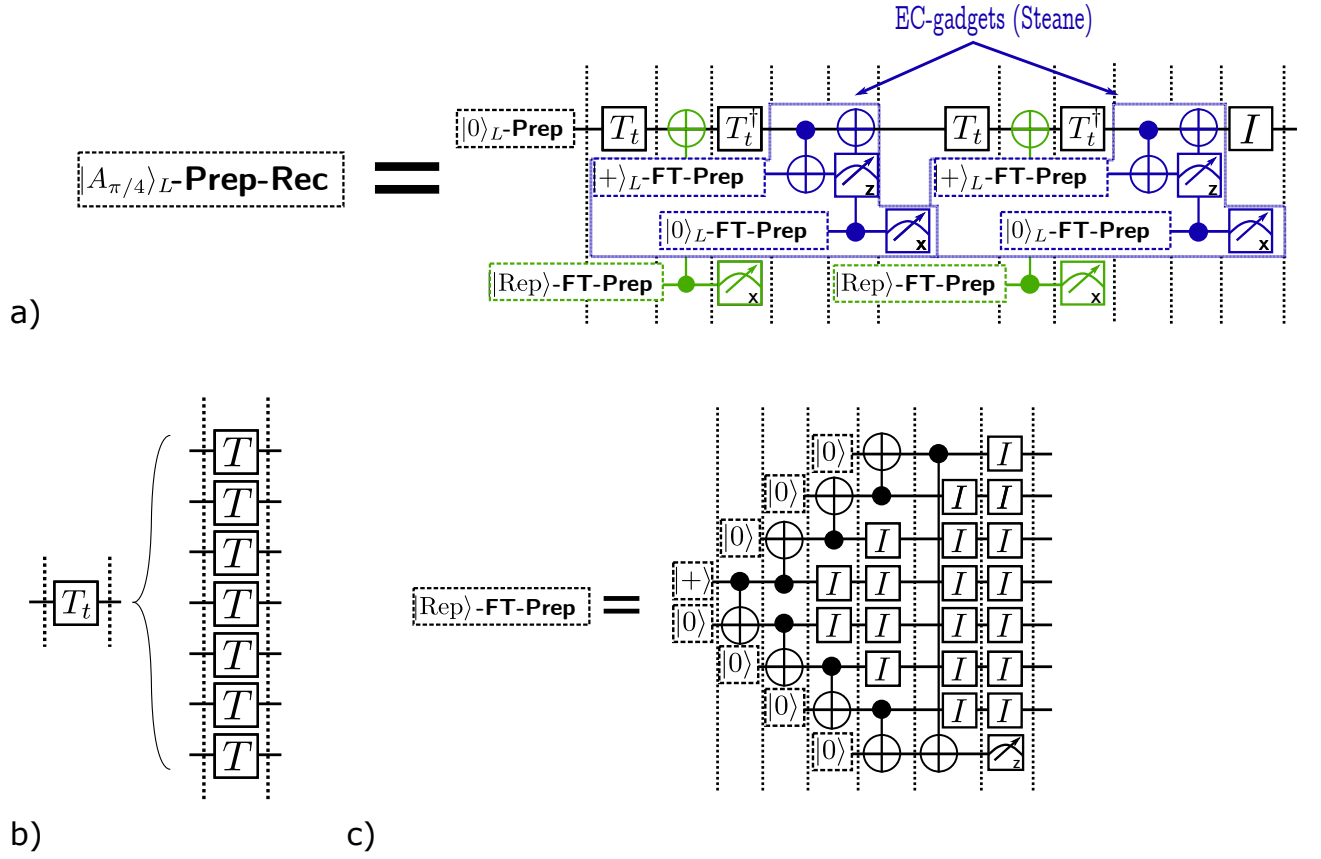


Figure 11. Magic-state preparation circuits for the 7-qubit code with Steane EC gadgets. (a) The 1-prep-Rec of the state $|A_{\pi/4}\rangle$ from Ref. [12] (indicated as $|A_{\pi/4}\rangle_L$ -Prep-Rec). Each horizontal line represents a logical qubit encoded in the 7-qubit code, with the exception of the two green lines connected to the $|\text{Rep}\rangle$ -FT-Prep boxes: Those represent logical qubits in the state $|\text{Rep}\rangle \equiv (|0\rangle^{\otimes 7} + |1\rangle^{\otimes 7})/\sqrt{2}$, the logical-+ state of the 7-qubit repetition code (sometimes called the cat state [12]). The gadgets drawn in green measure the logical observable TXT^\dagger on the top qubit (which eventually carries the magic state) through the use of the transversally defined T_t and T_t^\dagger gates [see (b)]. The first measurement projects the top qubit into the TXT^\dagger eigenstates $|A_{\pi/4}\rangle$ or $Z|A_{\pi/4}\rangle$; the latter can also be used for the T -gate [65]). The two Steane EC gadgets (in blue) and a second green gadget provide verification for a fault-tolerant preparation: The magic state passes the verification only if trivial syndromes are detected by the two EC gadgets, and if both measurements of TXT^\dagger give the same outcome (see Ref. [12]). (b) The definition of the gate T_t used in circuit in (a). (c) Fault-tolerant preparation of the state $|\text{Rep}\rangle$. In addition to the 7 qubits carrying $|\text{Rep}\rangle$, an extra qubit is used for verification: The state passes verification only if the Z measurement on that eight qubit gives +1.

reproduce here as

$$\begin{aligned}
 \lambda_{\text{EC}} &= \sum_{i=1}^{I_S} r_i \mu_i (n_i + v_i) \\
 \lambda_\psi &= \mu_\psi (n + v_\psi) \\
 \lambda_{\text{normal}} &= \lambda_\psi + \lambda_{\text{EC}}, \\
 \lambda_{\text{magic}} &= r_A \mu_A n, \\
 b &= \lambda_{\text{normal}} + r_A \mu_A v_A
 \end{aligned} \tag{33}$$

For the 7-qubit code, we have $n = 7$, and $v_\psi = 7$. $I_S = 2$ in λ_{EC} and the terms in its sum have $n_1 = n_2 = v_1 = v_2 = 7$. The four states we need to prepare are listed in Table I; our ψ labels in the formulas above thus take the values 0, 1, Rep, or A (short for $A_{\pi/4}$). Each one has a corresponding μ in Table I, with $\mu_{0/+}$ being the appropriate one for states $|0\rangle$ and $|+\rangle$, needed in λ_{normal} .

Next, we need the time multiplicity factors for the preparation of the different states. Those for the ancillary states needed in the EC gadget are calculated using Eq. (19); we find $r \equiv r_s = 3$ as listed in Table II. The calculation of r_A follows the same logic, but is more involved, so we explain it here. Let us initially assume a single concatenation level ($K = 1$). We apply the same logic already used for other ancillary states to derive Eq. (19). This gives $r_A \equiv \lceil \tau_{A,\text{anc}} / \tau_{T \rightarrow T} \rceil$, where $\tau_{T \rightarrow T}$ is the minimum time separating two consecutive T -gates, and $\tau_{A,\text{anc}}$ is the time to prepare, use, and measure the qubits carrying the magic state (or those qubits used to verify it). To evaluate $\tau_{T \rightarrow T}$, we note that T -gates are always separated by a Clifford gate (since $T^2 = S$ is a Clifford gate), and each T -gate lasts for $2\tau_L$ because of the state injection procedure (see fig. 10).

Hence, $\tau_T = 3\tau_L = 3D\tau_P$ where $D = 3$ is the number of timesteps to implement a Clifford gate. Here, τ_L is the duration of a level-1 logical gate, formally the duration of a 1-Rec including the syndrome extraction steps, and τ_P is the time for a single timestep for physical (level-0) qubits.

Turning to $\tau_{A,\text{anc}}$, Figs. 10 and 11 tell us that

$$\tau_{A,\text{anc}} = \tau_{A,\text{prep}} + \tau_L + \tau_P, \quad (34)$$

where $\tau_{A,\text{prep}}$ is the duration to prepare the magic state, and $\tau_L + \tau_P$ is the duration of the state-injection procedure (CNOT lasting for τ_L , and the magic-state measurement lasting for τ_P in Fig. 10). We get $\tau_{A,\text{prep}}$ from Fig. 11; the magic-state preparation starts with the preparation of the first repetition-code state, and ends when the last syndrome measurement is performed. Hence, we have: $\tau_{A,\text{prep}} = \tau_{\text{Rep,prep}} + 10\tau_P$. The duration to prepare the repetition-code state is $\tau_{\text{Rep,prep}} = 7\tau_P$; see Fig. 11c (one step to initialize the fourth qubit from the top in $|+\rangle$, 5 steps of CNOTs, and one measurement, with each of these steps lasting for τ_P). We thus have $\tau_{A,\text{anc}} = 21\tau_P$, and hence, $r_A = \lceil 21\tau_P / (9\tau_P) \rceil = 3$.

This reasoning for r_A generalizes to multiple concatenation levels, if one is careful with the following two facts. Firstly, while the preparation of a physical state takes $\tau_L(k=0) = \tau_P$ (and a measurement lasts for τ_P for all k), the fault-tolerant preparation of a level- k state takes longer than $\tau_L(k)$. Secondly, while the preparation of the $k=1$ magic state started with the preparation of the repetition-code state, it is not so clear for $k > 1$.

There, one must check which of the following tasks takes the longest time: (i) the preparation of the repetition-code state; (ii) the initialization in $|0\rangle$ of the qubits that carry the magic state; or (iii) the state injection necessary to implement T -gates at level- $(k-1)$ for $(k-1) > 0$. Despite these facts, one can check numerically that $r_A = 3$ is sufficient for general k .

In the calculation of the failure multiplicities we need to know the number of verifications per exRec, M . For Steane EC gadgets, we take the same M for all states, with that being the worst-case $M = 8$. This worst-case M is the number of verified syndrome states required in a CNOT exRec; each EC gadget requires two syndrome states, and the CNOT exRec contains four EC gadgets (each qubit in the CNOT has one before and one after the CNOT). This is clearly an overestimate of M for most states, so in fact this shows that M is in the interval $1 < M \leq 8$. However, the failure multiplicity only depends logarithmically on M , so we take $M = 8$ for simplicity, knowing that the failure multiplicity would barely change if we had taken a different value of M in this interval.

Now we have all necessary parameters, we find that for normal gates,

$$\begin{aligned} \lambda_{0/+} &= 14\mu_{0/+}, \\ \lambda_{\text{EC}} &= 28r_{\text{sv}}\mu_{0/+} = 84\mu_{0/+}. \end{aligned} \quad (35)$$

From this we get

$$\begin{aligned} \lambda_{\text{normal}} &= 98\mu_{0/+} \\ &= \begin{cases} 294 & \text{without shared prep.}, \\ 114 & \text{with shared prep.} \end{cases} \end{aligned} \quad (36)$$

where we use the values of $\mu_{0/+}$ in Table I, and round to the nearest integer. Although, finding the value of $\mu_{0/+}$ for shared state preparation (shared prep.) is postponed to sec. VII C.

Next, we turn to the parameters for magic gates, λ_{magic} and b , which involve the parameters associated with the magic-state preparation. We begin with v_A , the number of ancillary qubits needed to prepare the magic state $|A_{\pi/4}\rangle$. From Fig. 11, we see that the preparation of $|A_{\pi/4}\rangle$ requires an ancillary state $|\text{Rep}\rangle$ that needs to be fault-tolerantly prepared, employing 8 physical qubits in all, with one qubit used as a verification qubit. This $|\text{Rep}\rangle$ state preparation can fail, meaning that we require a failure multiplicity μ_{Rep} for it, and its multiple-time-step preparation circuit needs a time multiplicity r_{Rep} . Thus, the number of ancillary qubits needed for the $|\text{Rep}\rangle$ alone is $8r_{\text{Rep}}\mu_{\text{Rep}}$. In addition, the $|A_{\pi/4}\rangle$ state preparation circuit contains the Steane EC gadget. Altogether then, we have

$$v_A = \lambda_{\text{EC}} + 8r_{\text{Rep}}\mu_{\text{Rep}} = 84\mu_{0/+} + 16\mu_{\text{Rep}}. \quad (37)$$

Putting these into λ_{magic} and b , using the multiplicity values from Tables I and II, and rounding to the nearest integer, we get

$$\begin{aligned} \lambda_{\text{magic}} &= 7r_A\mu_A = 21\mu_A \\ &= \begin{cases} 84 & \text{without shared prep.}, \\ 27 & \text{with shared prep.} \end{cases} \end{aligned} \quad (38)$$

and finally, for b , we have

$$\begin{aligned} b &= 98\mu_{0/+} + 3\mu_A(84\mu_{0/+} + 16\mu_{\text{Rep}}) \\ &= \begin{cases} 3702 & \text{without shared prep.}, \\ 564 & \text{with shared prep.} \end{cases} \end{aligned} \quad (39)$$

As we take more and more levels of concatenation, the proportion of resources necessary for a given circuit compared to an equivalent one with only normal gates saturates at a finite value given by Eq. (6), which becomes

$$\begin{aligned} R(K) &\leq C = (Q_{\text{normal}}^{\text{algo}} + A_0 Q_{\text{magic}}^{\text{algo}}) / Q_{\text{total}}^{\text{algo}} \\ \text{with } A_0 &\equiv \frac{b}{\lambda_{\text{normal}} - \lambda_{\text{magic}}} \\ &= \begin{cases} 17.6 & \text{without shared prep.}, \\ 6.48 & \text{with shared prep.} \end{cases} \end{aligned} \quad (40)$$

Thus, we find that even in the worst-case scenario where the algorithm has a timestep where all gates are magic gates (hence $Q_{\text{magic}}^{\text{algo}} = Q_{\text{total}}^{\text{algo}}$), that algorithm will never

require more than 17.6 times the qubit costs of an equivalent-sized algorithm made entirely of normal gates. The factor of 17.6 is reduced to 6.48 if state preparation is shared.

However, as we discuss in Appendix A, magic gates are fairly rare in typical algorithms, and it is reasonable to assume only about 5% of gates are magic gates. To account for this we now make a simplifying assumption to avoid treating the time multiplicity at the logical level (level- K) differently from other levels in the concatenation. We recall that the time-multiplicity for magic gates was calculated knowing that a qubit only experiences (at most) a magic operation (T -gate) every two timesteps. This slightly complicates the estimation of the percentage of magic qubits at the logical level (level- K) in \mathcal{L}_{\max} . In short, when we take 5% of magic-operations in each level- K layer, we actually assume 10% of magic-operations occur every two level- K layers (and no magic-operations occur in between these two level- K layers). It guarantees that the computer has enough resources to implement 5% of magic-operations at each level- K layer. We do this because it allows us to use the same time-multiplicity at the logical level (level- K) as at other levels. This is what is done to get the 5% values in Figs. 1, 2 and 3, and corresponds to taking $Q_{\text{magic}}^{\text{algo}}/Q_{\text{total}}^{\text{algo}} \simeq 0.1$. Then the qubit costs for such a circuit is only 2.66 times that for an equivalent-sized logical circuit made entirely of normal gates. This factor of 2.66 is reduced to 1.55, if state preparation is shared.

In other words, in typical cases, the presence of gates that require magic states (the T -gates in this case), does not even triple the total qubit costs. Furthermore, it only adds about 50% to the total qubit costs when state preparation is shared. While this is clearly not a negligible contribution to the total resources, it is much less than implied in the literature; which insists on T -gates being extremely expensive in terms of resources [18–24]. This tells us that while optimizing magic-states (or optimizing circuits to minimize the number of magic-states) will reduce the qubits resources required by the quantum computer, any proposed (or hypothetical) optimization is unlikely to reduce the qubits resources by very much (probably much less than a factor of three). Of course, any such optimization is worthwhile, but it is extremely modest compared to other specific optimizations like sharing state preparation (which can reduce qubits costs by a couple of orders of magnitude), or replacing Steane EC gadgets by more resource efficient flag-qubit EC gadgets (which can reduce resources by four orders of magnitude). All this is shown in Fig. 1.

C. Shared state preparation for the Steane EC gadget

Sec. VIC explained the basic logic of evaluating the failure multiplicity factors for shared state preparation. Here, we explain how this logic applies for our current

example of the 7-qubit code scheme with the Steane EC gadget, and show how we obtained the failure multiplicities given in the last column of Table I, which were used above in Eqs. (36-40). Hence, our goal is to get rough estimates of V , M , K and $N_{\text{gates}}^{\text{level-1}}$ for Steane EC gadgets and magic-states. As explained in sec. VIC, we are not looking for a rigorous estimate here; we simply want to show with a simple argument the clear advantage in sharing state preparation and how it can significantly reduce the value of μ to something fairly close to 1. Here $K = 5$ is likely large enough for conceivable middle-term computers [64], and $M = 8$. This leaves us with estimating $N_{\text{gates}}^{\text{level-1}}$. For this, we start by counting the number of qubits at level 1 in a code with K levels of concatenations. We see it is equal to the total number of physical qubits in a code with $(K - 1)$ levels of concatenation, $Q_{\text{total}}^{\text{phys}}(K - 1)$. We multiply this number by the number of level-1 logical timesteps in the algorithm. For K total levels of concatenation, we would have about $D^{K-1} \times 2D_L$ level-1 timesteps (see Sec. VIC and footnote [63] for more details), where D is the number of timesteps required to implement a normal gate, and D_L is the depth of the algorithm implemented on the universal gateset (in this case Clifford gates plus T -gates); the factor of 2 is because a logical T -gate takes two logical steps to be implemented.

Hence, we have:

$$N_{\text{gates}}^{\text{level-1}} \approx Q_{\text{total}}^{\text{phys}}(K - 1) \times D^{K-1} \times 2D_L. \quad (41)$$

To show that sharing state preparation can significantly reduce the overheads, we will reason with a pessimistic scenario: for type ν states, we will find a value of S_ν satisfying Eq. (31) with Eqs. (28,41), and thus extract a value for its failure multiplicity μ_ν .

As an example, we assume the quantum computer is large enough to perform Shor’s algorithm to crack RSA-2048 [38], which requires $Q_{\text{total}}^{\text{algo}} \sim 10^4$ qubits and a depth $D^{\text{algo}} \sim 10^{10}$ at the level of the logical algorithm (level- K). We take $\kappa = 0.01$ and $K = 5$ [64], while taking the worst case scenario in which there is a timestep in the logical algorithm where all logical qubits (at the level- K) experience T -gates: $Q_{\text{magic}}^{\text{algo}} = Q_{\text{total}}^{\text{algo}}$. To get a lower bound on the right-hand side of Eq. (31), we take an overestimate of $Q_{\text{total}}^{\text{phys}}(K-1)$ for $K = 5$ by taking its value when state preparation is *not* shared from Fig 1 (this is a clear overestimate, because sharing the state preparation can only reduce this number); this gives $Q_{\text{total}}^{\text{phys}}(K - 1) = 10^{15}$ [66]. In this case, the ratio of physical depth to logical depth, $D = 3$. Using the fact $M = 8$, we know that Eq. (31) will be satisfied if we find the smallest S that ensures we take

$$p_{\text{Lack};\nu}^{\text{Share}}(S_\nu, p_{\text{thres}}) \leq 10^{-31}, \quad (42)$$

If we take $V = 100$, then the smallest S that satisfies the inequality Eq. (42) with Eqs. (28,41) depends on the number of fault-locations, N , in the type of state

being considered since N appears in the expression of $p_{\text{Lack};\nu}^{\text{Share}}(S_\nu, p_{\text{thres}})$. The failure multiplicity for that type of state is then given by $(V + S)/V$ with the S for that type of state. This gives the values of μ_s in the last column of Table I.

This raises the question of why we take $V = 100$ in our calculation of failure multiplicities, μ_ν where ν is “0/+”, “A” or “Rep”. Firstly, we note that μ_ν only depends weakly on V for the large V that is of interest to us, so any plausible choice of large V will give a similar μ_ν . Secondly, we note that μ_ν decays (slowly) with increasing V . Thus to get a worst case estimate of μ_ν with shared state preparation, we should take the smallest V likely to occur in the large-scale algorithm of interest to us. We now argue that $V = 100$ is a plausible such lower bound on V . To do this we assume the total number of qubits at the algorithmic level, Q_L , is at least 2000 (for comparison, $Q_L \sim 10^4$ for cracking RSA-2048 encryption [38]), and assume about 5% of the gates are magic gates (as explained below, our conclusion also holds for less than 5% of magic gates). Then we can expect at least 100 magic gates in parallel at the highest concatenation level (with more at lower concatenation levels), each of which will require a verified magic state. Hence, $V = 100$ is the smallest number of verified magic states an ancilla factory will have to produce in parallel, giving an upper bound on μ_ν . We thus use $V = 100$ for all the failure multiplicity in the last column of table I. In the case of ancillary states for EC gadgets, the smallest V is likely to be much larger (of order Q_L), which would reduce failure multiplicities below those in table I. However, those failure multiplicity is already fairly close to 1 with $V = 100$ (and it will not go below 1 for $V \rightarrow \infty$), so there is little practical gain in taking larger V .

Now turning to similar-sized circuits with less than 5% of magic gates, we note that the above value of V would be too large, so the value of μ_ν would be a bit too small. Despite this, we know that the cost of any circuit with less than 5% of magic gates is less than the cost of a circuit with 5% of magic gates, and more than the cost of a circuit with no magic gates. As these two costs are found to be close, this gives a good estimate of the cost of any circuit with less than 5% of magic gates.

As the arguments we made to get the numerical value on the right-hand side of Eq. (42) are rather simplistic, it is worth considering what happens if one takes a different numerical value on the right-hand side of Eq. (42). A simple numerical analysis indicates that a change in the choice of this value only causes a logarithmic change in the μ_s . For example, we replaced 10^{-31} with 10^{-39} in Eq. (42) (e.g., consider a logical circuit with 10^8 times more gate-operations), and found that it only changes the value of μ_A from 1.30 to 1.36. Thus we expect that the failure multiplicities in the last column of Table I are representative of a broad range of realistic situations.

The above analysis allows us to plot the blue curves in Fig. 1. They show that sharing state preparation can reduce the total qubit cost required for the computation

by a couple of orders of magnitude (for $K = 5$). It also makes the relative cost of magic states smaller; the solid and dashed blue curves are almost on top of each other in Fig. 1, corresponding to the fact that a circuit to implement an algorithm with a realistic number of magic gates only requires about 50% more resources than a circuit of equivalent size at level- K , that that has no magic gates.

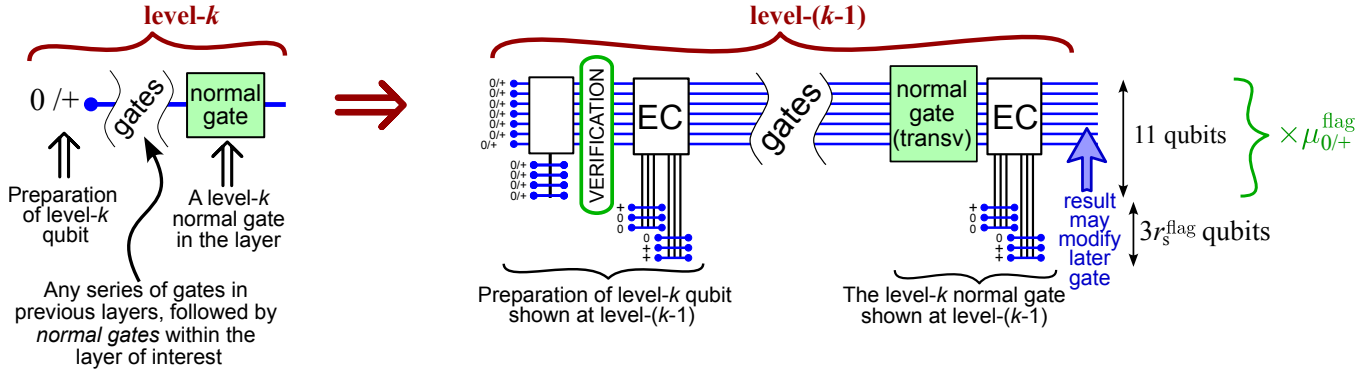
D. Evaluating qubit costs for a flag fault-tolerant scheme

The main conclusion of the previous subsection is that magic gates are not so costly compared to normal gates. Thus it may often be more efficient to minimize the qubit costs for the normal gates, rather than the magic gates. In particular, we observe that the EC gadget employs only normal gates, but it is used repeatedly throughout the entire computation. Having an EC gadget that uses fewer qubits might hence make a much larger impact. This naturally suggests repeating our analysis for the case of the flag-qubit approaches to error correction [40, 41]. We follow the flag fault-tolerant quantum computing scheme of Refs. [32, 40, 41], which requires only 6 ancillary qubits in each EC gadget (see Fig. 13a), much less costly than the earlier 28 ancillary qubits in each Steane EC gadget (see Fig. 12a).

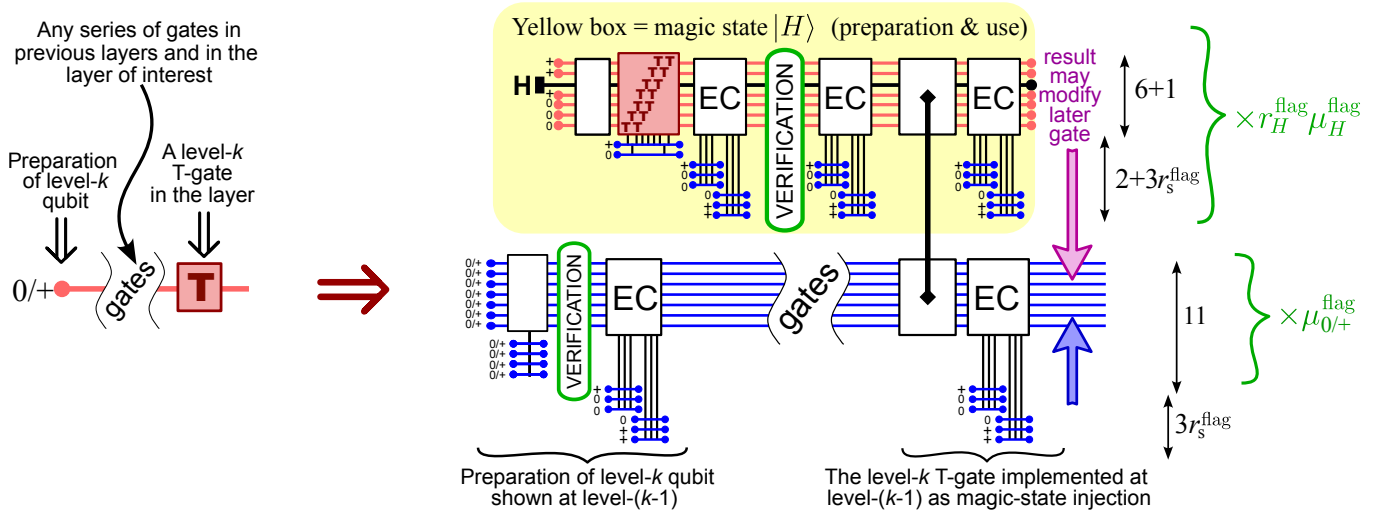
The detailed circuit diagrams for the flag scheme are given in Figs. 15-19, taken from Refs. [32] and [41]. The key differences from the Steane EC scheme of Sec. VII B are in the state preparation circuits, which now make use of flag qubits, rather than verification tests, and in the EC gadget that again uses flag qubits. Flag-qubit error-correction is argued to have a very similar threshold to Steane error-correction, see Appendix D so for simplicity we take its threshold to be the same as that of Steane error-correction; $p_{\text{thres}} = 2 \times 10^{-5}$. Fig. 13 is a simplified circuit diagram for the flag scheme; it shows the qubit costs at level- $(k-1)$ for normal and magic qubits at level k , while hiding details not needed when evaluating qubit costs. Note that this scheme implements the magic gate $T_Y \equiv \exp(-i\pi/8Y)$ [32], rather than the usual T gate $\exp(-i\pi/8Z)$. They are computationally equivalent up to normal gates (applying appropriate Clifford gates around T_Y can convert T_Y to a T -gate), and makes no difference in terms of resource costs. We will hence continue to refer to the magic gate in the flag scheme as a T gate.

We observe that the circuits are most easily written in terms of three types of qubit; one type of normal qubit and two types of magic qubit. The normal qubit (Fig. 13a) is one that starts in the state $|0\rangle$ or $|+\rangle$ and only experiences normal gates (Clifford gates). The first type of magic qubit is one that starts in the state $|0\rangle$ or $|+\rangle$, and experiences at least one magic gate (T -gate) at some point in the calculation. The second type of magic qubit is one that starts in the state $|H\rangle$ and experiences a magic gate (T -gate) at some point in the calculation.

(a) Normal qubit = qubit prepared in $|0\rangle$ or $|+\rangle$ experiencing only normal gates in layer where we evaluate resources.



(b) First type of magic qubit = qubit prepared in $|0\rangle$ or $|+\rangle$ experiencing a T-gate in the layer where we evaluate resources.



(c) Second type of magic qubit = qubit prepared in $|H\rangle$ experiencing a T-gate in the layer where we evaluate resources.

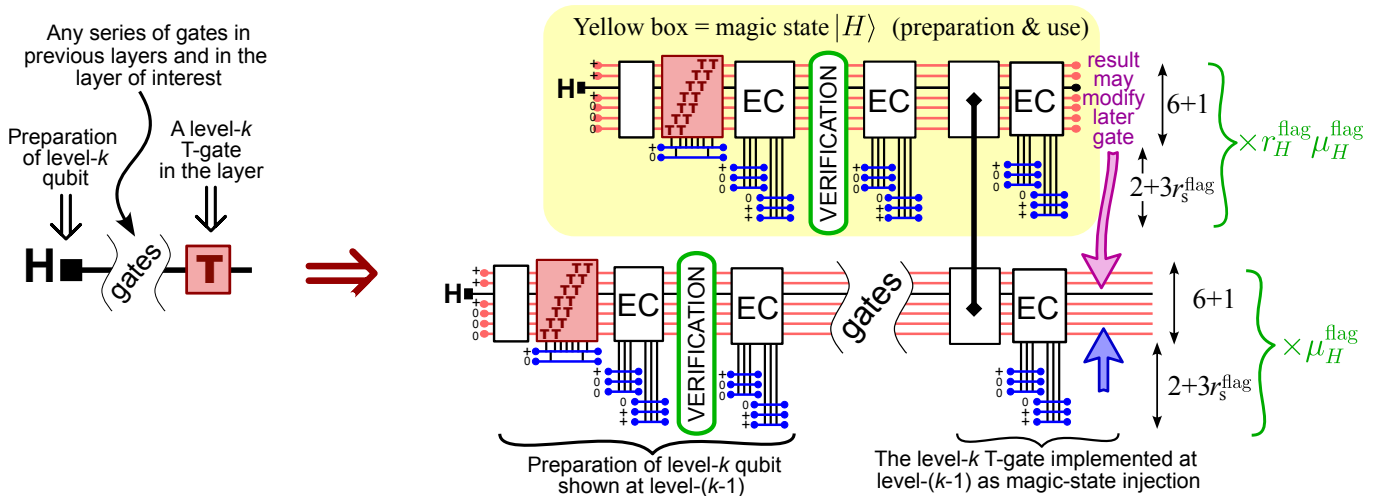


Figure 13. Simplified sketch of the error-correction circuitry for 7-qubit code with the flag-qubit approach, showing the aspects necessary to identify the qubit costs. The states at level k (to the left of the red arrows) are shown in terms of states at level $k - 1$ (to the right of the red arrows). Rectangles are blocks of gate-operations, whose details are in other figures in this work. The colored lines, arrows and symbols like “0/+” or “T” all have the same meaning as in Fig. 12. However, there is now also a black horizontal line indicating a qubit that starts in $|H\rangle$ and then experiences a T -gate.

Every qubit starting in $|H\rangle$ will experience a magic gate, as explained after Eq. (47) below. Let us define Q_{normal} as the number of normal qubits at level- k of concatenation, Q_{magic} as the number of magic qubits of the first type, and $Q_{\text{magic};H}$ as the number of magic qubits of the second type. Then, if there are K levels of concatenation, we have

$$\begin{pmatrix} Q_{\text{normal}}^{\text{phys}} \\ Q_{\text{magic}}^{\text{phys}} \\ Q_{\text{magic};H}^{\text{phys}} \end{pmatrix} = \mathbf{M}_{\text{flag}}^K \begin{pmatrix} Q_{\text{normal}}^{\text{algo}} \\ Q_{\text{magic}}^{\text{algo}} \\ 0 \end{pmatrix}. \quad (43)$$

The $Q_{\text{magic};H}^{\text{algo}} = 0$ entry in the vector on the right-hand side arises because the logical algorithm is written in terms of gates acting on $|0\rangle$, as indicated in our description of $\mathcal{C}_{\text{algo}}$ in Sec. III B 1, and so contains no $|H\rangle$ states. The matrix \mathbf{M}_{flag} can be derived in a similar manner as in earlier examples. We find,

$$\mathbf{M}_{\text{flag}} = \begin{pmatrix} \lambda_{\text{normal}}^{\text{flag}} & \lambda_{\text{normal}}^{\text{flag}} + \beta K_1 & \beta K_2 \\ 0 & 6K_1 & 6K_2 \\ 0 & K_1 & K_2 \end{pmatrix}. \quad (44)$$

The two zeros in the first column mean that \mathbf{M}_{flag} 's top-left matrix element is one of its eigenvalues; it is the one associated with normal qubits,

$$\lambda_{\text{normal}}^{\text{flag}} = 11\mu_{0/+}^{\text{flag}} + 3r_s^{\text{flag}} = 39. \quad (45)$$

For compactness, we have defined

$$\begin{aligned} \beta &\equiv 2 + 3r_s^{\text{flag}} = 8 \\ K_1 &\equiv r_H^{\text{flag}} \mu_H^{\text{flag}} = 8 \\ K_2 &\equiv (1 + r_H^{\text{flag}}) \mu_H^{\text{flag}} = 12 \end{aligned} \quad (46)$$

where we take μ_H^{flag} for the case without shared state preparation (see Table I). The assumptions allowing us to derive the time and failure multiplicities in Tables I and II are explained at the end of this section. Note the matrix element K_1 in the bottom row of the matrix \mathbf{M}_{flag} ; it is responsible for there being $|H\rangle$ states at lower concatenation levels even though there are none at the logical level (level K). This is a consequence of any T -gate at the logical level (level K) requiring a magic state that contains an $|H\rangle$ at level $(K-1)$; see Fig. 13(b), which in turn requires an $|H\rangle$ at level $(K-2)$, etc.

In addition to the eigenvalue in Eq. (45), \mathbf{M}_{flag} has two eigenvalues given by the two-by-two block in the lower-right corner of \mathbf{M}_{flag} . These are the eigenvalues for magic qubits. One of these two eigenvalues is zero and the other is

$$\lambda_{\text{magic}}^{\text{flag}} = 6K_1 + K_2 = (7r_H^{\text{flag}} + 1)\mu_H^{\text{flag}} = 60. \quad (47)$$

The zero eigenvalue plays no role in the scaling as we increase the number of levels of concatenation K ; it corresponds to a K -independent term. Hence, the K -scaling for normal qubits goes like $(\lambda_{\text{normal}}^{\text{flag}})^K$, while the K -scaling for magic qubits goes like $(\lambda_{\text{magic}}^{\text{flag}})^K$.

Now we see that, unlike the earlier scheme with Steane EC gadgets (Sec. VII B), this flag scheme has the magic-qubit eigenvalue larger than the normal one: $\lambda_{\text{magic}}^{\text{flag}} > \lambda_{\text{normal}}^{\text{flag}}$. This places it in the scaling regime where magic qubits increasingly dominate over normal qubits as K is increased, until the proportion of resources for magic gates goes to infinity as $K \rightarrow \infty$. However, the fact that $\lambda_{\text{magic}}^{\text{flag}}$ is only about 50% larger than $\lambda_{\text{normal}}^{\text{flag}}$ means that the two will remain comparable for practically relevant K s, such as $K \leq 5$ [64].

To quantify this, the method in App. B allows us to find the total physical qubit costs for these parameters. For K levels of concatenation, the total physical qubit costs are

$$Q_{\text{total:flag}}^{\text{phys}} = 39^K Q_{\text{normal}}^{\text{algo}} + \frac{82 \times 60^K - 65 \times 39^K}{15} Q_{\text{magic}}^{\text{algo}} \quad (48)$$

where the terms that go like 39^K and 60^K come from $\lambda_{\text{normal}}^{\text{flag}}$ and $\lambda_{\text{magic}}^{\text{flag}}$ respectively. Hence, the ratio of resources for a logical algorithm to an equivalent circuit in which all magic gates have replaced by normal gates at the algorithmic level (level K), as defined in Eq. (1) is

$$R_{\text{flag}}(K) = \frac{Q_{\text{normal}}^{\text{algo}}}{Q_{\text{total}}^{\text{algo}}} + \frac{82 \times 60^K - 65 \times 39^K}{15 \times 39^K} \frac{Q_{\text{magic}}^{\text{algo}}}{Q_{\text{total}}^{\text{algo}}}. \quad (49)$$

This grows exponentially with K , but for $K = 5$ this corresponds to a magic gate (T -gate) being about 43 times more costly than a normal gate (Clifford gate). So a worst-case algorithm which has a timestep in which all logical (level- K) are magic gates (i.e., with $Q_{\text{magic}}^{\text{algo}} = Q_{\text{total}}^{\text{algo}}$) will require about 43 times the amount of qubit costs as an equivalent-sized algorithm with no magic gates. However, many typical algorithms have only 5% of gates being magic gates (see App. A) for which we can take $Q_{\text{magic}}^{\text{algo}}/Q_{\text{total}}^{\text{algo}} \simeq 0.1$ (as explained below Eq. 40), the magic gates (with their associated magic states) only consume about 5.2 times as many qubit costs as the normal gates.

Such a factor of five is clearly not negligible; it is seen as the difference between the solid and dashed green curves in Fig. 1. However, it is tiny compared to the factor of 10^4 reduction in resources achieved (at $K = 5$) by switching from Steane EC gadgets to Flag-qubit gadgets (compare the black and green curves in Fig. 1).

E. Shared state preparation for the flag-qubit approach

Now we turn to the case of flag scheme with shared state preparation, for which we will be more approximate than elsewhere in this work.

The logic of treating shared state preparation for flag-qubits is the same as for the Steane EC gadgets. However, such an evaluation would require knowing a certain

factor $J_{\text{EC-repeat}}^{\text{flag}}$ which contributes to the factor D in Eq. (41). We recall that D is the number of timesteps at level $(k-1)$ required to implement a normal gate at level- k , and this depends on the number of repetitions of the flag-qubit EC gadget that are required, a number which we call $J_{\text{EC-repeat}}^{\text{flag}}$. A look at the circuit from Figure 16 shows that $D = 1 + 12 \times J_{\text{EC-repeat}}^{\text{flag}}$ (1 time step to implement the transversal gate, $12 \times J_{\text{EC-repeat}}^{\text{flag}}$ to perform error-correction).

The exact value of $J_{\text{EC-repeat}}^{\text{flag}}$ varies depending on details of the error-correction gadget. Typically its value is fairly close to 1, with $J_{\text{EC-repeat}}^{\text{flag}} = 3, 4$ or 5 appearing in the literature [67, 68]. However, it turns out that we do not need the precise value of $J_{\text{EC-repeat}}^{\text{flag}}$, because it only enters our failure multiplicities, and they depend very weakly on $J_{\text{EC-repeat}}^{\text{flag}}$. Let us take the same example of implementing Shor's cracking of RSA-2048 as in Sec. VII C (so $K = 5$, $Q_{\text{total}}^{\text{algo}} \sim 10^4$, $D^{\text{algo}} \sim 10^{10}$, $\kappa = 0.01$). If we take an under-estimate with $J_{\text{EC-repeat}}^{\text{flag}} = 1$, we get $\mu_{0/+}^{\text{flag}} = 1.14$ and $\mu_H^{\text{flag}} = 1.24$. If we then take an *extreme* overestimate with $J_{\text{EC-repeat}}^{\text{flag}} = 1000$, we get $\mu_{0/+}^{\text{flag}} = 1.19$ and $\mu_H^{\text{flag}} = 1.31$. Thus varying $J_{\text{EC-repeat}}^{\text{flag}}$ between 1 and 1000 only causes a few percent change in the failure multiplicities, $\mu_{0/+}^{\text{flag}}$ and μ_H^{flag} . For the sake of caution, we put the larger of these values in Table I, and then use them for the orange curves in Fig. 1, knowing that this can only be an overestimate.

This shows that sharing the state preparation reduces the qubit cost by nearly two orders of magnitude. Then reducing the cost of the magic states can never reduce qubit costs more than about a factor of two for $K \leq 5$ [64]. Furthermore, achieving that factor of two would require finding an optimization that makes magic gates no more costly than normal gates, which currently seems unrealistic. This again shows that, while magic-states should be optimized, other optimizations are more important. Hence, magic states should be considered as the last resource to optimize.

VIII. STRONG EFFECT OF EC GADGET SIZE ON THE QUBIT COSTS

We have seen that changing from the Steane scheme (with larger EC gadgets) to the flag-qubit scheme (with smaller EC gadgets) vastly reduces the resources. These reductions are a few orders of magnitude at $K = 5$, see Fig. 1. However, the switch from Steane to flag-qubit schemes does not only reduce the number of qubits in the EC gadget, it also reduces the number of qubits in the magic-state preparation. So to confirm that the dominant effect is the reduction of the number of qubits in the EC gadget, we finish this article with a toy model to directly explore how the size of the EC gadget affects the resource costs of normal and magic gates.

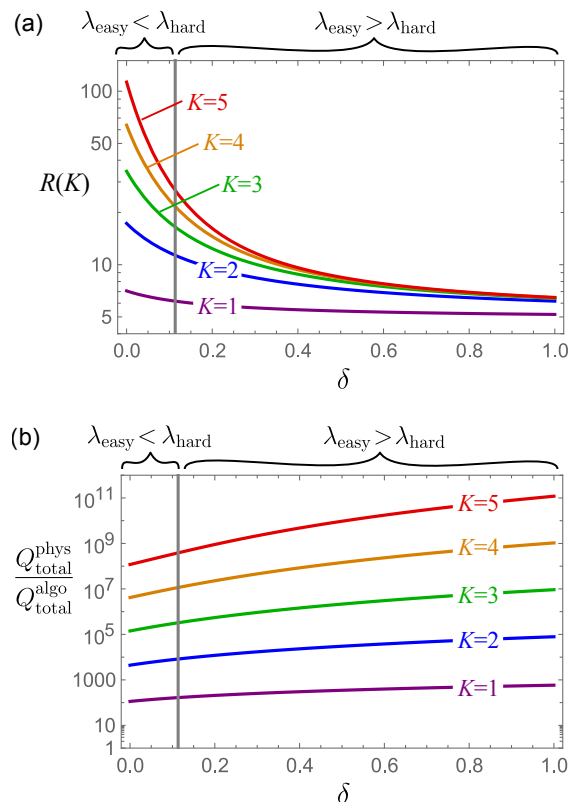


Figure 14. Plots of the toy-model in sec. VIII, where we vary the size of the error-correction gadget by varying δ . Here $\delta = 1$ corresponds to the Steane EC gadget in sec. VII B, and reducing δ reduces the size of the EC gadget to the point where $\delta = 0$ corresponds to a fictional case where the EC gadget requires no ancillary qubits at all. All curves are for the (unrealistic) worst-case scenario where the circuit is made only of magic gates at the level of the logical algorithm (level- K), so $Q_{\text{magic}}^{\text{algo}} = Q_{\text{total}}^{\text{algo}}$ and $Q_{\text{normal}}^{\text{algo}} = 0$. (a) The relative cost of magic gates to normal gates, as quantified by $R(K)$ in Eq. (52), which is the ratio of physical qubits in a circuit that contains only magic logical gates to physical qubits in an equivalent-sized circuit that contains only normal logical gates. (b) The number of physical qubits required to encode a single logical qubit in the algorithm, $Q_{\text{total}}^{\text{phys}}/Q_{\text{total}}^{\text{algo}}$, as in Eq. (51). In both plots, the gray vertical line indicates the value of δ for which $\lambda_{\text{magic}} = \lambda_{\text{normal}}$. Comparing the vertical scales of the two plots (which are both logarithmic), we see from (a) that when we reduce δ there is an increase in the relative cost of magic gates, despite this we see from (b) that the total physical qubit costs are reduced by multiple orders of magnitude.

For this, we take a toy model based on the scaling approach for the simple case of the 2-by-2 matrix \mathbf{M} in Sec. IV B, and allow ourselves to vary its parameters in a continuous manner, without worrying about whether there are fault-tolerant circuits that achieve any given value of the parameters. Here, we vary λ_{normal} and b for fixed λ_{magic} . From this, we find that reducing the size of the EC gadget causes an increase in the relative weight of resources of the magic gates to normal gates. Despite

this, reducing the size of the EC gadget causes the total physical qubit costs (for normal and magic operations) to be significantly reduced. It is thus always worthwhile finding ways to reduce the size of the EC gadget.

Specifically here, our toy model begins with the parameters for 7-qubit code scheme using Steane EC gadgets with shared state preparation [see Eqs. (36)-(39) and surrounding text], but replaces $r_s = 3$ by 3δ , where we recall that the number of ancillary qubits in the EC gadget is proportional to r_s . Then δ is the toy-model parameter that we can vary to change the resources required by the EC gadget. In this case,

$$\lambda_{\text{normal}} = 97\delta + 16 \quad (50a)$$

$$\lambda_{\text{magic}} = 27 \quad (50b)$$

$$b = 477\delta + 87 \quad (50c)$$

where we round coefficients to the nearest integer. When $\delta = 1$ these equations coincide with our earlier example of Steane error correction with shared state preparation in Eqs. (36-39). In contrast, $\delta = 0$ corresponds to a likely fictitious situation in which the EC gadget requires no ancillary qubits at all. Then, Eq. (4) gives the number of physical qubits necessary for a given algorithm. In the rare worst-case scenario where all gates are magic gates so $Q_{\text{magic}}^{\text{algo}} = Q_{\text{total}}^{\text{algo}}$ and $Q_{\text{normal}}^{\text{algo}} = 0$, this gives the number of physical qubits required to encode a single logical qubit in the algorithm,

$$\frac{Q_{\text{total}}^{\text{phys}}}{Q_{\text{total}}^{\text{algo}}} = 27^K + (477\delta + 87) \frac{(97\delta + 16)^K - 27^K}{97\delta - 11}. \quad (51)$$

Similarly, Eq. (5) with $Q_{\text{magic}}^{\text{algo}} = Q_{\text{total}}^{\text{algo}}$ and $Q_{\text{normal}}^{\text{algo}} = 0$ gives the ratio of physical qubits necessary for a circuit that contains only magic gates at the level of the logical algorithm (level- K) compared to an equivalent-sized circuit that contains only normal gates at that level (level- K),

$$R(K) = \frac{477\delta + 87}{97\delta - 11} - \frac{380\delta + 98}{97\delta - 11} \left(\frac{27}{97\delta + 16} \right)^K. \quad (52)$$

Fig. 14 plots Eqs. (51) and (52) for various K values, as δ varies between 0 and 1, thereby varying the size of the EC gadget.

When analysing Fig. 14, we assume that the EC gadget's capacity to correct errors is independent of δ . In other words, we assume that while the “cost” varies with δ in the manner shown in Fig. 14, the “benefit” (the amount of error correction) does not vary with δ . If both cost and benefit varied with δ , then Fig. 14 would not be a fair comparison of different δ s. However, we observe that the benefits (capacity to correct errors) do not vary with δ in our earlier examples of the Steane EC gadget versus the flag-qubit EC gadget; their capacity to correct errors is quantified by the fault-tolerance threshold, p_{thres} , and this is similar for both schemes (see appendix D). In short, the reason is that a flag-qubit EC gadget contains fewer ancillary qubits, but takes more time-steps,

so its number of fault locations in the largest exRec — which determine p_{thres} in the manner mentioned below Eq. (7) — is not so different from that for a Steane-EC gadget. Thus, it seems natural to reflect this in our toy-model by assuming the capacity for error-correction to be δ -independent.

With this in mind, we conclude from the plots in Fig. (14)(a) that reducing δ (reducing the number of ancillary qubits required by each EC gadget), increases the relative cost of magic gates to normal gates (as quantified by $R(K)$). Nonetheless, we see from Fig. (14)(b) that reducing δ can cause the total physical qubit costs to be reduced by multiple orders of magnitude. Minimizing the EC gadget size is thus an excellent way to reduce the physical qubit costs.

IX. CONCLUSIONS

We have devised a simple, yet powerful, scaling approach to evaluate the qubit costs of concatenated fault-tolerant quantum computing. Our approach yields closed-form expressions that remain simple at arbitrary levels of concatenation, especially for recursively concatenated schemes. This makes it a useful tool for comparing qubit costs between different schemes and their variants, as we have done in the examples of Fig. 1. While we focused on specific examples in the main text, our approach is applicable for more general schemes, as explained in Appendix B 2.

We have seen from our analysis that qubit costs are determined only by a small number of parameters (only three in the simplest case) which can be extracted from the circuit designs of the scheme in question. However, to get reliable values of these parameters, for accurate estimates of qubits costs, there are two particularly critical factors: the time and failure multiplicity factors. These account for, respectively, the costs associated with the time taken to prepare ancillary qubit states and the additional costs needed to compensate for failed verification of quantum states. For the latter, we had to analyze the impact of these failures on the fault-tolerance threshold. The multiplicity factors can have a large impact on the qubit costs: For the examples in Fig. 1, reducing the failure multiplicity by sharing state preparation resources reduces qubit costs by orders of magnitude.

Understandably, the optimizations most effective at reducing qubit costs are those that affect all operations, rather than optimizations restricted to magic states. While one can naturally expect that optimizations affecting all operations are more efficient than optimizations only affecting magic-states, the surprising conclusion of our work is that the former can reduce the costs by several orders of magnitude while the latter only by a marginal amount. This is particularly surprising given that numerous works in the literature emphasize specific optimizations that only affect magic-states. This is also surprising given the current trend in the field to design

algorithms that minimize the use of magic operations. We have shown how the switch from the Steane EC gadget to a flag-qubit scheme significantly lowers the qubit costs, with the bulk of the reduction attributable to the use of flag qubits in place of standard state verification in the EC gadget used for every operation, normal or magic (see Fig. 1 and Sec. VIII). In contrast, the optimization of magic states can bring only marginal improvements. The best (i.e., least costly) case in our Fig. 1 is flag-qubits with shared state preparation. In that case, even if one could find a way to completely eliminate the additional cost of magic states, so that magic and normal gates have equal costs, we find a qubit-cost reduction of only a factor of two.

We thus conclude that magic-state optimizations are less important than one might think. Instead, optimizing ingredients that go into every operation can reap the most benefits. We have shown how resource sharing can reduce failure multiplicities, leading to sizable cost reductions. One can also expect that circuit designs that reduce time multiplicities to also have significant impact. Our scaling approach elucidates how each ingredient affects the qubit costs, and provides a means of identifying the most worthwhile optimizations to minimize the qubit costs of concatenated fault-tolerant quantum computing schemes.

X. ACKNOWLEDGEMENTS

We warmly thank A. Auffèves, J.H. Chai, C. Vuillot for many useful discussions and inputs.

This work was supported by the European Union (EU) Horizon 2020 research and innovation program via “Quantum Large Scale Integration in Silicon” (QLSI) (Grant No. 951852), the Singapore National Research Foundation (NRF) and French National Research Agency (ANR) joint project “QuRes” (Grant No. ANR-PRC-CES47-0019; NRF2021-NRF-ANR005), the Merlion Project (Grant No. 7.06.17), the ANR program “Investissements d’avenir” (Grant No. ANR-15-IDEX-02), the Laboratories of Excellence (Labex) Laboratoire d’Alliances Nanosciences-Energies du Futur (LANEF), and the “Quantum Optical Technologies” project within the International Research Agendas program of the Foundation for Polish Science cofinanced by the EU European Regional Development Fund. H.K.N. acknowledges the support of the National Research Foundation, Singapore and A*STAR under its CQT Bridging Grant. M.F.A also acknowledges the funding from the European Union’s Horizon Europe Research and Innovation programme under the Marie Skłodowska-Curie Actions & Support to Experts programme (MSCA Postdoctoral Fellowships) - grant agreement No. 101108284.

Appendix A: Proportion of magic gates (T -gates) in typical algorithms

At various points in this work we need a reasonable estimate of the number of magic gates that occur in the timestep of the algorithm with the most magic gates. This time step at level- K of concatenation defines a layer of code which contains multiple gates in series on each qubit at lower concatenation levels $k < K$. This is the layer of the algorithm that requires the largest number of physical qubits, and so determines the number of physical qubits that the quantum computer must have. In the body of the text we quantify this as the proportion of magic gates in that step of the algorithm, $Q_{\text{magic}}^{\text{algo}}/Q_{\text{total}}^{\text{algo}}$, where $Q_{\text{total}}^{\text{algo}}$ is the total number of qubits in the algorithm, and $Q_{\text{magic}}^{\text{algo}}$ is the number of magic qubits at that timestep with the most magic qubits (with magic qubits being those involved in magic gates at that timestep).

In principle, we could plunge in the circuit detail for each algorithm in the literature to find the largest value of $Q_{\text{magic}}^{\text{algo}}/Q_{\text{total}}^{\text{algo}}$ in that algorithm. However, here we prefer to get simple estimates from easily available information summarized in Table III. That table gives the proportion of gates in the algorithm that are magic gates (where magic gates are T -gates in our examples) for various computing task, and calls the proportion $P_{\text{magic}}^{\text{algo}}$. Table III shows that most algorithm’s implementations have a very low proportion of T -gates (with the exception of the last line of the table); this proportion is a few percent or less. We will now use $P_{\text{magic}}^{\text{algo}}$ to estimate $Q_{\text{magic}}^{\text{algo}}/Q_{\text{total}}^{\text{algo}}$ for such computing tasks.

To get a lower limit on $Q_{\text{magic}}^{\text{algo}}/Q_{\text{total}}^{\text{algo}}$, we can assume each time-step has the same number of magic gates, then we have

$$\frac{Q_{\text{magic}}^{\text{algo}}}{Q_{\text{total}}^{\text{algo}}} \sim P_{\text{magic}}^{\text{algo}}. \quad (\text{A1})$$

Thus the lower bound on $Q_{\text{magic}}^{\text{algo}}/Q_{\text{total}}^{\text{algo}}$ is a few percent or less in most algorithms.

To get an upper limit on $Q_{\text{magic}}^{\text{algo}}/Q_{\text{total}}^{\text{algo}}$, we can assume there are a few time-step where all qubits experience magic gates, and many time-steps where there are no magic gates. Then the proportion of timesteps with magic gates would then be $P_{\text{magic}}^{\text{algo}}$. We do not believe that any of the examples in Table III have the property, but we cannot rule it out as a worst case scenario. In this unlikely case $Q_{\text{magic}}^{\text{algo}}/Q_{\text{total}}^{\text{algo}} = 1$, however it is easy to reduce it [74]. For example, to reduce $Q_{\text{magic}}^{\text{algo}}/Q_{\text{total}}^{\text{algo}}$, we imagine taking that one timestep of the algorithm that involve all magic gates, and spreading it out over 20 timesteps, where each of those twenty timesteps only involves 5% of the qubits having magic gates (while the rest of the qubits do nothing). At the same time, any timesteps that involve less than 5% of magic gates will be left unchanged. As the proportion of the algorithm’s

Computing Task	Reference & assumptions	Proportion of T -gates $P_{\text{magic}}^{\text{algo}}$
Shor's algorithm for cracking an RSA n -bit encryption key.	Eqs. (39-41) of Ref. [69]. If Toffolis are implemented as Cliffords+ T -gates in the usual manner: $Q_{\text{total}}^{\text{algo}} = 5n$, $N_T = 364n^3$, $D = 5400n^2$.	$P_{\text{magic}}^{\text{algo}} = 0.0135$
Elliptic curve discrete logarithm problem (a crucial part of Shor's algorithm) for 256, 384 & 521 bits elliptic curves.	Table 1 of Ref. [7] has results optimized for low T -count, low $Q_{\text{total}}^{\text{algo}}$ or low depth. See also Ref. [70].	$P_{\text{magic}}^{\text{algo}} < 0.001$ (low T -count) $P_{\text{magic}}^{\text{algo}} < 0.001$ (low $Q_{\text{total}}^{\text{algo}}$) $P_{\text{magic}}^{\text{algo}} < 0.0125$ (low depth)
Quantum linear-system algorithm for electromagnetic scattering cross-section of a 2D target.	Ref. [71], including oracles in its Table 2	$P_{\text{magic}}^{\text{algo}} < 10^{-8}$
Finance: Estimates for a quantum advantage in derivative pricing.	Table 1 of Ref. [72] indicates the T -count and T -depth for various examples.	$P_{\text{magic}}^{\text{algo}} < 0.05$ (all examples)
Quantum chemistry: Obtaining energies of FeMoco.	Table 1 of Ref. [73] with results for serial and parallelized implementations.	$P_{\text{magic}}^{\text{algo}} < 0.01$ (serial) $P_{\text{magic}}^{\text{algo}} \sim 0.5$ (parallel)

Table III. The proportion of the algorithm's gates that are T -gates for various computing tasks in the literature. These T -gates correspond to magic gates in our 7-qubit code examples (since they are the gates requiring magic-state injection). This proportion of magic gates is take as $P_{\text{magic}}^{\text{algo}} = N_T/(Q_{\text{total}}^{\text{algo}}D)$, where N_T is the number of T -gates, $Q_{\text{total}}^{\text{algo}}$ is number of logical qubits, and D is the logical depth.

timesteps that are spread in this manner is only $P_{\text{magic}}^{\text{algo}}$, this will only increase the algorithm's depth by a factor of

$$20P_{\text{magic}}^{\text{algo}} + (1 - P_{\text{magic}}^{\text{algo}}) \quad (\text{A2})$$

As $P_{\text{magic}}^{\text{algo}}$ is small, this is a modest increase in depth. For example, in those algorithms where $P_{\text{magic}}^{\text{algo}} = 0.01$, we can ensure that $Q_{\text{magic}}^{\text{algo}}/Q_{\text{total}}^{\text{algo}} \leq 0.05$ at the cost of increasing the algorithm's depth by $\leq 19\%$. In those algorithms where $P_{\text{magic}}^{\text{algo}} = 0.05$, we can ensure that $Q_{\text{magic}}^{\text{algo}}/Q_{\text{total}}^{\text{algo}} \leq 0.05$ at the cost of doubling the algorithm's depth.

However, we emphasize that these are worst case scenarios, and the increase in depth is likely to be much less than that given above. This is because it is rare that all magic gates occur in the same timestep. If this were to occur, it would be rare that one cannot reorganize the gate-operations so that the magic gates are spread over multiple timesteps, but qubits that are not doing magic gates are doing other gates-operations useful for the algorithm (rather than just waiting doing nothing). This would ensure the depth is less than if all such qubits just waited, as assumed in Eq. (A2). Indeed, developing methods to do this would be an excellent way of reducing the qubits resource costs of an algorithm in which many magic gates (gates requiring magic states) must be done in the same time-step. One such method is discussed in Ref. [74]. In such cases, re-designing the circuit to spread magic gates more evenly in time could be more important for resource efficiency than reducing the qubit costs of each magic state.

Whatever the scenario, we estimate that such relatively modest increases in depth as given in Eq. (A2) will only very rarely impact the number of qubits required by error-correction. To understand why, we recall that the goal of fault-tolerance is to make the error per logical gate at level- K logical gate-operation, p_K , small enough that the total algorithm only fails a small proportion of the time; let us assume we can accept that this proportion to be ϵ_{algo} . Then if the algorithm contains N_{algo} level- K gate-operations, we require that $p_K N_{\text{algo}} \leq \epsilon_{\text{algo}}$. Now recalling that p_K is given by Eq. (22), and considering fault-tolerant codes with $t = 1$ (like those in the examples considered here), we get

$$K = \left\lceil \frac{1}{\ln(2)} \ln \left(\frac{\ln(p_{\text{thres}} N_{\text{algo}} / \epsilon_{\text{algo}})}{\ln(p_{\text{thres}} / p_0)} \right) \right\rceil \quad (\text{A3})$$

where we recall that $\lceil x \rceil$ is the ceiling function (defined as giving the smallest integer larger than x). The argument of the ceiling function in Eq. (A3) varies extremely slowly with N_{algo} — it scales like $\ln(\ln(p_{\text{thres}} N_{\text{algo}} / \epsilon_{\text{algo}}))$ — and so a change of N_{algo} by the factor in Eq. (A2) (which is typically $\lesssim 2$) is very unlikely to change the argument of the ceiling function enough that K increases by one. Hence, in the vast majority of cases, K will be completely unchanged when the depth is increased by the factor in Eq. (A2). Then this depth increase has no effect on the physical qubit costs.

In those rare cases, where increasing the depth by the factor in Eq. (A2) causes K to increase by one, the physical qubit costs will increase significantly (as seen in Fig. 1). This would be a case where K was already

extremely close to increasing by one anyway; for example a slightly larger p_0 would also make K increase by one. In such cases, one strategy may be able to keep K unchanged, and compensate by accepting a larger value of ϵ_{algo} . This requires no increase in the physical qubit costs, but one must run the circuit a few more times before being sure that it is giving the correct result. To be more precise, we remark that if one runs the circuit multiple times, all runs of the circuit that are error-free give the same correct result, but each run with a random error will give a different wrong result. Hence, even if a fairly high proportion of the runs fail due to a random error (say $\epsilon_{\text{algo}} \sim 0.2$), one can identify the correct result by running the circuit a few $1/\epsilon_{\text{algo}}$ times (e.g. 10-15 times if $\epsilon_{\text{algo}} \sim 0.2$). Only one of the calculation's results will be repeated multiple times in these runs, and that will be the error-free result.

The conclusion of this section is that for most algorithms in Table III with $P_{\text{magic}}^{\text{algo}}$ of a few percent or less, it is reasonable to assume a logical algorithm will only have about 5% of magic gates in the layer with the most magic gates, and this is what we do in the body of this article.

Appendix B: Scaling approach in the general case

1. Definition of qubit's type

When we observe that a fault-tolerant scheme requires multiple types of normal qubits or multiple types of magic qubits, the scaling is not described by Eq. (2), which only has one type of each. That is when we need the general case, based on a matrix \mathbf{M} of larger dimensions.

However, while we have no simple way to say *a priori* how many types of qubit a given fault-tolerant scheme requires (it is necessary to look at the details of the circuits), we can explain the procedure we followed in our examples. We first identify every combination of initial states, gate-operations, and measurements that is required by the scheme in question. We then group the qubits into "qubit's types". A type of qubit is defined as a specific combination of state-preparation, gates, and measurements that a qubit can go through. Then, the (i,j) element of the matrix \mathbf{M} represents the number of qubits of type "i" at level-(k-1) that are required inside one qubit of type "j" at level-k. This approach suggests that there could have a huge number of qubit's type (because many combinations of state-preparation gates and measurements are possible). In practice, however, one can often group the qubits into a small number of qubit's type (2 or 3 in the examples we considered in the main text). This is because many qubit's types are equivalent. We will say that two qubit types " j_0 " and " j_1 " are equivalent if, for any K , it is sufficient to know the sum of the number of level- K j_0 and j_1 qubits there are (and the number of qubits of type j_i for $i \notin \{0,1\}$) to deduce

the number of level-0 qubits they would require. In this case, it is not useful to separate the qubits " j_0 " and " j_1 " into two different types: we can merge them into a single one, meaning that the matrix \mathbf{M} can have its dimension reduced by one. In different terms, two qubit's type are equivalent if, for any K , they require the same number of level-0 qubits. For instance, in our flag and Steane EC-gadgets examples, for any K , every level- K normal qubit initialized in either $|0\rangle$ or $|+\rangle$ and measured in the Pauli X or Z bases requires the same number of level-0 qubits: it is not necessary to separate them into different qubit's type. A natural example of where two types are not equivalent is the difference between normal and magic qubits: because level- K magic qubits require state injection, they will usually require more level-0 qubits than normal qubits, hence, they must be classified into different types. It can also be that two magic qubits (or two normal qubits) do not belong to the same type. We have such examples for the flag scheme, with the introduction of two types of magic qubits: see Eq. (44) where the shape of \mathbf{M} indicates that the second type of level- k magic qubits requires a different number of level- $(k-1)$ qubits than the first type of magic qubits. Finding a minimum number of qubit's type thus requires a careful look at the circuit in order to identify the few types of qubits that require a different number of level-0 qubits, with the help of sketches like Figs. 12 or 13. Often, the resulting matrix will be of low dimension.

Outside of this section, when we specify a number of types of qubits, we assume that the reduction described here has already been performed in the sense that all equivalent types of qubits have already been merged into a single type.

2. Formalism for the general case

Here we give details of how to generalize the scaling approach introduced in Sec. IV to cases where there are multiple types of normal and magic qubits (for instance because some normal gates require more qubits than other normal gates, or because there are different type of magic gates, each requiring a different number of qubits to prepare their magic state). We first generalize our approach in Sec. B 2 a, before giving relatively general results about the cost of a circuit composed of magic gates in the limit of large K , compared to a circuit only composed of normal gates, in concatenated schemes, in Sec. B 2 b. These results illustrate the flexibility of our scaling approach, showing how it can be used as a tool to analyze concatenation schemes that are more complicated than the examples treated in detail in this article.

a. Generalizing the matrix structures

Here, we use the main assumption that our work is built on, namely, assumptions 1 & 2 in Sec. IV. Then in

general, there may be j_{normal} types of normal qubits at level k , each requiring different resources at level $(k-1)$, and j_{magic} types of magic qubits, each requiring different resources at level $(k-1)$.

To explain how to deal with this case, we make a few assumptions to keep the explanation compact, these include the assumptions about the circuit $\mathcal{C}_{\text{algo}}$ in Sec. III B 1. We also assume that the magic gates are single-qubit magic gates (like the T -gate in our examples in Sec. VII). If this is not the case the following argument will not fundamentally change, but it will be a bit uglier (particularly if there are magic two-qubit gates as well as magic single-qubit gates).

In this case the matrix recursion relation looks like that for the 2-by-2 matrix \mathbf{M} in Eq. (2), but now it contains a larger matrix. It is written as

$$\begin{pmatrix} Q_{\text{normal}}(k-1) \\ Q_{\text{magic}}(k-1) \end{pmatrix} = \mathbf{M} \begin{pmatrix} Q_{\text{normal}}(k) \\ Q_{\text{magic}}(k) \end{pmatrix}, \quad (\text{B1})$$

where now $Q_{\text{normal}}(k)$ is a vector with j_{normal} elements, whose i th element is the i th type of normal qubit (at level k). Similarly, $Q_{\text{magic}}(k)$ is a vector with j_{magic} elements, whose i th element is the i th type of magic qubit (at level k). This means that \mathbf{M} is the $(j_{\text{normal}} + j_{\text{magic}})$ -by- $(j_{\text{normal}} + j_{\text{magic}})$ matrix that takes the form

$$\mathbf{M} = \begin{pmatrix} \mathbf{M}_{\text{normal}} & \mathbf{B} \\ 0 & \mathbf{M}_{\text{magic}} \end{pmatrix}. \quad (\text{B2})$$

whose ij th element is the number of level- $(k-1)$ qubits of type i necessary for a level- k qubit of type j . Here $\mathbf{M}_{\text{normal}}$ is a j_{normal} -by- j_{normal} matrix, $\mathbf{M}_{\text{magic}}$ is a j_{magic} -by- j_{magic} matrix, and \mathbf{B} is a rectangular j_{normal} -by- j_{magic} matrix. The zero in \mathbf{M} is a j_{magic} -by- j_{normal} null matrix. It is there because normal qubits at level k are only made from normal qubits at level $(k-1)$. The matrix \mathbf{M} thus has $[(j_{\text{normal}} + j_{\text{magic}})^2 - j_{\text{normal}}j_{\text{magic}}]$ positive elements, so the resources will depend on $[(j_{\text{normal}} + j_{\text{normal}})^2 - j_{\text{normal}}j_{\text{magic}}]$ parameters of the error-correction circuitry. These can be extracted from a given fault-tolerant scheme in the manner outlined at the end of sec. V B.

To find the resources with K levels of concatenation, we have (in analogy with Eq.(3)),

$$\begin{pmatrix} Q_{\text{normal}}^{\text{phys}} \\ Q_{\text{magic}}^{\text{phys}} \end{pmatrix} = \mathbf{M}^K \begin{pmatrix} Q_{\text{normal}}^{\text{algo}} \\ Q_{\text{magic}}^{\text{algo}} \end{pmatrix}. \quad (\text{B3})$$

Here $Q_{\text{normal}}^{\text{algo}}$ and $Q_{\text{magic}}^{\text{algo}}$ are vectors whose elements are the number of logical (level- K) qubits of that subtype in the bottleneck layer of the algorithm, \mathcal{L}_{max} . Then $Q_{\text{normal}}^{\text{phys}}$ and $Q_{\text{magic}}^{\text{phys}}$ are the same vectors for the number of physical (level-0) qubits in the layer \mathcal{L}_{max} .

In this case, it is unlikely that there is an easy way to find the bottleneck layer, \mathcal{L}_{max} , which we recall corresponds to the time-step of the logical (level- K) circuit

that requires the most physical (level-0) qubits. Thus, the method used in Sec. IV A is likely to be too simplistic. It is likely that we will have to use our scaling approach to calculate the physical qubit cost for each plausible candidate for the bottleneck layer, and only the result of these calculations will reveal to us which one is the true bottleneck layer, \mathcal{L}_{max} .

At this point, we assume $\mathbf{M}_{\text{normal}}$, $\mathbf{M}_{\text{magic}}$ and \mathbf{M} are all diagonalizable and we diagonalize \mathbf{M} in the textbook manner to get $\mathbf{M} = \mathbf{U}\mathbf{M}_{\text{diag}}\mathbf{U}^{-1}$. Here, \mathbf{M}_{diag} is the diagonal matrix of eigenvalues. The zero in \mathbf{M} 's lower-left corner means that the eigenvalues of \mathbf{M} are those of $\mathbf{M}_{\text{normal}}$ and $\mathbf{M}_{\text{magic}}$. We chose \mathbf{M}_{diag} so that its first j_{normal} diagonal elements are eigenvalues of $\mathbf{M}_{\text{normal}}$, and its remaining j_{magic} diagonal elements are eigenvalues of $\mathbf{M}_{\text{magic}}$. Then \mathbf{U} 's j th column is the right eigenvector for \mathbf{M}_{diag} 's j th eigenvalue. The number of physical qubits for K level of concatenation is then given by

$$Q_{\text{total}}^{\text{physical}} = \sum_{i,j,j'=1}^{j_{\text{normal}}+j_{\text{magic}}} \left(\mathbf{U}_{ij'} [\mathbf{U}^{-1}]_{j'j} Q_j^{\text{algo}} \right) \lambda_{j'}^K. \quad (\text{B4})$$

Here, $\lambda_{j'}$ for $1 \leq j' \leq j_{\text{normal}}$ correspond to the eigenvalues of $\mathbf{M}_{\text{normal}}$ and $\lambda_{j'}$ for $j_{\text{normal}} < j' \leq j_{\text{normal}} + j_{\text{magic}}$ to the eigenvalues of $\mathbf{M}_{\text{magic}}$. This is the general analytic result for the total physical qubit costs required when there are multiple types of normal and magic gates.

Now we turn to evaluating R , we recall that it was previously defined as a ratio; it is the physical qubit costs required by a given algorithm, divided by the resources required a fictitious algorithm of the same size in which all level- K magic operations are replaced by level- K normal operations. Equivalently, this means we replace the magic qubits by normal qubits at level- K . However, this replacement is ambiguous whenever there are multiple types of normal qubits at level- K with different physical qubit costs, unless we specify which type of level- K normal qubits replaces the level- K magic qubits. So we define R as the physical qubit costs required by a given algorithm, divided by the resources required a fictitious algorithm of the same size in which all magic qubits are replaced by normal qubits of type m . To evaluate the resources for this fictitious algorithm we first note that the number of magic gates in the bottleneck layer \mathcal{L}_{max} of the real algorithm is $Q_{\text{magic}}^{\text{algo}} = \sum_{i=j_{\text{normal}}+1}^{(j_{\text{normal}}+j_{\text{magic}})} Q_i^{\text{algo}}$. Thus in the fictional algorithm where all magic gates are replaced by normal gates of type m we have Q_j^{algo} replaced by Q_j^{fict} where

$$Q_j^{\text{fict}} = \begin{cases} Q_j^{\text{algo}} + \delta_{jm} Q_{\text{magic}}^{\text{algo}} & \text{for } j \leq j_{\text{normal}} \\ 0 & \text{for } j > j_{\text{normal}} \end{cases} \quad (\text{B5})$$

where δ_{jm} is a Kronecker delta-function. In this case the numerator of R is given by Eq. (B4), while the denominator of R is given by Eq. (B4) with Q_j^{algo} replaced by

Q_j^{fict} . Here, we write R in an equivalent manner as

$$R = \frac{\sum_{i,j,j'=1}^{j_{\text{normal}}+j_{\text{magic}}} \left(\mathbf{U}_{ij'} [\mathbf{U}^{-1}]_{j'j} Q_j^{\text{algo}} \right) \lambda_{j'}^K}{\sum_{i,j,j'=1}^{j_{\text{normal}}} \left(\tilde{\mathbf{U}}_{ij'} [\tilde{\mathbf{U}}^{-1}]_{j'j} Q_j^{\text{fict}} \right) \lambda_{j'}^K}, \quad (\text{B6})$$

where the denominator contains the matrix $\tilde{\mathbf{U}}$ which diagonalizes $\mathbf{M}_{\text{normal}}$. This is because the denominator assumes a circuit with only normal qubits, hence its physical qubit's count can be found through $\mathbf{M}_{\text{normal}}$ alone.

b. Behaviour of R in the large- K limit

Now we look at the behavior of R in the large K limit, to see if a circuit containing at least one magic gate-operation requires more physical qubits than a circuit exclusively composed of normal gate-operations, when there are a large number of concatenations. For this simple, but useful, conclusions can be derived from our scaling approach by looking at the eigenvalues of \mathbf{M} in the numerator and denominator of R in (B6). We note that the numerator of Eq. (B6) contains eigenvalues for both magic and normal qubits, while the denominator contains only eigenvalues for normal qubits. If the largest eigenvalue appearing in the numerator of R is larger than the largest one appearing on the denominator, R will diverge as K increases. If not, R will go to a finite constant value at $K \rightarrow \infty$. One may have $R \rightarrow 0$ in the limit $K \rightarrow \infty$, but only if magic gates are less costly than normal gates of type m ; this is not impossible, but is made unlikely in most schemes by arguments similar to the argument below Eq. (14) that $b > \lambda_{\text{normal}}$.

Note that the choice of m , i.e., the choice of the type of normal qubits that replace magic qubits to make the fictional circuit, changes the denominator in Eq. (B6), hence it changes the value of R . However, so long we choose m among the types of normal qubits that are already in the original logical algorithm, then the choice of m simply changes the value of the prefactors on the different eigenvalues in the denominator, which does not change how the denominator scales as $K \rightarrow \infty$. Hence, this choice of m does not change whether R diverges or remains constant as $K \rightarrow \infty$.

This shows the interest of our scaling approach in more complicated situations with multiple types of normal and magic qubits. It tells us the physical qubit cost in the large K limit can very easily be identified from inspecting the eigenvalues of the matrix \mathbf{M} . While we do not explore the general case for finite K here, we do a detailed analysis of such an example in Sec. VII D, where \mathbf{M} is a 3-by-3 matrix because that is a 7-qubit scheme with one type of normal qubit, but two types of magic qubit.

Appendix C: Circuit diagrams and parameters for flag qubits

Here we give some details on how we arrive at the values of parameters used to evaluate the qubit costs for flag-qubit error correction in sec. VII D. For completeness, we give the circuit diagrams for various parts of the flag-qubit fault-tolerant scheme in Figs. 15-19; these circuits are copied from Refs. [32, 40, 41]. Many parameters can be read directly off these circuits, just as for the Steane EC gadgets, and these are summarized in Fig. 13. However, the time multiplicity and failure multiplicities require a little more explanation, so we address them here.

As mentioned in Sec. VII D the magic gate in the flag-qubit scheme is $T_Y \equiv \exp[-i\pi/8Y]$ (while the usual T -gate is $T_Z \equiv \exp[-i\pi/8Z]$). However, we simply call it a T -gate, because T_Y and T_Z are computationally equivalent (they represent the same rotation but around a different Pauli axis).

1. Time multiplicities for flag-qubits

We need to estimate the time multiplicity coefficients shown in Table II. There r_s^{flag} is the time multiplicity for the ancillary states used in the flag EC gadget, while r_H^{flag} is the time multiplicity for the $|H\rangle$ magic-state. To be more precise, we assume that the flag EC gadget uses a pool of 3 ancillary qubits that it might re-use later. This pool corresponds to the first 3 ancillary qubits in Fig. 16 (meaning that if $r_s^{\text{flag}} = 1$, we would only have 3 ancillary qubits in Fig. 16, not 6). The time multiplicities are estimated through a formula $r_i^{\text{flag}} = \lceil \tau_{i,\text{anc}} / \tau_{i,\Delta\text{anc}} \rceil$, where $\tau_{i,\text{anc}}$ is the time to prepare, use and measure the $i \in \{s, H\}$ type of ancilla, and $\tau_{i,\Delta\text{anc}}$ is the minimum time separating two consecutive usage of this ancilla. We recall that the T -gate performed with magic-state injection lasts for $2\tau_L$ (see the state-injection gadget in Fig. 7), and two T -gates are always separated by one Clifford, so we have $\tau_{H,\Delta\text{anc}} = 3\tau_L$. Now, each r_i can in practice be fully determined from the circuits we provide in Figs. 15, 16, 17, 18, 19. There here we acknowledge a crucial point; the EC gadget in Fig. 16 need to be repeated $J_{\text{EC-repeat}}^{\text{flag}}$ times to guarantee fault-tolerance. However, for any for any $J_{\text{EC-repeat}}^{\text{flag}} \geq 1$, a numerical estimate of each r_i^{flag} shows that the values in Table II are sufficient to guarantee that enough qubits are in the computer (without needing the exact value of $J_{\text{EC-repeat}}^{\text{flag}}$). We say "sufficient", because, strictly speaking, the values in Table II are upper bounds on the required time multiplicities.

2. Failure multiplicities for flag-qubits

Here we explain the assumptions we used in order to find the values of $N_{0/+}^{\text{flag}}$ and N_H^{flag} given in Table I (they

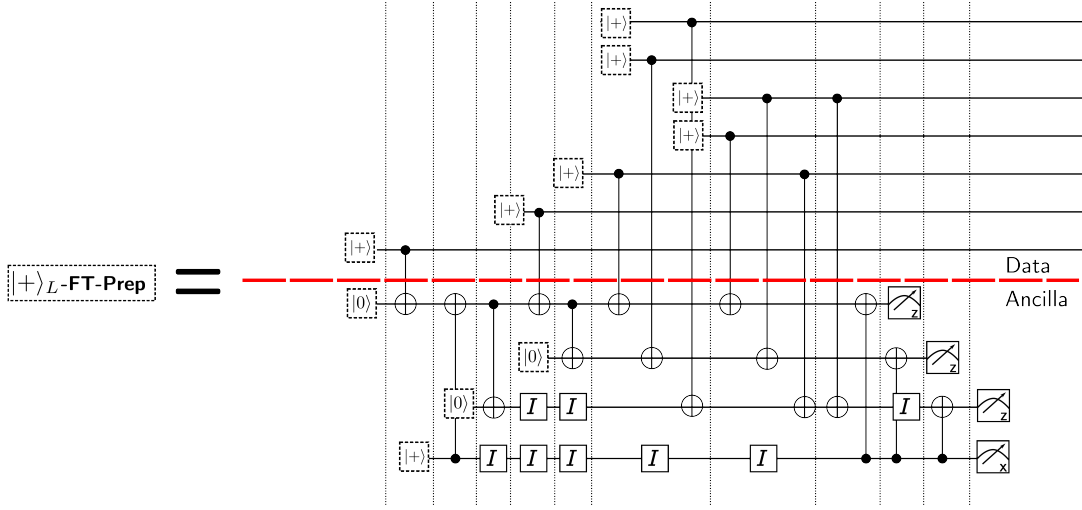


Figure 15. Fault-tolerant preparation of the logical $|+\rangle$: $|+\rangle$ -FT-Prep encoded in Steane code (top 7 qubits), with a verification based on flag qubits, from Refs [32] and [40]. The verification requires 4 ancillary qubits, at the bottom, see [40] and appendix C.1 of [32]. The bottom ancillary qubit is the flag qubit: if it is measured in $|-\rangle$, the state is rejected. There are numerous identity gates in this circuit (timesteps at which the qubit does nothing except stores its state for a later gate), however we mark with “I” those identity gates whose failure could lead to a state rejection, and thereby contribute to the state’s failure probability. The fault-tolerant preparation of the logical $|0\rangle$ -FT-Prep can be found by swapping the roles of Pauli X and Z everywhere in the circuit, i.e. swapping target and control for all CNOTs, exchanging the role of X and Z measurements, and $|0\rangle$ and $|+\rangle$ preparation.

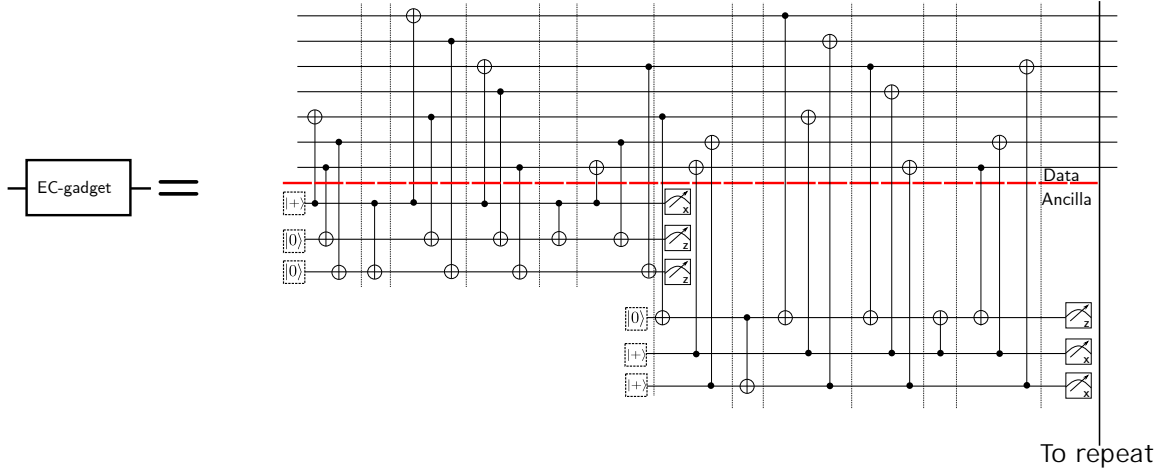


Figure 16. Error correction gadget based on flag qubits. The top 7 lines represent the Steane encoded qubit. It requires 3 ancillary qubits to extract the syndrome, but $3r_s^{\text{flag}} = 6$ in practice due to the fact the ancillary states take multiple time-steps to be fault-tolerantly prepared, in particular for $k > 1$. Hence, the two pairs of 3 ancillary qubit at the bottom are extracting the 6 stabilizers of Steane code (see [41] for the original proposal). To guarantee fault-tolerance, this circuit is repeated a few times, however the number of repetitions, $J_{\text{EC-repeat}}^{\text{flag}}$, does not appear in our evaluation of qubit costs. This is because our resource estimates would depend on $J_{\text{EC-repeat}}^{\text{flag}}$ in a negligible manner, as explained in Sec. VII E and at the end of Sec. C 1. Hence, we neglect this dependence.

correspond to, respectively, the first and second line of the fourth column of the flag-qubit section in Table I). For this, we need to find $N_{0/+}^{\text{flag}}$ and N_H^{flag} . They are then used in Eq. (27) to determine the values of failure multiplicities, $\mu_{0/+}^{\text{flag}}$ and μ_H^{flag} , given in the penultimate column of Table I.

We start with $N_{0/+}^{\text{flag}}$, which is estimated from the state preparation circuit shown in Fig. 15 taken from Ref. [32]. This circuit prepares the state $|+\rangle$. The same circuit prepares $|0\rangle$ under permutation of Pauli X and Z everywhere in the circuit (see the caption of Fig. 15), so the following explanation for $|+\rangle$ preparation applies equally for $|0\rangle$ preparation. To guarantee fault-tolerance, this

$$|H\rangle_L\text{-FT-Prep} = |H\rangle_L\text{-Prep} \xrightarrow{H_m} \text{EC-gadget}$$

Figure 17. Fault-tolerant preparation of the magic state $|H\rangle\text{-FT-Prep}$, taken from [32]. It takes as an input the state $|H\rangle\text{-Prep}$ whose preparation is shown on figure 18, while the circuit for the gadget H_m is in Fig. 19, and the circuit for the EC gadget is that already shown in Fig. 16. Note that the formal definition of the state $|H\rangle = T_Y|0\rangle$.

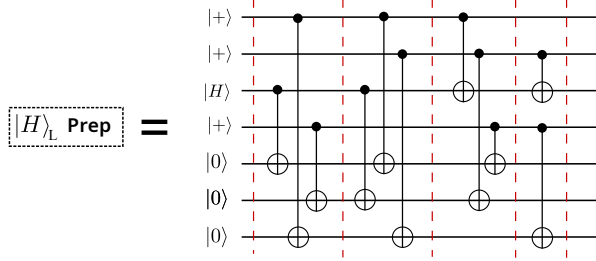


Figure 18. Non-fault-tolerant preparation of the state $|H\rangle \equiv T_Y|0\rangle$ in Steane code. This preparation is not fault-tolerant as a single fault for any of the CNOTs (or idling locations) can introduce more than one error on the logical qubit. The circuit in figure 17 allows to make the preparation fault-tolerant, according to the description provided in the text of the appendix.

circuit relies on post-selecting the states for which the flag is measured in $|+\rangle$ (the bottom ancillary qubit in Fig. 15). This guarantees that a single fault leads to at most a weight-one X error and a weight one Z -error on the output state, see Ref. [40]. Hence, such a post-selection satisfies the axioms of a 1-prep (see for instance appendix A of Ref. [32] for CSS codes such as the 7 qubit code considered here). This means that $N_{0/+}^{\text{flag}}$ is the number of ways a single fault could imply that the result of the verification fails — with verification failing when the flag (the bottom ancillary qubit in Fig. 15) ending up in the state $|-\rangle$ (rather than $|+\rangle$). For this, we count all the gates, state preparation and identity gates for which one fault could make the flag qubit measured in $|-\rangle$. From Fig. 15, we have 11 state preparations, 15 CNOTs, 9 identity gates, and 1 measurement that could lead to verification failure: it gives $N_{0/+}^{\text{flag}} = 36$.

We move on with N_H^{flag} . Here, we assumed $N_H^{\text{flag}} = \sqrt{2/p_{\text{thres}}}$. This is motivated by the fact $1/p_{\text{thres}}$ counts the number of malignant pair of fault-locations in the biggest exRec of the computation. A malignant pair of fault-locations, is a pair of fault-locations for which the introduction of faults introduces an uncorrectable error on the logical qubit of the computation. While not all pairs of fault-locations are necessarily malignant, the numbers are usually sufficiently close for our purpose, since we recall that μ_H^{flag} only depends *logarithmically* on N_H^{flag} (see Eq. (27)), hence an order of magnitude estimate is sufficient. To illustrate the legitimacy of our assumption, we can mention that the number of fault-locations

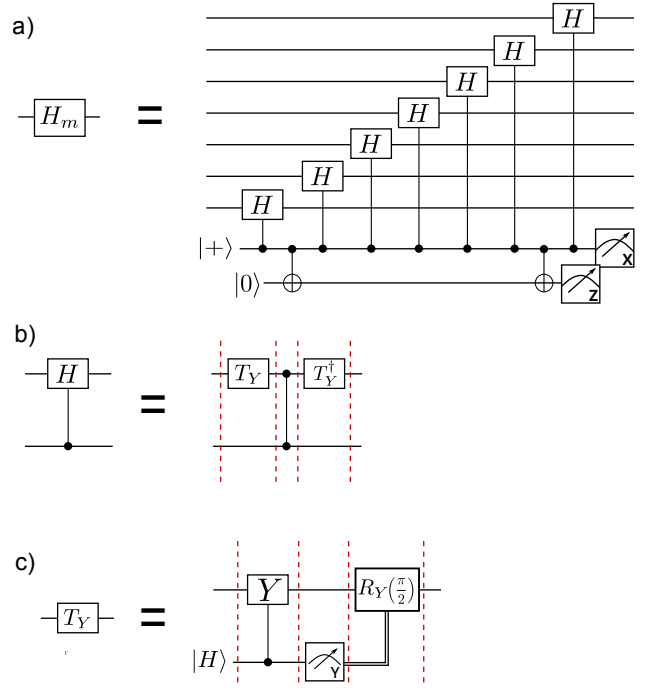


Figure 19. a) The top 7 qubits represent a logical qubit encoded in Steane code. The 2 ancillary qubits at the bottom are doing a flag fault-tolerant measurement of the logical Hadamard operator of the logical qubit: the top one will provide the outcome of the logical Hadamard measurement while the bottom one is the flag, used to make the overall preparation of the $|H\rangle$ state (shown on figure 17) fault-tolerant. b) The controlled Hadamard is decomposed as indicated here. State injection for the T_Y and T_Y^\dagger gates will be done for $k \geq 1$. To keep notations light, the T_Y -gate is simply labeled T in the parts referring to flag qubits. Yet, it does represent the $T_Y = \exp(-i\pi/8Y)$ gate. Note that T_Y is computationally equivalent to the "usual" T -gate ($\exp(-i\pi/8Z)$): they are the same rotation, but performed on two different Pauli axes (Y or Z). c) State injection gadget allowing to implement T_Y on the data qubit (top qubit). The gate T_Y^\dagger can be implemented by applying an extra Clifford $R_Y(\pi/2)$ on the top qubit after cY . T_Y^\dagger will have the same effective duration than T_Y as the extra $R_Y(\pi/2)$ can be combined with the classically controlled feedback which either implements a logical identity or $R_Y(\pi/2)$. For $k = 0$, T_Y (or T_Y^\dagger) can directly be implemented at the physical level (i.e., no need to perform state injection).

in the largest exRec for Steane EC gadget is 575, while $\sqrt{2/p_{\text{thres}}} = 316$: these are close estimate given the logarithmic dependence of the failure multiplicities.

Appendix D: Values of the error-correction threshold

Throughout this work, we assume that the error-correction threshold is similar for different error-correction schemes, even when they require very different physical qubit costs. This greatly simplifies our analysis,

because it means we can compare “costs” (i.e. physical qubit costs) for different error-correction schemes, while assuming the “benefits” of those schemes (i.e. their capacity to correct errors) are about equivalent. For simplicity, we assume that all error-correction schemes that we consider in this work (Steane, flag-qubit, and our toy-model) have the same threshold as for Steane error-correction [12]; $p_{\text{thres}} = 2 \times 10^{-5}$.

However, this assumption needs justifying, as it may seem surprising that a flag-qubit EC gadget has a similar capacity to correct errors as a Steane EC gadget, when the flag-qubit gadget is much smaller. Yet, the literature strongly implies that this is the case. In short, this is because flag-qubit EC gadgets require less ancillary qubits, but use them for more timesteps, so the number of fault-locations that determine the threshold appears to be similar to that for Steane EC gadgets.

Having said that, there is not yet a consensus in the literature on the *true* threshold for flag-qubits. Such a *true* threshold would be one that applies for any gate operation and a reasonably-general noise model ($p_{\text{thres}} = 2 \times 10^{-5}$ for Steane EC gadgets under an adversarial independent stochastic noise model [12] is such a true threshold). Instead, different works (listed below) calculate what are called *pseudothresholds* for flag-qubits; these are thresholds that only apply for specific gate-operations exposed to specific noise, and are in principle only applicable for a single level of concatenation. As expected, each gate-operation and noise model gives different pseudothresholds. The works listed below show that some of these pseudothresholds for flag-qubits EC gadgets are better than the equivalent pseudothreshold for Steane EC gadgets, and some are worse. However, most of these pseudothresholds for flag-qubits EC gadgets are the same order of magnitude as the equivalent one for Steane EC gadgets. We therefore assume, as a reasonable working hypothesis, that the true threshold for flag-qubits EC gadgets is also similar to that for Steane EC gadgets, so for simplicity we take it to be the same.

To justify the above claim about the pseudothresholds, we now list one by one various works, and the pseudothresholds that they found for particular gate op-

erations and noise models. Ref. [75] evaluated the pseudothreshold for a quantum memory (i.e. a logical identity gate) depolarizing noise model and different noise strength for identity gates compared to two-qubit gates. When the identity gates had a comparable noise strength to two-qubit gates, the pseudothreshold for flag-qubit EC gadgets was 3.39×10^{-5} , while that for the Steane EC gadget was 6.29×10^{-4} , which is about eighteen times bigger. When the noise of the identity gates is 100 times less than that of the two-qubit gate, the pseudothreshold for flag-qubit EC gadgets was 1.41×10^{-5} , while that for Steane EC gadgets was 3.84×10^{-5} , which is more than two time bigger. This suggests that the advantage in one scheme compared to the other heavily depends on the noise model. Ref. [76] did numerical simulations for a quantum memory with depolarizing noise. They defined the pseudothreshold differently, through the leading order term in the expression of the logical error-rate. They then found this the pseudothreshold for flag-qubit EC gadgets was about 2×10^{-3} , while that for Steane EC gadgets was 1.4×10^{-3} . So a pseudothreshold defined in this way is very similar for the two types of EC gadgets, while, this time, the flag-qubit EC-gadget has a slightly bigger pseudothreshold than Steane.

Ref. [77] went beyond a quantum memory, and considered the pseudothreshold for a logical CNOT gate. Again they took depolarizing noise, and found a pseudothreshold for flag was 3.02×10^{-5} . This is smaller than the equivalent pseudothreshold for Steane EC gadgets in Ref. [12], which was 9.3×10^{-5} .

All these results strongly suggest that the threshold for the two types of error-correction are similar, despite the fact they have very different qubit costs. As this work is concentrating on the analysis of qubit costs, it is a natural simplification to assume the true threshold is the same in all cases. As the true threshold is closer to that for logical CNOT gates than to that for quantum memory, it can be expected that it is a bit below the pseudothreshold in Ref. [77]. Hence, it seems reasonable to assume the flag-qubit error-correction threshold is about $p_{\text{thres}} = 2 \times 10^{-5}$, the same as the Steane error-correction threshold for an adversarial independent stochastic noise model [12].

-
- [1] E. Farhi, J. Goldstone, and S. Gutmann, A Quantum Approximate Optimization Algorithm, arXiv 10.48550/arXiv.1411.4028 (2014), 1411.4028.
- [2] D. Amaro, C. Modica, M. Rosenkranz, M. Fiorentini, M. Benedetti, and M. Lubasch, Filtering variational quantum algorithms for combinatorial optimization, Quantum Sci. Technol. **7**, 015021 (2022).
- [3] B. Bauer, S. Bravyi, M. Motta, and G. K.-L. Chan, Quantum Algorithms for Quantum Chemistry and Quantum Materials Science, Chem. Rev. **120**, 12685 (2020).
- [4] Y. Cao, J. Romero, J. P. Olson, M. Degroote, P. D. Johnson, M. Kieferová, I. D. Kivlichan, T. Menke, B. Peropadre, N. P. D. Sawaya, S. Sim, L. Veis, and A. Aspuru-Guzik, Quantum Chemistry in the Age of Quantum Computing, Chem. Rev. **119**, 10856 (2019).
- [5] H. Ma, M. Govoni, and G. Galli, Quantum simulations of materials on near-term quantum computers, npj Comput. Mater. **6**, 1 (2020).
- [6] P. W. Shor, Polynomial-Time Algorithms for Prime Factorization and Discrete Logarithms on a Quantum Computer, SIAM J. Comput. 10.1137/S0097539795293172 (2006).
- [7] T. Häner, S. Jaques, M. Naehrig, M. Roetteler, and M. Soeken, Improved Quantum Circuits for Elliptic

- Curve Discrete Logarithms, in *Post-Quantum Cryptography* (Springer, Cham, Switzerland, 2020) pp. 425–444.
- [8] P. Shor, Fault-tolerant quantum computation, in *Proceedings of 37th Conference on Foundations of Computer Science* (1996) pp. 56–65.
- [9] E. Knill, R. Laflamme, and W. H. Zurek, Resilient quantum computation: error models and thresholds, *Proceedings of the Royal Society of London. Series A: Mathematical, Physical and Engineering Sciences* **454**, 365 (1998).
- [10] J. Preskill, Reliable quantum computers, *Proceedings of the Royal Society of London. Series A: Mathematical, Physical and Engineering Sciences* **454**, 385 (1998).
- [11] D. Aharonov and M. Ben-Or, Fault-tolerant quantum computation with constant error rate, *SIAM Journal on Computing* **38**, 1207 (2008), <https://doi.org/10.1137/S0097539799359385>.
- [12] P. Aliferis, D. Gottesman, and J. Preskill, Quantum accuracy threshold for concatenated distance-3 codes (2005), arXiv:quant-ph/0504218.
- [13] B. M. Terhal, Quantum error correction for quantum memories, *Rev. Mod. Phys.* **87**, 307 (2015).
- [14] E. T. Campbell, B. M. Terhal, and C. Vuillot, Roads towards fault-tolerant universal quantum computation, *Nature* **549**, 172 (2017).
- [15] J. Roffe, Quantum error correction: an introductory guide, *Contemp. Phys.* **60**, 226 (2019).
- [16] A. G. Fowler, M. Mariantoni, J. M. Martinis, and A. N. Cleland, Surface codes: Towards practical large-scale quantum computation, *Phys. Rev. A* **86**, 032324 (2012).
- [17] Y. Liu, Z. Ma, L. Luo, C. Du, Y. Fei, H. Wang, Q. Duan, and J. Yang, Magic state distillation and cost analysis in fault-tolerant universal quantum computation, *Quantum Science and Technology* **8**, 043001 (2023).
- [18] A. Krishna and J.-P. Tillich, Towards Low Overhead Magic State Distillation, *Physical Review Letters* **123**, 070507 (2019).
- [19] E. Nikahd, M. S. Zamani, and M. Sedighi, A Low-Overhead Hybrid Approach for Universal Fault-Tolerant Quantum Computation (2017), arXiv:1610.03309.
- [20] S. Bravyi and J. Haah, Magic state distillation with low overhead, *Physical Review A* **86**, 052329 (2012), arXiv:1209.2426.
- [21] P. Webster, S. D. Bartlett, and D. Poulin, Reducing the overhead for quantum computation when noise is biased, *Physical Review A* **92**, 062309 (2015).
- [22] J. Haah and M. B. Hastings, Codes and Protocols for Distilling T , controlled- S , and Toffoli Gates, *Quantum* **2**, 71 (2018), arXiv:1709.02832.
- [23] M. B. Hastings and J. Haah, Distillation with Sublogarithmic Overhead, *Physical Review Letters* **120**, 050504 (2018).
- [24] H. Goto, Step-by-step magic state encoding for efficient fault-tolerant quantum computation, *Scientific Reports* **4**, 7501 (2014).
- [25] A. Kissinger and J. van de Wetering, Reducing the number of non-Clifford gates in quantum circuits, *Phys. Rev. A* **102**, 022406 (2020).
- [26] A. G. Fowler, S. J. Devitt, and C. Jones, Surface code implementation of block code state distillation, *Scientific Reports* **3**, 1939 (2013).
- [27] Y. Li, A magic state’s fidelity can be superior to the operations that created it, *New J. Phys.* **17**, 023037 (2015).
- [28] C. Chamberland, T. Jochym-O’Connor, and R. Laflamme, Overhead analysis of universal concatenated quantum codes, *Phys. Rev. A* **95**, 022313 (2017).
- [29] J. O’Gorman and E. T. Campbell, Quantum computation with realistic magic-state factories, *Phys. Rev. A* **95**, 032338 (2017).
- [30] J. Haah, M. B. Hastings, D. Poulin, and D. Wecker, Magic State Distillation with Low Space Overhead and Optimal Asymptotic Input Count, *Quantum* **1**, 31 (2017), arXiv:1703.07847.
- [31] E. T. Campbell and M. Howard, Magic state parity-checker with pre-distilled components (2018), arXiv:1709.02214.
- [32] C. Chamberland and A. W. Cross, Fault-tolerant magic state preparation with flag qubits, *Quantum* **3**, 143 (2019), arXiv:1811.00566.
- [33] C. Chamberland and K. Noh, Very low overhead fault-tolerant magic state preparation using redundant ancilla encoding and flag qubits, *npj Quantum Information* **6**, 91 (2020).
- [34] C. Chamberland, T. Jochym-O’Connor, and R. Laflamme, Thresholds for Universal Concatenated Quantum Codes, *Physical Review Letters* **117**, 010501 (2016).
- [35] T. Jochym-O’Connor and R. Laflamme, Using concatenated quantum codes for universal fault-tolerant quantum gates, *Physical Review Letters* **112**, 010505 (2014), arXiv:1309.3310.
- [36] D. Litinski, Magic State Distillation: Not as Costly as You Think, *Quantum* **3**, 205 (2019), 1905.06903v3.
- [37] C. Gidney, N. Shutty, and C. Jones, Magic state cultivation: growing T states as cheap as CNOT gates, arXiv 10.48550/arXiv.2409.17595 (2024), 2409.17595.
- [38] C. Gidney and M. Ekerå, How to factor 2048 bit RSA integers in 8 hours using 20 million noisy qubits, *Quantum* **5**, 433 (2021), 1905.09749v3.
- [39] Ref. [24] also only considered resources in an example where *both* magic states and CNOTs are implemented via state injection; in our language, this means it considered all operations as magic operations. Our approach evaluates resources for both normal and magic operations.
- [40] R. Chao and B. W. Reichardt, Quantum error correction with only two extra qubits, *Physical Review Letters* **121**, 050502 (2018), arXiv:1705.02329.
- [41] B. W. Reichardt, Fault-tolerant quantum error correction for Steane’s seven-qubit color code with few or no extra qubits, *Quantum Science and Technology* **6**, 015007 (2021), arXiv:1804.06995.
- [42] The verification is probabilistic because it is a probabilistic process with a finite chance of failing verification.
- [43] As we were finishing this work, we became aware of a new proposal to further reduce the resources needed for error correction [78], but we have not yet analyzed it.
- [44] The flag-qubit scheme that we consider not only has a different size EC gadget from the Steane scheme, it also has other differences (such as slightly less-costly magic states). This toy-model is intended to explore only the effect of the EC gadget’s size, so it does not capture other aspects of the flag-qubit scheme.
- [45] To avoid any ambiguity, we explicitly state that we only use the term “level- k ” to refer to the level- k circuit in which magic gates have not yet been replaced by state-injection gadgets. We only implement the state-injection as part of the protocol that writes level- k operations in terms of level- $(k - 1)$ operations.

- [46] M. Fellous-Asiani, J. H. Chai, R. S. Whitney, A. Auffèves, and H. K. Ng, Limitations in Quantum Computing from Resource Constraints, *PRX Quantum* **2**, 040335 (2021).
- [47] M. Fellous-Asiani, J. H. Chai, Y. Thonnart, H. K. Ng, R. S. Whitney, and A. Auffèves, Optimizing Resource Efficiencies for Scalable Full-Stack Quantum Computers, *PRX Quantum* **4**, 040319 (2023).
- [48] F. Góis, M. Pezzutto, and Y. Omar, Towards Energetic Quantum Advantage in Trapped-Ion Quantum Computation, arXiv 10.48550/arXiv.2404.11572 (2024), 2404.11572.
- [49] M. C. Volpato and P.-L. de Assis, Estimating the electrical energy cost of performing arbitrary state preparation using qubits and qudits in integrated photonic circuits, arXiv 10.48550/arXiv.2402.16603 (2024), 2402.16603.
- [50] In contrast, for a completely arbitrary algorithm, one may need to use our method to evaluate the physical qubit cost of every layer before discovering which one is the bottleneck layer, \mathcal{L}_{\max} . There may even be some cases where the highest qubit cost is not during the calculation, but rather at the moment of preparation of the logical qubits that will be used in the calculation, or (in very atypical cases) at the moment all logical qubits are measured at the end of the calculation.
- [51] An algorithm implementing \mathcal{L}_{\max} at every step, requires more qubits than an algorithm implementing \mathcal{L}_{\max} only once. This is because the latter would not need to be preparing ancillary states for future layers (or reading ancillary states from preceding layers) at the same time as carrying out \mathcal{L}_{\max} . The extra resources required to implement \mathcal{L}_{\max} at every step will be quantified by the “time multiplicity” introduced in Sec. V B.
- [52] We note that this treats an ancillary qubit that undergoes a single magic operation during its usage as if it experienced a magic operation at *every* time step. This clearly overestimates the qubit cost of such a magic qubit. However, as we show that this cost is not so large, a better estimate would only reinforce this conclusion.
- [53] This can be found using Eq. (7) in the standard manner.
- [54] Monotonic growth with K is guaranteed by two observations. Firstly, λ_{normal} , λ_{magic} , and b are positive numbers. Secondly, for the regime where $\lambda_{\text{normal}} > \lambda_{\text{magic}}$, we use $b > \lambda_{\text{normal}}$, which holds for the reasons explained below Eq. (14).
- [55] As explained in Appendix B, λ_{normal} , λ_{magic} and b can become matrices when there are multiple types. Then the upper-bound for each one is the largest matrix element in the respective matrix, multiplied by the number of rows in that matrix.
- [56] Here $\lceil x \rceil$ is the ceiling function, so $\lfloor x \rfloor$ is the smallest integer greater than x .
- [57] In the case where $\tau_{\text{anc}}(k)/\tau_{\text{L}}(k)$ is unbounded when k grows (which never occurs in the examples we treat later on), one can simply redefine $r \equiv \max_{k \in [1, K]} \lceil \tau_{\text{anc}}(k)/\tau_{\text{L}}(k) \rceil$ so that the maximum is well-defined over the targeted concatenations levels the experimentalist wish to implement.
- [58] C. Chamberland and A. W. Cross, Fault-tolerant magic state preparation with flag qubits, *Quantum* **3**, 143 (2019), 1811.00566v2.
- [59] The upper-bound of Np does not require independent errors. However, when errors are independent, such a probability takes the form $1 - (1 - p)^N$, for which the upper bound Np is quite tight for the concrete values in Table I.
- [60] If there are multiple exRecs with different M s, we simplify our analysis (while getting an upper bound) by replacing all these M s by whichever M is largest.
- [61] These values are still significantly larger than that given by the law of large numbers, $1/(1 - Np_{\text{thres}})$. This shows that even very large computations will not be large enough to be approximated by the law of large numbers.
- [62] D. Bluvstein, S. J. Evered, A. A. Geim, S. H. Li, H. Zhou, T. Manovitz, S. Ebadi, M. Cain, M. Kalinowski, D. Hangleiter, J. P. Bonilla Ataides, N. Maskara, I. Cong, X. Gao, P. Sales Rodriguez, T. Karolyshyn, G. Semeghini, M. J. Gullans, M. Greiner, V. Vuletić, and M. D. Lukin, Logical quantum processor based on reconfigurable atom arrays, *Nature* **626**, 58 (2024).
- [63] Rigorously speaking, $N_{\text{gates}}^{\text{level-1}}$ could be bigger than $Q_{\text{total}}^{\text{phys}}(K-1) \times D^{K-1} \times 2D_L$. This is because, $D^{K-1} \times 2D_L$ does not account for the duration required to prepare the ancillary level- $(K-1)$ states required to implement the level- K circuit (for instance the qubits required by the magic states). Their duration of preparation may be long enough that they must be being prepared before the first-step of the level- K circuit. Yet, for any typical algorithm, this extra duration will be negligible compared to the total algorithm’s duration. This is why $D^{K-1} \times 2D_L$ is a good over-estimate of the physical circuit depth for $(K-1)$ concatenations.
- [64] We think it plausible to assume that practical quantum computers will not have concatenation level, $K > 5$. This is because Fig. 1 shows that at $K = 5$ all error-correction schemes considered here require millions of physical qubit for each qubit in the logical algorithm (with Steane scheme requiring billions). A large-scale quantum algorithm (like Shor code to crack RSA-2048 [38]) needs about a thousand logical qubits. It seems impractical to assume a real quantum computer with more than billions of physical qubits in the near future.
- [65] The gadget in figure 11a will prepare $Z|A_{\pi/4}\rangle$ instead of $|A_{\pi/4}\rangle$, whenever the logical X measurement of the repetition qubits in both gadgets indicated -1 , and both Steane EC-gadgets detect no error. This $Z|A_{\pi/4}\rangle$ can be injected and used to perform a T -gate, one would simply have to apply an additional logical Z in the block marked “S” in Fig. 10. This additional logical Z will not change our qubit’s resource estimate.
- [66] For this we start with the dashed curve for Steane code without shared state preparation in Fig. 1, which corresponds to a circuit without magic gates. We then multiply it by 17.6 (taken from Eq. 40) to arrive at the case where all gates are magic gates, and round to the nearest order of magnitude.
- [67] T. Tansuwannont, B. Pato, and K. R. Brown, Adaptive syndrome measurements for shor-style error correction, *Quantum* **7**, 1075 (2023).
- [68] B. Pato, T. Tansuwannont, S. Huang, and K. R. Brown, Optimization tools for distance-preserving flag fault-tolerant error correction, *PRX Quantum* **5**, 020336 (2024).
- [69] C. Zalka, Fast versions of Shor’s quantum factoring algorithm, arXiv 10.48550/arXiv.quant-ph/9806084 (1998), quant-ph/9806084.
- [70] G. Banegas, D. J. Bernstein, I. van Hoof, and T. Lange, Concrete quantum cryptanalysis of binary elliptic curves, *TCHES*, 451 (2021).

- [71] A. Scherer, B. Valiron, S.-C. Mau, S. Alexander, E. van den Berg, and T. E. Chapuran, Concrete resource analysis of the quantum linear-system algorithm used to compute the electromagnetic scattering cross section of a 2D target, *Quantum Inf. Process.* **16**, 60 (2017).
- [72] S. Chakrabarti, R. Krishnakumar, G. Mazzola, N. Stamatopoulos, S. Woerner, and W. J. Zeng, A Threshold for Quantum Advantage in Derivative Pricing, *Quantum* **5**, 463 (2021), 2012.03819v3.
- [73] M. Reiher, N. Wiebe, K. M. Svore, D. Wecker, and M. Troyer, Elucidating reaction mechanisms on quantum computers, *Proc. Natl. Acad. Sci. U.S.A.* **114**, 7555 (2017).
- [74] C. Gidney, Quantum block lookahead adders and the wait for magic states, arXiv 10.48550/arXiv.2012.01624 (2020), 2012.01624.
- [75] C. Chamberland and M. E. Beverland, Flag fault-tolerant error correction with arbitrary distance codes, *Quantum* **2**, 53 (2018), 1708.02246v3.
- [76] R. Chao and B. W. Reichardt, Quantum Error Correction with Only Two Extra Qubits, *Phys. Rev. Lett.* **121**, 050502 (2018).
- [77] P.-H. Liou and C.-Y. Lai, Parallel syndrome extraction with shared flag qubits for Calderbank-Shor-Steane codes of distance three, *Phys. Rev. A* **107**, 022614 (2023).
- [78] B. Pato, T. Tansuwannont, and K. R. Brown, Concatenated Steane code with single-flag syndrome checks, arXiv 10.48550/arXiv.2403.09978 (2024), 2403.09978.